UNIVERSITY OF LIVERPOOL

HCCI ENGINE MODELLING FOR CONTROL

Thesis submitted in accordance with the
requirements of the University of Liverpool
for the degree of Doctor in Philosophy

in

Department of Electrical Engineering and Electronics

by

Nan Jia

January 2009

To my parents

Acknowledgements

I would like to give my greatest thanks to my supervisor, Dr. Jihong Wang, for her invaluable support, dedication and enthusiasm. Her scientific belief and her persistent efforts constitute the essential part of the project, and her knowledge and passions in science exceptionally inspire and enrich my growth as a student, a researcher and an engineer want to be.

I gratefully acknowledge Dr. Keith Nuttall for the great experience and expertise he brings to the project. His drive, enthusiasm, work and knowledge have triggered and nourished my intellectual maturity that I will benefit from, for a long time to come.

Many thanks go to Dr. Hongming Xu, for sharing his invaluable knowledge and experience in the field of HCCI engine research from the very early stage of the project. His much important advice and guidance gave me extraordinary experiences throughout the work. Many thanks also go to Prof. Miroslaw Wyszynski, for his valuable advice in science discussion and giving his critical comments about my publications.

I gratefully thank Prof. Qinghua Wu for his important advice and encouragement along the way. My thanks also go to Prof. Jinling Zhang who always kindly grants me her time for answering my unintelligent question about thermodynamics.

It is a pleasure to pay tribute to my colleagues. Many thanks go to Dr. Jianlin Wei for valuable discussion and the pleasure working together in the project. I also benefited by outstanding works from Dr. Yin Yong and Mr. Xing Luo, especially in the field of HILST. I would also acknowledge Dr. Steve

Mangan for sharing his experience on vehicle modelling. I would also like to thank Dr. Nan Lu for sharing his bright thoughts with me.

I gratefully thank Jaguar Car Ltd for the financial support of the project. I also acknowledge Mr. Jacek Misztal and Dr. Daniel Yap for providing me the experimental data.

I should say thanks to my friends for their kindly helps and supports during my studying. There are greatest memories – we work hard and have fun together and we will never walk alone. Special acknowledgements to Dr. Jia Ke and Ms. Liuying Wu, two very special people in my life. Heartily thanks for standing by my side all the time over the period of my studying.

Finally, I am greatly indebted to my parents, for their encouragement, support and understanding. With love, they have always been there for me, whenever good time or bad.

Abstract

To meet future environmental challenges and more stringent emission legislation, Homogeneous Charge Compression Ignition (HCCI) has been proposed as a promising alternative to conventional combustion strategies. HCCI engines offer thermal efficiencies comparable to those attained by high compression ratio diesel engines while maintaining the smoke free operation of spark ignition engines. HCCI engines operate on the principle of having a premixed charge that auto-ignites and burns spontaneously throughout the cylinder as it is compressed by the piston. However, combustion control is a significant challenge for HCCI engines that must be solved if they are to become a commercial success. In order to investigate the control strategies for solving the fundamental challenges, the original project specification set by the sponsor, Jaguar Cars Ltd, does not require that the models predict the HCCI combustion in every detailed aspect, but the models must be sufficient to capture most control relevant behaviours of HCCI process and are desired an inherent simple structure to reduce the simulation time.

This thesis summarises research work in the development of HCCI engine models for control purposes. The work was initially inspired from the investigations of HCCI research development that introduces the technologies to achieve HCCI combustion and reviews the modelling approaches by different methodologies. The single-zone model was proposed and utilised with Arrhenius-type equations to describe the process of propane combustion. And then, gasoline fuelled HCCI engine was developed by utilising Wiebe function and using Genetic Algorisms (GAs) to identify unknown parameters in the combustion segments. The relevant simulation results show that the models are able to adequately simulate the combustion

process and capture the combustion timing and in-cylinder pressure evolution.

The aforementioned models were extended to investigate the general behaviours of the HCCI dynamic process, including cycle-to-cycle coupling, modulating the inducted gases composition and cyclic in-cylinder pressure evolutions. After the extensive simulation studies were conducted, a vehicle driveline model was then integrated into the model to investigate the feasible control strategy. By applying a simple proportional-integral controller, the vehicle velocity and engine output were both controlled by modulating intake and exhaust valves timing. The successful cycle-resolved simulation results indicate that the simplifications inherent in the model are not critical to the successful prediction of trend of ignition timing, work output variation and cyclic coupling – the most challenging problems of HCCI engines. Furthermore, the reduced complexity of the simulation offers the prospect of achieving simulation speeds that will allow real time predictions so that the model can be used as a practical engineering tool and a valuable testing facility in the development of suitable control strategies.

CONTENTS

LIST OF FIGURE

LIST OF TABLES

ABBREVIATION

AR	Active Radical
ATAC	Active Thermo Atmosphere Combustion
ATDC	After Top Dead Centre
BTDC	Before Top Dead Centre
CAD	Crank Angle Degree
CAI	Controlled Auto Ignition
CFD	Computational Fluid Dynamics
CIDI	Compression Ignition Direct Injection
DI	Direct Injection
EGR	Exhaust Gas Recirculation
EVC	Exhaust Valve Closing
EVO	Exhaust Valve Opening
GDI	Gasoline Direct Injection
HC	Hydrocarbon
HCCI	Homogeneous Charge Compression Ignition
IC	Internal Combustion
IVC	Intake Valve Closing
IVO	Intake Valve Opening
MK	Modulated Kinetics
MOP	Maximum Opened Position
NVO	Negative Valve Overlap
PCCI	Premixed Charge Compression Ignition
PDF	Probability Density Function
RGF	Residual Gas Fraction
SI	Spark-Ignited
SULEV	Super Ultra Low Emission Vehicles

TS	Toyota-Soken
VCR	Variable Compression Ratio
VVT	Variable Valve Timing

Chapter 1

INTRODUCTION

1.1 ENVIRONMENT CHALLENGE AND NEW PROPULSION SYSTEM

With the economic development, the number of vehicles is rapidly increasing. According to report from Department for Transport [1], with 3.2% annual growth rates, there are 35 million vehicles on the road in the United Kingdom alone, resulting in 100 billion gallons of fuel being consumed in each year. Most of the vehicles are driven by internal combustion (IC) engine, which associate with large-scale consumption of limited fossil-fuel reserves and the production of harmful exhaust gases. Considering the continuously increasing of the number of people and their energy needs, the fuel consumption and emissions can only realistically be reduced if an alternative for the IC engine is developed with characteristics significantly better than those of present engines. Ideally, such an alternative should not be dependent on fossil fuels, emit no harmful products and are more efficient. The research works concentrate on the developments of advanced internal combustion strategies, hybrid system and fuel cells system.

Fuel cells system would be the most promising concept for next generation propulsion systems. However, it may take another twenty years or more to make this novel propulsion technology applicable in daily life, due to its high costs and the difficulty of hydrogen storage. Furthermore, the well-to-wheel efficiency of fuel cell powertrain with all the necessary auxiliary equipment is estimated to be similar than that of optimised diesel engines [2, 3], unless the hydrogen can be generated in the vehicle directly from renewable sources, such as solar energy. However, as the present technological standards in the renewable energy field are newly developed, it is still far from realistic to expect that a substantial portion of the fossil fuel used for vehicle propulsion could be replaced by sustainable alternatives in the near future.

A hybrid vehicle is usually equipped with IC engine and additional distinct power storage, i.e. rechargeable battery, which is able to recapture inertial energy that would otherwise be wasted in a conventional vehicle. Fuel-electricity system is the most common hybrid propulsion system in the market. Benefits from its energy recycle concept, a hybrid system can reduce fuel consumption up to 30% compared with conventional propulsion system [4]. Furthermore, it is recently reported that the energy recovery rate of hydraulic/pneumatic hybrid vehicles, which use an engine to charge a pressure accumulator to drive the wheels via hydraulic/pneumatic drive units *i.e.* compressed air, is higher and they are more efficient than battery charged hybrids, demonstrating a 60% to 70% increase in energy economy [5].

However, no matter in a hybrid vehicle or in a conventional vehicle, IC engine always plays the major role in the system. There were impressive evolutionary improvements in the development of the IC engine in the past few decades: fuel consumption and emissions have been substantially decreased, while power output has been raised, mainly due to the application of new technologies, such as the three-way catalyst and advanced engine

management system. Furthermore, since more strict legislation on vehicle emissions will be applied in the world, other innovative IC engine strategies with a wide range of features have recently been introduced, including: variable valve operation, cycle-to-cycle model-based engine control system, fuel direct-injection, *etc.* Among these advanced IC engine strategies, the most promising one is Homogeneous Charge Compression Ignition (HCCI), the compression-induced auto-ignition of a uniform fuel and air mixture.

1.2 HOMOGENEOUS CHARGE COMPRESSION IGNITION

In this thesis, HCCI is defined as the process in which the homogeneous mixtures of air and fuel, diluted with residual combustion products, are compressed to a certain conditions that auto-ignition occurs close to TDC, and a uniform combustion process follows that is usually significantly faster than 4-stroke conventional IC engine. Propane and gasoline are used as the fuel, while early Exhaust Valve Close (EVC) and later Intake Valve Open (IVO) are applied to facilitate combustion products trapping the process so-called Negative Valve Overlap (NVO). The NVO cycle is illustrated in Figure 1-1. An important characteristic of the HCCI combustion is that there is no direct trigger for its combustion initiation. In the conventional Spark Ignition (SI) and diesel engine the onset of the combustion event is triggered with the application of a spark and fuel injection, respectively. The HCCI combustion process is only dominated by local chemical-kinetic reaction rate that depends on internal energy of the mixtures. This characteristic indicates that the HCCI process is sensitive to temperature since temperature is one of the key functions of chemical kinetics. [6].

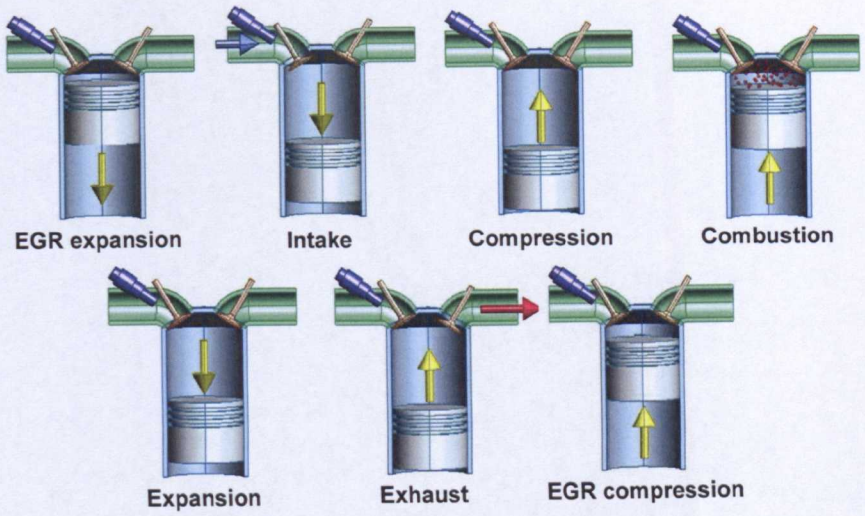

Figure 1-1 Key processes for HCCI adopting NVO

In the definition, homogeneous mixture and uniform combustion are assumed, which can be explained as: the temperature, pressure and composition of a perfectly homogeneous mixture of air and fuel are uniform throughout the combustion chamber; after the auto-ignition, combustion would occur uniformly throughout the combustion chamber, the perfectly mixed reactants will release all the heat of combustion simultaneously [7, 8]. These assumptions are made for HCCI simulation using a single-zone model that will be discussed in following chapters. However, in a real engine, the mixtures are not perfectly homogeneous, and the mixture temperature, equivalence ratio and residual gas fraction (RGF) are stratified present in the combustion chamber. The degree of stratification affects the combustion duration and may limits the load range indirectly where stable HCCI operation is possible; a too fast heat release gives rise to violent, knocking combustion, whereas a too long burn duration causes incomplete combustion, or even misfiring, due to the falling mixture temperature in the expansion stroke [9].

1.3 ADVANTAGES AND CHALLENGES OF HCCI ENGINE

Having introduced the HCCI combustion concept, this section will give an overview of the advantages of HCCI engine and the challenges with making HCCI practical.

1.3.1 ADVANTAGES OF HCCI ENGINE

The potential advantages of HCCI are numerous and depend on the combustion system to which it is compared. Comparing to SI gasoline engine, HCCI engine is more efficient, approaching the efficiency of a diesel engine. According to the reports, within the HCCI operating range, fuel consumption is up to 30% lower at (part-load) steady-state conditions than for conventional, throttled SI engine operation [10, 11]. The improved efficiency results from three sources listed as follows:

1. The elimination of throttling losses. Since HCCI engines can be run with wide-open throttle, even for part-load operation, the pumping losses are significantly lower than those for SI operation at low and intermediate loads.

2. The use of high compression ratios. HCCI can be operated at very low equivalence ratios, thus the compression ratio can be achieved as higher as a diesel engine.

3. Faster combustion. It is not necessary for a flame to propagate across the cylinder, which means that the process is closer to theoretical constant volume combustion, and heat losses are reduced, due to the lower combustion temperatures characteristic of HCCI operation.

In comparison with to diesel engines, HCCI engines have substantially lower emissions of Particulate Matter (PM) and NO_x (Emissions of PM and NO_x are the major impediments to diesel engines in order to meet future emissions standards and are the focus of extensive current research.). The low emissions of PM and NO_x in HCCI engines are a result of the dilute homogeneous air and fuel mixture in addition to low combustion temperatures. The charge in an HCCI engine may be made dilute by being very lean, by using exhaust gas recirculation (EGR), or a combination of them. As flame propagation is not required, dilution levels can be much higher than the levels tolerated by either SI or diesel engines. Combustion is induced throughout the charge volume by compression heating due to the piston motion, and it will occur in almost any fuel/air/exhaust-gas mixture once the 800 to 1100 K ignition temperature (depending on the type of fuel) is reached. Once combustion occurs, the temperature will rise above the ignition temperature, but complete combustion can only be achieved at temperatures below those at which significant NO_x is produced. In contrast, in diesel engines, minimum flame temperatures are 1900 to 2100 K, high enough to make unacceptable levels of NO_x [11, 12]. Additionally, the combustion duration in HCCI engines is much shorter than in diesel engines since it is not limited by the rate of fuel/air mixing. This shorter combustion duration makes the HCCI engine more efficient.

1.3.2 Challenges with making HCCI practical

Although HCCI engine and its substantial benefits have been demonstrated at selected conditions, there are some fundamental challenges with regards to combustion control. Specially, high proportion internal/external EGR are adopted to achieve HCCI combustion, the cycle-to-cycle coupling through the residual gas temperature plays a critical role.

1. AS aforementioned in the previous section, there is no specific initiator to trigger the HCCI combustion. Hence, how to control and ensure that combustion occurs with acceptable timing is more complicated and challenging than in the case of either SI or diesel combustion. Combustion timing in HCCI is dominated by chemical kinetics, which depends on the in-cylinder concentrations of reactants and products, their temperature and the amount of compression.

2. In this thesis, HCCI is achieved by adopting NVO strategy to trap residual combustion products, and then subsequent engine cycles are coupled through the residual temperature. Since the residual combustion products will elevate the temperature of fresh reactants the amount of residual product and relevant internal energy from an engine cycle directly affects the combustion occurrence and the reactants oxidation process on the subsequent. The cyclic coupling plays a fundamental role in steady state and transient operation.

3. For any practical HCCI strategy, the reactants are diluted with either residual gas or air. As much as 50% of the gas in the combustion chamber can consist of residual products prior to combustion. As a result, the dilution leads to the presence of the upper load limit that is significantly lower than the one for SI engines. Furthermore, the dilution decreases the amount of work that can be extracted from a given engine geometry. For these reasons, practical HCCI will be accompanied with either conventional SI or diesel strategies in a multi-mode engine that will switch between HCCI mode at lower/medium loads and conventional engine operation at high loads.

In the past a few years, substantial progress has been made in HCCI engine developments. However, the issues listed above are still the obstacle on the way leading to a commercial success for HCCI engine.

1.4 PROJECT OBJECTIVES

In order to investigate the control strategies for solving the fundamental challenges of HCCI engine, the original project specification set by Jaguar Cars Ltd required a modelling approach that can be used as a test bed for control developments. However, it was not necessary that engine model can predict the HCCI combustion in every detailed aspect - it would be sufficient if the model could capture most control relevant behaviours of HCCI process in both steady states and transients. Furthermore, the model was desired an inherent simple structure to reduce the simulation time.

The first step to achieve the final goal of the project would be the development of HCCI engine models for investigating real-time control strategy. The physics models were expected to capture most control relevant behaviours of the engine *i.e.* in-cylinder pressure evolutions, in-cylinder temperature and combustion timing. The following step was to develop the cycle-to-cycle model in order to investigate the most important insights of NVO HCCI engine control, *i.e.* the residual gases cyclic coupling, self-stabilising nature and the NVO modulation of gas composition. Afterwards, the models would be extended with a simplified vehicle driveline model to carry on the investigation of valve timing control strategy and dynamic process analysis.

1.5 THESIS CONTRIBUTIONS

In the thesis, the developments of HCCI research are studied and a number of different modelling approaches are reviewed in order to develop the new HCCI engine models for control strategy developments. The simplified simulation models are developed and implemented to predict the effects of the NVO system on the HCCI combustion. By utilising the Arrhenius rate equations and Wiebe functions, the single-zone models capture the most control related behaviours of HCCI engine. Through the comparisons, the simulation studies show general good agreements with experiments of in-cylinder pressure evolutions, the combustion timings and the peak pressure values. The developments of cycle-to-cycle model demonstrate the capability of the model to predict the dynamic behaviours of NVO HCCI process. After extending the simulation models with vehicle driveline model, a number of valve timing strategies are investigated and the dynamics of operation changing points are captured as well. With minor modifications, the modelling approach is able to capture the thermal dynamic behaviours of scroll motor. The validations exhibit that single-zone models are capable for different dynamics system analysis. The contributions are summarised as follows:

NVO HCCI engine models

The model captures the most control relevant behaviours of HCCI engines, include: rates of pressure/temperature rise, combustion timing, in-cylinder pressure/temperature evolutions and work outputs. The HCCI combustion process is simulated by Arrhenius rates and Wiebe functions for propane fuelled and gasoline fuelled engine separately. Genetic Algorithms (GAs) is applied to identify and optimise the unknown parameters for the gasoline HCCI combustion simulation. The inherent simple structures offer that the

simulation run times are at between 0.05 and 0.1 seconds for one completed engine cycle of gasoline and propane HCCI separately.

Engine and vehicle dynamic modelling

The engine models are extended for cycle-to-cycle simulations to investigate the HCCI dynamics behaviours, including: the cyclic in-cylinder pressure evolution, combustion timing, work output and residual gas coupling. The simulation studies indicate the key insights of the nature of HCCI can be predicted by the models - modulation of inducted gas composition, the self-stabilise nature of HCCI engine adopting negative valve overlap scheme and the cycle-to-cycle coupling. The investigations of these important characterises not only indicate that the model can be applied for control strategy testing, but also provide important clues for control strategy design.

A simplified driveline model and a PID controller are developed and integrated into the system to test the valve timing control strategy. The simulation studies demonstrate that the engine power output can be controlled by tuning the intake and exhaust valve timing. A certain range of intake/exhaust valve timing pairs is investigated for obtaining the operation boundary condition. The studies also indicate that although the HCCI process can be controlled by tuning the timings of IVO and EVC, more controllable factors must be considered into the controller design for extending the operation window of HCCI engine, such as boosting the intake pressure, advanced thermal management of the engine, variable compression ratio.

1.6 THESIS OUTLINE

The thesis is organised as follows:

Chapter 2 gives an overview on the developments of HCCI engine research. The technologies for HCCI combustion control are introduced, such as variable compression ratio, variable induction temperature and variable valve timing (VVT). And an overview of a wide variety of HCCI engine modelling is given where the approaches are categorised by the types of modelling methods and the levels of complexity.

Chapter 3 covers the development of a propane fuelled HCCI engine model that the valve motion is modulated as NVO scheme. The Arrhenius-type relations are used to describe the combustion. The influence of valve timing and intake temperature has been investigated. The simulation model is validated against the experimental results from a single cylinder HCCI research engine.

Chapter 4 formulates an accurate, simple and intuitive model of the gasoline HCCI process. The simulation shows the model can real-timely capture the response of the system outputs, which are most relevant to the control problem: combustion timing, in-cylinder pressure evolution, gas temperature and work output. The model uses Wiebe function to describe the combustion process and uses GAs to identify the unknown parameters in the segment of the combustion process. Subsequent validation with variety engine operations shows that the model is capable of reproducing the engine cycles of gasoline HCCI process.

Chapter 5 develops the cycle-to-cycle engine modelling. With the simulation results, the key characteristics of NVO HCCI engine are

discussed, which include: the residual gas coupling between subsequent engine cycles; the self-stabilising behaviour; the modulation of gas composition. The engine model is extended with a vehicle driveline dynamics model for HCCI control strategy investigation. The simulation studies demonstrate the vehicle velocity can be controlled by modulating IVO and EVC. Furthermore, the operating range of valve timing control is investigated.

Chapter 2

OVERVIEW OF HCCI ENGINE RESEARCH

This chapter gives an overview of HCCI engine research which is essential for understanding HCCI – the next generation IC engine. In the chapter, the first section introduces the developments of HCCI engine, which covers the time period from very earliest concept to the latest demo car. The key technologies of HCCI control are then introduced, which focus on the field of four-stroke HCCI engine control. A wide variety of numerical modelling approaches for HCCI engine are reviewed and categorised in the last section, according to the variety types of modelling methods and the levels of complexity.

2.1 DEVELOPMENTS OF HCCI ENGINE

The earliest HCCI concept can be traced back to the end of 19 century, when Herbert Stuart established the hot bulb engine that used a hot vaporisation chamber to help mix fuel with air. The extra heat combined with

compression induced the conditions for combustion to occur. However, it was not until 1979; that the first application of HCCI had been introduced into modern IC engine by Onishi, *et al.* [13]. They applied the HCCI process to the two-stroke engines that were named Active Thermo-Atmosphere Combustion (ATAC) engine. Concurrently, the same phenomena was observed by Noguchi, *et al.* [14], which named as Toyota-Soken (TS) combustion. They concluded that new lean combustion process could be applied most easily to two-stroke cycle gasoline engines; stable combustion occurred at low load over a wide speed range; the fuel consumption and exhaust emissions are remarkably improved together with the reduced noise and vibration. And several of the key characteristics of HCCI combustion were identified, including the importance of achieving necessary levels of hot residual to achieve auto-ignition, uniform mixing between residual combustion products and reactant, and repeatable presence of residual gases on a cycle-to-cycle basis.

Furthermore, Najt, *et al.* [6] were able to achieve HCCI combustion in a four stroke engine in 1983. The engine used a pancake combustion chamber with a shrouded valve. Experiments were performed with blends of paraffinic and aromatic fuels over a range of engine speed and dilution levels. The process was analyzed, considering that HCCI is mainly controlled by chemical kinetics excepting negligible influence from physical effects, first of all turbulence and mixing. In the development process, a simplified kinetics model was used to predict heat release as a function of pressure, temperature, and species concentration in the combustion chamber. This assumption permitted to show that the HCCI combustion could be divided into two semi independent processes - ignition and energy release: HCCI auto-ignition is controlled by the same low temperature chemistry leading to knock in SI engines. The energy release is controlled by the high temperature chemistry, dominated by *CO* oxidation [6].

Based on Najt's work, Thring, *et al.* [15] examined the use of a gasoline fuel in 4-stroke HCCI engine. Experiments were undertaken on the engine using the conventional SI operation at high loads and HCCI at part loads (SI-HCCI). The performance of the HCCI engine operated with fully blended gasoline and diesel fuel with possible combinations of λ and Exhaust Gas Recirculation (EGR) were examined. It claims that a low compression ratio was necessary to be used in a diesel engine [16], since auto-ignition occurred too early during the compression stroke. Also studies of the HCCI combustion with diesel fuel, illustrate that successful operation with EGR rates in the range from 0 to 50 %. The experiments with pre-chambered ceramic-heat isolating combustion chamber have also been carried out [17]. A standard 1.6 litre VW SI engine was converted and adopted to HCCI mode in 1992 [18]. The tests demonstrated the part load efficiency was higher up to 34%. Aoyama, *et al.* [19] compared the auto-ignition conditions with Premixed Charge Compression Ignition (PCCI) engine and diesel engine, and the a PCCI diesel engine had been compared with a Gasoline Direct Injection (GDI) engine at optimum λ. The investigations shown that PCCI engine has the lowest fuel consumption and NO_x emissions, but relatively higher *HC*. Gentill [20] optimised HCCI combustion process at the time of ignition by means of throttling either the exhaust or inlet duct. The research indicated that the combustion timing was advanced and the burn duration decreased when the engine was operated with the orifice plates on the transfer ports [17].

In 2001, Kong, *et al.* [21], examined the phenomena that the turbulence affects the rate of HCCI combustion. Zhao, *et al.* [22, 23] investigated the effects of residual gas and fuel distribution on a multi-cylinder Controlled Auto-Ignition (CAI) engine in 2001 and 2002. The cylinder head had intake ports with high swirl ratio and correspondingly large gradients were observed in the fuel distribution inside the cylinder. The conclusion drawn

from those experiments was that the main effect of residual gas on HCCI auto-ignition was thermal, and that the primary influence of charge dilution was on the combustion chamber [23]. Also the impact of residual gas and in-homogeneity of charge on HCCI combustion process of natural gas was precisely investigated by Morimoto, *et al.* [24]. It performed series of experiments *i.e.* influences of EGR and in-homogeneity on combustion control. All experiments were performed on a single cylinder engine with compression ratio 16 supplied by means of methane and propane as a fuel. The experiments rely on comparison between engine performances when the engine was supplied by fuel injected upstream homogeneously and by the fuel injected closer to the intake port – in-homogeneously. After many series of experiments and engine model simulations it was concluded that the combustion phasing was insensitive to in-homogeneity, but the emissions of NO_x rapidly increase with increasing un-mixedness [17]. In 2002, the experiments were performed in order to study the effect of turbulence on HCCI combustion process by Christensen, *et al.* [25, 26]. Different turbulence levels were created by changing the detachable piston crown thereby combustion chamber geometry and swirl ratios. It was concluded that influence of mixture motion and turbulence on HCCI auto-ignition and combustion is low as compared to SI and CI combustion because HCCI combustion process is a reaction zone where the entire charge is gradually consumed almost at the same time. In 2003, Agrell, *et al.* [27] used valve timings to effectively alter the compression ratio and control combustion timing. Bengtsson *et al.* [28] modulated the fuel amount to vary the work output while altering the mixture ratio of two fuels to control combustion timing. Further investigations [29] were initiated by using compression ratio instead of fuel mixture to shift combustion timing. These researches indicated the usefulness of effective compression ratio and inducted gas composition as control inputs for HCCI [17].

Currently, in automotive industry, General Motors (GM), Ford, Nissan, Honda, Toyota and Volkswagen are all working on HCCI engines, although it has not been reported that when the HCCI engine would actually become a full production real life. Honda and Nissan demonstrated their commercially available engines running in HCCI mode over part of their duty cycle. Active Radical (AR) engine from Honda is a dual-mode two-stroke engine that was reported the fuel consumption is at least 27% better than a normal two stroke engine [30]. In 2005, Honda Car Ltd announced that significant progress had been made on HCCI engine for hybrid applications. The advanced technology claim up to 65% fuel consumption reduction. The "Modulated Kinetics" (MK) system, developed by Nissan [31], incorporates in a regular Compression-Ignition-Direct-Injection (CIDI) engine using diesel fuel. At light load, the engine operates with high swirl, high EGR, and retarded injection timing. Under these conditions, the time required to achieve nearly complete mixing is shorter than the time required for fuel auto-ignition. Therefore, near-homogeneous combustion occurs. At these low loads, the equivalence ratio is low; therefore, the homogeneous combustion results in extremely low NO_x and particulate matter emissions. The new generation MK engine was announced as part of Nissan Green Program 2010 in order to achieve cleaner diesel emission for meeting California's standard for Super-Ultra-Low Emission Vehicles (SULEVs). In 2008, GM started to test HCCI engine on road. It is the first time that HCCI engines are fitted in driveable production vehicles where the HCCI gasoline engines operate in SI-HCCI-SI mixed mode. The engines were set up to use SI when starting, driving over 55 mph or higher loads and revert to HCCI when loads are lower and over certain temperature conditions. At least 15% fuel benefits achieved with additional help from direct injection, variable valve lift, dual electric camshaft phasers and individual cylinder pressure transducers to control the combustion as well as deliver a smooth transition between combustion modes.

2.2 HCCI CONTROL TECHNOLOGIES

As discussed in Chapter 1, controlling HCCI is a major hurdle to more widespread commercialization. HCCI is more difficult to control than conventional SI and diesel. In a SI engine, a spark is used to ignite the pre-mixed fuel and air. In Diesel engines, combustion begins when the fuel is injected into compressed air. In both cases, the timing of combustion is explicitly controlled. In an HCCI engine, however, the homogeneous mixture of fuel and air is compressed and combustion begins whenever the appropriate conditions are reached. This means that there is no well-defined combustion initiator that can be directly controlled. Engines can be designed in such a way that the ignition conditions occur at a desirable timing. To achieve dynamic operation in an HCCI engine, the control system must change the conditions that induce combustion. Thus, the control system must control either the compression ratio, inducted gas temperature, inducted gas pressure, fuel-air ratio, or quantity of retained or re-inducted exhaust. Several existing control approaches are discussed below.

2.2.1 VARIABLE COMPRESSION RATIO (VCR)

Since HCCI combustion is strongly affected by the compression ratio of the engine, a VCR engine has the potential to achieve satisfactory operation in HCCI mode over a wide range of conditions because the compression ratio can be adjusted as the operating conditions change. There are several methods of modulating both the geometric and effective compression ratio, where the effective compression ratio can be reduced from the geometric ratio by VVT which will be introduced in later section. The geometric compression ratio can be changed with a movable plunger at the top of the cylinder head whose position can be varied to change the compression ratio [32]. The compression ratio could also be varied by using an opposed-piston

engine design having variable phase-shifting between the two crankshafts [12]. Szybist, *et al.* [33] used a hydraulic cylinder to rotate the crankshaft cradle where the crankshaft is mounted eccentrically, changing the crankshaft centreline height, and thus the cylinder clearance volume and compression ratio. The experiments shown that the VCR system is capable of controlling HCCI ignition timing to maintain optimal combustion phasing across a very wide range of intake temperatures and fuel types of varying octane number with sufficiently fast response time.

2.2.2 VARIABLE VALVE ACTUATION (VVT)

VVT has been proven to extend the HCCI operating region by giving finer control over the temperature-pressure-time history within the combustion chamber. One application of VVT is to change the trapped compression ratio of the engine (i.e., the amount of compression after the gases are trapped by intake-valve closure), and therefore VVT can achieve a similar effect on HCCI combustion as varying the geometric compression ratio of the engine. An engine could be built with a high geometric compression ratio, with lower trapped compression-ratios being obtained by delaying the closing of the intake valve during the compression stroke. Also engines with VVT have the added benefit of allowing changes in the temperature and composition of the incoming charge by retaining hot residual gases from the previous cycle in the cylinder. By varying the amount of hot residual, the temperature and mixture of the new charge can be adjusted. Increasing the temperature of the charge in this manner can be used to induce HCCI combustion even with relatively low geometric compression ratios or under cold-engine conditions. In addition, altering the charge composition with partial mixing of the residual could benefit combustion rate control [34, 35]. Compared with VCR, VVT is relatively cheaper and less complicated. If the the desired VVT

characteristic is known, then it is relatively simple to configure such systems to achieve the necessary control over the valve lift curve [36].

2.2.3 Engine Thermal control

The possibility also exists to control HCCI combustion by controlling the temperature, pressure, and composition of the mixture at the beginning of the compression stroke. Here, thermal energy from EGR and compression work from a supercharger are either recycled or rejected to obtain satisfactory combustion [37]. The main advantage of this method is its simplicity, since it does not require major engine modifications or use of fuel additives. The disadvantage of this method is that it may be too slow to react to the rapidly changing conditions that typically exist in transportation applications [36]. A full transient response analysis of this type of system had performed in [38].

2.2.4 Other control approaches

HCCI engine control could be achieved by using two fuels with different octane ratings [39-42]. The system could be designed to have a main fuel with a high octane number, while the secondary fuel, with a low octane number, is injected as needed to advance combustion. This procedure has recently been studied for a combination of methane and dimethyl ether (DME) [40, 41]. However, this method typically requires carrying and refilling two fuel tanks. Ideally, the amount of the secondary fuel being consumed would be minimal, and the tank could be re-fuelled only at the maintenance intervals. Flowers, *et al.* [43] and Persson *et al.* [35] demonstrated combustion timing is controllable via varying intake temperature. The auto-ignition event is highly sensitive to temperature. They used either resistance heaters to vary the inlet temperature or mixing hot and cold streams to rapidly vary the cycle to cycle intake charge temperature.

However the system is also expensive to implement and has limited bandwidth associated with actuator energy.

2.3 HCCI MODELLING APPROACHES

Depending on different types, HCCI engine models are not only used for understanding the physical phenomena that occur in HCCI engine, but also able to validate and test the control strategy. This section gives an overview of a wide variety of HCCI engine modelling where the approaches are categorised by the types of modelling methods and the levels of complexity as follows:

1. Single-zone, zero-dimension models.
2. Multi-zone, quasi-dimension models.
3. PDF models.
4. Cyclic simulation models.
5. CFD, multi-dimension models.
6. Other modelling approaches.

2.3.1 SINGLE-ZONE, ZERO-DIMENSION MODELS

Models of this type utilise a single-zone approach to modelling the in-cylinder gases. There are a large number of efforts in this area [22, 44-51]. Most of the single-zone models are very similar: The first law of thermodynamics is applied to a homogeneous mixture of in-cylinder gases and the properties of gases in a closed-volume are evaluated from IVC to EVO. The composition of the gases are either determined with standard valve flow relations or through approximation from steady state experiment. The volume change of the combustion chamber is described by a slider-

crank model. Assumptions that are often made are that the effects of the fluid mechanics are not directly considered except, in some cases, when deriving relevant heat transfer coefficients that is often calculated by applying Woschni's correlation. The heat loss is usually based on the difference of the average wall temperature and gas temperature. The blow-by and radiation heat losses are negligible, the only heat losses occur due to convection affecting the whole volume equally.

The zero-dimensional approaches are benefited from their inherently simplicity and relatively short calculation times by homogeneity assumption of the in-cylinder gases. The aforementioned models can capture main HCCI engine outputs, including work output, combustion timing and peak in-cylinder pressures. However, since the homogeneity assumption has been made, near wall/piston quenching effects are difficult to capture [52], leading to inaccurately predicting emissions and completeness of combustion. Additionally these approaches can not capture the mixing process during induction.

2.3.2 MULTI-ZONE, QUASI-DIMENSION MODELS

A wide variety of modelling approaches are reported in [53-63], where the cylinder is divided into different zones for analysis. The definitions of the zones are varied by different analysis methodologies, *i.e.* the types of zones include core zones, boundary layers, crevices and mass exchange zones; the types of interaction that occur between zones; the types of heat transfer models. The number of zones could be different from as small as 2 to as large as 30 [54, 56, 59]. Generally, the model becomes more accurate with an increasing number of zones, but calculation times become significantly longer as well [56]. The number of zones in a multi-zone model is still much smaller than the number of cells in a CFD mesh. The rationale for adapting a

multi-zone model instead of a single-zone model is that the multi-zone model can account for the mixture in-homogeneity present in the combustion chamber. Thus, multi-zone models usually consist of a number of core zones with different initial temperatures, equivalence ratio and EGR rates [58, 61, 64], but they are often difficult to choose. Some researchers use CFD modelling to calculate initial values for multi-zone models [62-65]. One solution is to perform a multi-dimensional CFD simulation prior to the multi-zone calculations, and to use the parameter distributions obtained from the CFD results as input for the zones in the multi-zone model [52, 66]. The best method [52] is to represent the engine geometry by a 3-D mesh and to include the gas exchange process in the CFD calculations as well, since this allows the mixture in-homogeneity present in the cylinder during the compression stroke to be captured [63, 64, 67]. Simulating the gas exchange process is important for HCCI combustion based on internal EGR trapping, since the mixing of a large fraction of high temperature internal EGR and low temperature inducted reactants gives rise to greater mixture in-homogeneity than is the case for HCCI-types without internal EGR [68, 69]. For cases in which minor fractions of EGR are used and direct-injection takes place after IVC, it might not be necessary to evaluate the gas exchange processes by means of CFD and the mixture can be assumed to be homogeneous at IVC. This might explain why some researchers have started CFD simulations at IVC, assuming a uniform mixture, before switching to a multi-zone model just before auto-ignition is expected [53, 70]. Furthermore, by applying a 2-D CFD mesh, if the gas exchange processes are not taken into accounts, the simulation time may be reduced.

Compared with single-zone model, the advantage of multi-zone models is that they can be applied to predict more accurate heat release curves than single-zone models. The influences of the distribution of zones, heat transfer from the wall, mass and heat exchange between zones and boundary layer

thickness and temperature stratification can be considered [55]. Thus, the formation of emissions can also be modelled. To this end, many multi-zone models contain zones representing crevices and boundary layers as well as mass exchange zones [17, 52]. Thus, the multi-zone model is capable to predict and investigate the operating range for different engine speeds by changing initial temperature and equivalence ratio – the two critical factors for expanding the operating range of HCCI engines [61]. In some models, the boundary layers can exchange mass with both the crevices and a mass exchange core zone to model the trapping of unburned mixture in relatively cold regions near the end of the compression stroke [57, 63, 64]. The different zones in the model interact with each other in several ways. Most models calculate the pressure-volume workout that indicates that the compression or expansion of one zone influences the other zones. As which mentioned above, the mass exchange between certain zones can be implemented to account as well. Core zones do not usually exchange mass with each other and most models do not consider the heat transfer between zones, because it has been shown that HCCI combustion is very fast for heat transfer to have a significant effect [53].

Overall, Multi-zone models is overcome more advantage than single-zone counterparts, since they can represent the in-homogeneity present in the cylinder prior to combustion [67, 69]. The multi-zone quasi-dimensional thermo-kinetic models can be used for emission analysis and lead to a considerable improvement of combustion prediction, albeit at the expense of increased modelling complexity and long computation time.

2.3.3 PDF MODELS

Apart using a multi-zone model to account for in-homogeneities gases in the combustion chamber, a number of researchers [65, 66, 71-75] attempt to

simulate the HCCI process by a Probability Density Function (PDF). There are some widely used methodologies to calculate time-average values for variables such as species concentrations and temperature for engine modelling, for example, Reynolds-averaged Navier–Stokes (RANS) equations. On the other hand, the effects of variable fluctuations are accounted by PDF models at a sub-grid level: PDFs can be applied to describe the range of possible values and to calculate the corresponding probabilities for a fluctuating variable [66, 76]. The parameters used for combustion modelling are typically the species mass fractions, as well as the temperature and combustion velocity. As an alternative to solve RANS equations, a transport equation for the Joint PDF can be formulated similarly with typical RANS equations for combustion cases. It contains a convection term, a diffusion term, a term representing small-scale mixing and a chemical source term [77]. When the number of species is large, it becomes impractical to solve the transport equation for the Joint PDF by means of a finite-difference or finite-volume technique. Instead, the so-called Monte-Carlo method is frequently used [65, 73, 78]. Examples of micro-mixing models used in practical simulations are the Curl model [79] and models based on interaction by exchange. Some PDF based models describe the combustion chamber as a single cell containing 100 particles [66]. in this case, Mass density functions (MDFs) were applied instead of classic PDFs to account for the variable density [52]. In a single-cell approach, the convection and diffusion terms were neglected, while terms describing heat losses and piston motion were added. By using Curl's approach [80], the mixing term was modelled, while the heat transfer to the walls was simulated by Woschni model incorporating stochastic fluctuations. The calculation time for two engine cycles in the literature was seven hours on one processor using 100 particles and a reaction mechanism consisting of 157 species and 1552 reactions [75]. The model managed to accurately predict emissions of

HC, *CO* and *NOx*, as well as the cylinder pressure trace during combustion [72, 74].

The PDF models allow the effects of in-homogeneity on auto-ignition process can be explicitly captured. The main advantage of PDF applications over using RANS equation is the ability to predict emission accurately although calculation times are significant long.

2.3.4 CYCLIC SIMULATION MODELS

One major disadvantage of aforementioned models is that they can only evaluate the processes in the combustion chamber during the intervals when the valves are closed. The models usually start calculating from intake valve close (IVC) and stop at exhaust valve open (EVO). This means that initial values of parameters have to be specified at IVC *i.e.* average mixture temperature, equivalence ratio and EGR rates, and they are hard to choose. To solve this problem, those models can be combined with engine cycle simulation codes that can predict the desired values at IVC [60, 73, 81-84]. These codes are often one dimensional, predicting result for the complete engine flow system from air intake to exhaust pipe. Since the results are calculated for the complete engine cycle, gas exchange processes are modelled as well. As there are a variety of different combustion models implemented in the cycle simulation code, the completed cyclic model can be attempted accordingly, at a number of levels of complexity. It is possible to implement simplified models [81], single-zone models [85, 86] or multi-zone models [54, 60, 77, 84, 86-88]. For instance, the simple models have been reported [89, 90], in which the auto-ignition timing are predicted by using temperature threshold and Livengood-Wu auto-ignition integral [91]; the combustion duration is specified by an algebraic equation or the Wiebe function.

Engine cycle simulation is able to provide initial conditions for CFD modelling [21, 67, 69, 92, 93]. Ideally, a one-dimensional cycle simulation code is applied with a combustion model based on detailed kinetics, to predict boundary conditions of HCCI combustion, which are reported in [45, 94]. Typical boundary conditions are the pressure and temperature in the intake and exhaust ports for CFD calculations that include the gas exchange processes. When the CFD simulation starts at IVC, the cycle simulation code can provide average values for the mixture temperature, RGF and equivalence ratio. It is also possible to integrate three different modelling techniques, for example, Koopmans *et al.* [68] used results from detailed-chemistry cycle-simulation code runs as boundary conditions for motored, 3-D CFD calculations. These CFD simulations evaluated the gas exchange processes as well as part of the compression stroke, after which the predicted in-cylinder distributions were used to specify initial values for detailed-chemistry, single-zone and multi-zone calculations. The switch from the CFD simulation to the single-zone or multi-zone calculation was made near the end of the compression stroke [45, 95], when chemical processes are still slow [52].

2.3.5 MULTI-DIMENSIONAL CFD MODELS

Computational fluid dynamics (CFD) is one of the branches of fluid mechanics that uses numerical methods and algorithms to solve and analyse problems which involve fluid flows. Computers are used to perform the millions of calculations required to simulate the interaction of fluids and gases with the complex surfaces used in engineering. For example, it takes weeks to carry out a calculation with a detailed-chemistry model, which would be necessary for accurate HCCI modelling [96].

Winter *et al.* [97] carried out a 3-D modelling which adopted both a detailed reaction mechanism for *n*-heptane and a reduced mechanism approach. The reduced model assumed the low and intermediate temperature chemistry to consist. Researchers who have used 2-D models have implemented reaction mechanisms ranging from simple chemistry that is a four-step reaction model for low temperature oxidation [98] to reaction mechanisms including approximately 100 species and 500 reactions [99, 100] of eight reactions, while modelling the high temperature hydrocarbon oxidation process as a single-step process. With both approaches a good match with measured cylinder pressure was obtained, when applying a mixing-controlled combustion model. Kong *et al.* [21] also included the effect of turbulent mixing on combustion chemistry as well.

Generally, as the most complex and computationally intensive methodology, multi-dimensional CFD models have the highest potential for predicting the combustion by the combination of applying the detailed-chemistry approaches and the geometry of the combustion chamber is resolved in full details [97, 101]. However, as the fact, the combustion process may involve a large number of species participate in an even greater number of elemental reactions during the oxidation of hydrocarbons. Including all these species and reactions in a detailed reaction mechanism leads to unacceptably long calculation times. More research work [95, 96, 102] has been focused on reducing the complexity of the reaction mechanism.

2.3.6 OTHER MODELLING APPROACHES

Martinez-Frias *et al.* [37] developed an engine model including a detailed-chemistry, single-zone combustion model as well as models for different components, such as a pre-heater, supercharger and intercooler. Flowers *et al.* [103], combined a multi-zone model and a CFD code, as a optimised

HCCI modelling approach. In their approach, the two codes calculated in parallel during the compression and expansion strokes. At each time step, the CFD code accounted for fluid dynamics, while the multi-zone model performed the detailed-chemistry calculations. Information transferred between the two codes took place at each time step. The advantage with this approach was that the fluid mechanics processes were calculated on a highly resolved grid, while the much more computationally intensive chemical kinetics processes could be solved for a limited number of computational zones. Furthermore, the prediction of hydrocarbon and *CO* emissions improved significantly compared with the previous model [64, 104]. This was due to the mixing of fluid from burnt mixture and cold unburned mixture zones during the expansion process, by means of the CFD code that accounted for fluid mechanics. As a result, fuel and intermediates from cold, partially burnt regions diffused to hotter regions during expansion. The fuel might then have reacted partially, after which reactions were quenched due to the low temperature [52].

Shaver *et al.* [105] investigated three methods to predict auto-ignition timing; a temperature threshold, an integrated threshold based on both temperature and species concentrations and a model utilizing a two-step kinetic mechanism. The last two methods predicted combustion phasing well and the second method was preferred due to its simplicity [106, 107].Without detailed-chemistry, the Livengood-Wu auto-ignition integral [91], provides a simple and fast way of predicting auto-ignition timing. The model input consists of an expression for the ignition delay, which is used to calculate the ignition delay time at each moment during the compression stroke. Ryan and Callahan presented a relationship with five constants and the variables oxygen concentration, fuel concentration, density and air temperature [16]. Agrell *et al.* calculated ignition delay times using an Arrhenius correlation including pressure, temperature and three constants

[81]. Qin [88], *et al.* reported that by using s-curve fitting, the heat release process was modelled in a simple way. The heat release is based on a single zone model where empirical expressions are applied. The disadvantage of Qin's method is that it may need to re-tune or re-calibrate if the codes are applied for other applications.

Chapter 3

PROPANE FUELLED HCCI ENGINE MODELLING FOR CONTROL

The detailed models of HCCI combustion have been developed by using detailed chemistry to capture the combustion process and the chemical kinetics, such as multi-zone models, multi-dimension CFD model and flame spread etc. These models offer the capability for accurately predicting the overall process of HCCI combustion, in particular the chemical kinetics and the emissions. However these models are often far too detailed for control strategy development or validation.

Instead of modelling every aspect of the engine cycle, this chapter covers the development of a propane fuelled HCCI engine model that the valve motion is modulated as negative valve overlap scheme. The simplified HCCI engine model that is to just the necessary factors for control purpose, such as combustion timing, in-cylinder gas temperature and in-cylinder pressure evolutions. The Arrhenius-type relations are used to simulate the combustion.

The simulation model is validated against the experimental results from a single cylinder HCCI research engine.

3.1 STRUCTURE OF THE MODEL

The modelling work is based on the first law of thermodynamics for an open system, the model includes ten states, namely, the cylinder volume, V, the in-cylinder temperature T, the concentrations of propane $[C_3H_8]$, oxygen $[O_2]$, nitrogen $[N_2]$, carbon dioxide $[CO_2]$, water $[H_2O]$ and carbon monoxide $[CO]$, crank angle θ, and in-cylinder pressure P. For perform HCCI combustion, the engine adopts negative valve overlap scheme to trap certain level internal energy in the cylinder. Based on that structure, the modelling procedure partitioned into seven stages during a completed engine cycle (Figure 3-1):

1. Residual gas expansion: the residual combustion products are expended from TDC to IVO.
2. Intake: the air/fuel mixtures are injected into the cylinder and mixing with residual products from IVO to IVC.
3. Compression: the residual products and the fresh reactants are mixing and compressed from IVC to TDC
4. Combustion: auto-ignition and combustion occurred after TDC
5. Expansion: combustion products are expended from TDC to EVO.
6. Exhaust: combustion products are exhausted from EVO to EVC.
7. Residual gas compression: the residual combustion products are compressed from EVC to TDC.

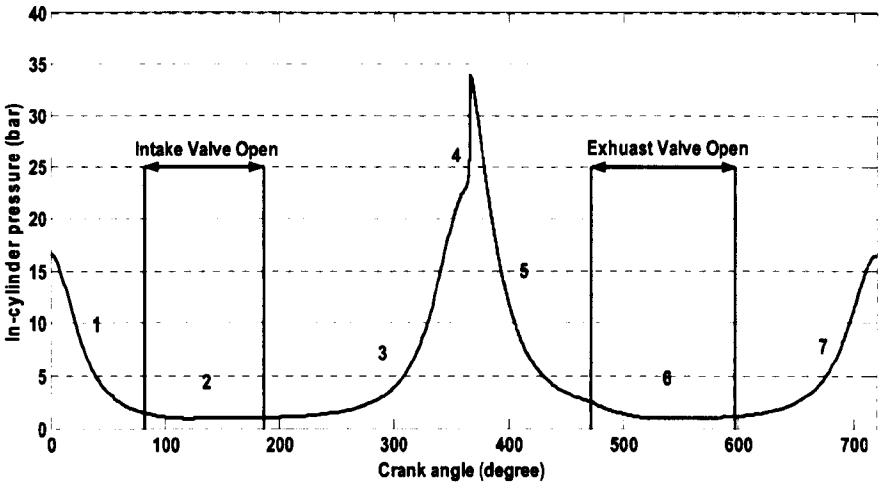

Figure 3-1 Framework of completed engine cycle

3.2 DESCRIPTION OF CYLINDER GEOMETRICS

Based on the geometry analysis of reciprocating engine, some basic geometrical relationships and the parameters commonly used to characterise HCCI engine had been developed for modelling. The equations from 3.1 to 3.7 define the basic geometry of a HCCI engine cylinder. Figure 3-2 shows general cylinder geometric details and Figure 3-3 also shows the general shape of the cylinder volume and surface profiles used for the experimental validation of the simulation model.

$$r_c = \frac{V_d + V_c}{V_c} \tag{3.1}$$

where r_c is compression ratio.

V_d is the displaced volume.

V_c is the clearance volume.

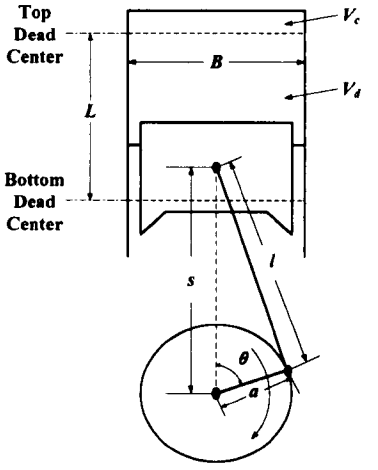

Figure 3-2 Cylinder geometrics diagram

The cylinder volume V at any crank position θ is:

$$V = V_c + \frac{\pi B^2}{4}(l + a - s) \tag{3.2}$$

where B is cylinder bore.

l is connecting road length.

a is crank radius.

θ is crank angle.

s is the distance between the crank axis and piston pin axis.

It is given by equation 3.3:

$$s = a\cos\theta + (l^2 - a^2\sin^2\theta)^{1/2} \tag{3.3}$$

And its derivative is related by:

$$\dot{V} = \frac{\pi}{4}B^2 a\dot{\theta}\sin\theta\left(1 + a\frac{\cos\theta}{\sqrt{(L^2 - a^2\sin^2\theta)}}\right)$$

where a is the half of stroke length.

$\dot{\theta}$ is the rotational speed of the crankshaft.

The combustion chamber surface area can be approximated by:

$$A_s \cong \frac{\pi}{2}B^2 + \pi Ba\left[R+1-\cos\theta+(R^2-\sin\theta)^{0.5}\right], \tag{3.5}$$

where A_s is the surface area of cylinder.

An important characteristic speed is the mean piston speed $\overline{S}_p$:

$$\overline{S}_p = 2L\dot{\theta} \tag{3.6}$$

Mean piston speed is often more appropriate parameter than crank rotational speed for correlating engine behaviour as a function of speed [108]. The instantaneous piston velocity S_p is obtained from:

$$S_p = \frac{ds}{dt} = \frac{\pi}{2}\sin\theta[1+\frac{\cos\theta}{(R^2-\sin^2\theta)^{1/2}}]\overline{S}_p \tag{3.7}$$

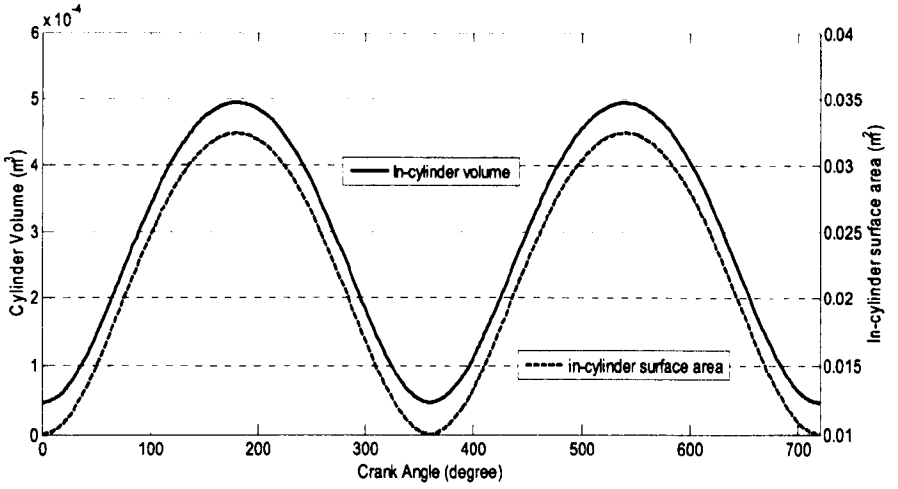

Figure 3-3 In-cylinder volume and surface area

3.3 DESCRIPTION OF MASS FLOW IN/OUT OF THE CYLINDER CHAMBERS

In the thesis, equations for the mass flow rates are developed using a compressible, steady state, one-dimensional, isentropic flow analysis for a restriction, where real gas flow effects are included by means of a discharge coefficient, C_D.

$$C_D = \frac{actual\ mass\ flow}{ideal\ mass\ flow} \tag{3.8}$$

The instantaneous valve flow area depends on valve lift (Figure 3-4) and the geometric details of the valve head, seat, and stem. Due to the constant opening and closing of the valves, the cross sectional area through which the flow passes through changes. This area is referred to as the effective area A_e that is determined by the valve profile and the position of maximum opening point (MOP). The MOP for the intake valve is with reference to (after) the conventional induction TDC (ATDC) and for the exhaust valve it is with reference to (before) the conventional combustion TDC (BTDC) [109]. Since the geometric minimum flow area is a complex function of valve and valve seat dimensions. In this report, the most convenient reference area, A_c the curtain area and the discharge coefficient C_D are linked together to assume the effective area that is defined as:

$$A_e = A_c \cdot C_D \tag{3.9}$$

$$A_c \approx \pi \cdot D_V \cdot L_V \tag{3.10}$$

The discharge coefficient varies with the crank angle and usually is determined experimentally. This coefficient accounts for the real gas flow effects. The discharge coefficient decreases slightly with lift since the jet fills

less of the reference curtain area as it transforms from an attached jet to a separated free jet [1].

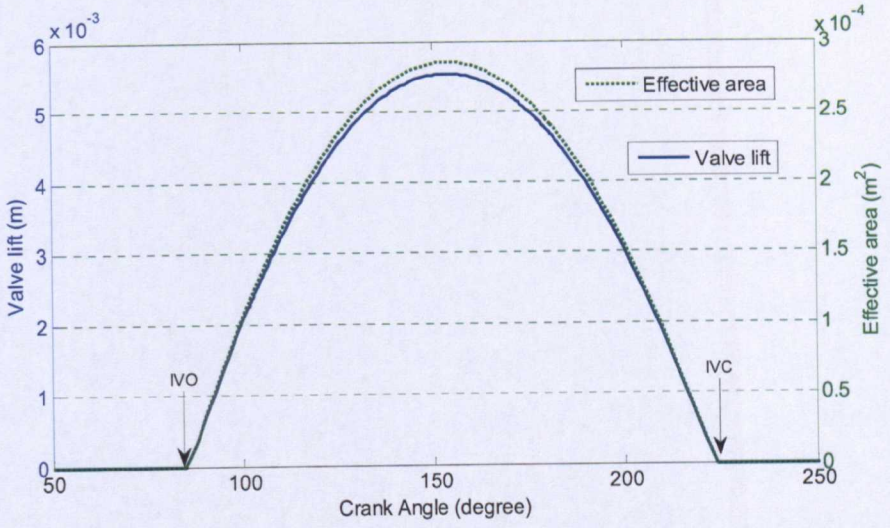

Figure 3-4 Valve profile used for experimental engine testing

The mass flow rate through a valve is usually described by the equations 3.11 and 3.12 for compressible flow through a flow restriction:

for un-choked flow ($P_T / P_0 > [2/(\gamma+1)]^{\gamma/(\gamma-1)}$):

$$\dot{m} = \frac{C_D A_C P_0}{\sqrt{RT_0}} \left(\frac{P_T}{P_0}\right)^{1/\gamma} \left[\frac{2\gamma}{\gamma-1}\left[1-\left(\frac{P_T}{P_0}\right)^{(\gamma-1)/\gamma}\right]\right]^{1/2} \tag{3.11}$$

for choked flow ($P_T / P_0 \leq [2/(\gamma+1)]^{\gamma/(\gamma-1)}$):

$$\dot{m} = \frac{C_D A_C P_0}{\sqrt{RT_0}} \sqrt{\gamma} \left[\frac{2}{\gamma+1}\right]^{(\gamma+1)/2(\gamma-1)} \tag{3.12}$$

where P_0 is upstream stagnation pressure.

P_T is downstream stagnation pressure.

T_0 is the downstream stagnation temperature.

R is mixture gas constant.

γ is the specific heat ratio.

3.4 HEAT TRANSFER ANALYSIS

The peak burned gas temperature in the cylinder of an internal combustion engine is of order 2500 K. However the maximum metal temperatures for the inside of the combustion chamber space are limited to much lower values by a number of considerations, and cooling for the cylinder head, cylinder and piston must be provided. In regions of high heat flux, thermal stresses must be kept below levels that would cause fatigue cracking, so that the temperatures must be less than about 700 K for cast iron and 600 K for aluminium alloys. The heat transfer is usually presented as conduction, convection and radiation. For simplified modelling and due to the steady-flow assumptions, only convection heat transfer is considered into the model. In convection heat transfer, heat is transferred though fluids in motion and between a fluid and solid surface in relative motion. When the motion is produced by forces other than gravity, the term forced convection is used. The heat is transferred by forced convection between the in-cylinder gases and the cylinder head, valves, cylinder wall and piston during induction, compression, expansion and exhaust processes [36, 108].

Newton determined that the heat transfer rate, $\frac{\dot{Q}}{A_S}$, is proportional to the fluid solid temperature difference $T_{solid} - T_{fluid}$ as the equation 3.13 shows:

$$\dot{Q} = A_s(\theta)h(T_{solid}(\theta) - T_{fluid}) \tag{3.13}$$

The temperature difference usually occurs across a thin layer of fluid adjacent to the solid surface. This thin fluid layer is called a boundary layer and the constant of proportionality is called the heat transfer coefficient, h, which is replaced by h_c - the instantaneous convective average coefficient for simplified the calculation. The following convective heat-transfer correlation had been developed by Annand [110] to match the experimental data on instantaneous heat fluxes:

$$\frac{h_c B}{k} = a\left(\frac{\rho \bar{S}_p B}{\mu}\right)^b \tag{3.14}$$

where B is the cylinder bore size.

k is the gas thermal conductivity.

ρ is the characteristic gas velocity.

μ is the dynamic viscosity.

Woschni [111] assumed a correlation of the form below by using Nusselt and Reynolds number relationship:

$$Nu = 0.035\,\mathrm{Re}^m \tag{3.15}$$

The above correlation can be written as equation 3.16 where the heat transfer coefficient changes with the crank angle since it is a function of pressure, temperature and the average cylinder gas velocity, which vary with crank angle.

$$h_c = CB^{m-1}P^m T^{0.075-1.62m} w^m \tag{3.16}$$

where w is the local average gas velocity in the cylinder.

P is the in-cylinder pressure.

With the exponent in equation 3.15 equal to 0.8, Woschni's correlation can be re-summarised as:

$$h_c = 194 .7 B^{-0.2} P^{0.8} T^{-0.55} w^{0.8} \quad (3.17)$$

where the average gas velocity, $w = \left[C_1 S_p + C_2 \frac{V_d T_{IVC}}{P_{IVC} V_{IVC}} (P - P_{motored}) \right]$. The two constant C_1 and C_2 equal to 2.28 (6.18 for gas exchange).

In this thesis, the rate of in-cylinder heat transfer, $\dot{Q}$, is presented by the following relation:

$$\dot{Q} = A_s(\theta) h_c (T_{wall} - T(\theta)) \quad (3.18)$$

where A_s is the surface area of cylinder.

T_{wall} is the average cylinder wall temperature that is approximated as 400K a common assumption for evaporativly cooled engines [112]

3.5 MODELLING THERMODYNAMICS PROCESS

In order to model the complexity of thermodynamics process of HCCI engine, the thermodynamics cycle has been represented as five different phases which are essential to give the correct trends under different control strategies. They are induction phase, compression phase, combustion phase, expansion phase and exhaust phase. The modelling is based on the analysis of the first law of thermodynamics for an open system that can be represented as following:

$$\frac{d(mu)}{dt} = \dot{Q} - \dot{W} + \dot{m}_I h_I - \dot{m}_E h_E \quad (3.19)$$

where m is the total reactant mass in cylinder.

u is the specific internal energy.

h is the enthalpy.

mu is the total internal energy in the cylinder.

$\dot{Q}$ is the rate of energy transfer as heat.

$\dot{W}$ is the rate of energy transfer as work ($=P\dot{V}$).

$\dot{m}_I$ and $\dot{m}_E$ represent the rates of intake mass flow and exhaust mass flow. The subscripts I and E represent intake and exhaust respectively. In this phase, $\dot{m}_E$ and $\dot{m}_I$

In order to simplify the analysis and modeling, the following assumptions are made:

1. The mixture in the engine system is a perfect gas;
2. Temperature and species concentrations are uniformly distributed in the cylinder;
3. Heat transfer takes place only due to convection; radiation and crevice flows are neglected.

Based on the aforementioned assumptions, it is convenient to commence the analysis with the induction phase, during which the valves are open or close.

3.5.1 INDUCTION PHASE

For this phase, it is supposed that the following assumptions hold:

1. The pre-mixed air/fuel species are present in the intake manifold. The air/fuel ratio is a constant and has been kept λ=1.
2. The intake manifold conditions remain unchanged during the induction process and there is no gas flow from cylinder to intake manifold during the valve opening. However, allowing flow from cylinder to intake manifold would be simple to include in the model if necessary.
3. The pressure in intake manifold is assumed to 1 bar, but could be setting with different value if desire as turbo charger implementation.

As enthalpy is defined by $h = u + Pv = u + PV/m$, the first law of thermodynamics can be re-written as following:

$$\frac{d(mu)}{dt} = \frac{d(m(h - PV/m)}{dt} = \frac{d(mh)}{dt} - \dot{P}V - P\dot{V} \tag{3.20}$$

$$\frac{d(mh)}{dt} = \dot{Q} + \dot{P}V + \dot{m}_1 h_1 \tag{3.21}$$

Here the in-cylinder pressure and its derivative can be related to the concentrations and temperature though the ideal gas law as:

$$P = \sum[\frac{N_i}{V}]RT = \sum[X_i]RT \tag{3.22}$$

$$\dot{P} = \frac{P\sum[\dot{X}_i]}{\sum[X_i]} + \frac{P\dot{T}}{T} \tag{3.23}$$

where N_i is the number of moles of species i and $X_i = \frac{N_i}{V}$ is the molar volumetric concentration of species i.

Expanding the enthalpy to show the contributions:

$$mh = \sum N_i \hat{h}_i \tag{3.24}$$

where $\hat{h}_i$ is the specific enthalpy of species i on a molar basis, $\dot{\hat{h}}_i = C_{p,i}(T)\dot{T}$. Here $C_{p,i}(T)$ is the specific heat of species i per mole at temperature T.

The rate of change of concentration for species i denoted by $[\dot{X}_i]$ is related to N_i and can be obtained by:

$$[\dot{X}_i] = \frac{d}{dt}\left(\frac{N_i}{V}\right) = \frac{\dot{N}_i}{V} - \frac{\dot{V}N_i}{V^2} = w_i - \frac{\dot{V}N_i}{V^2} \tag{3.25}$$

where, w_i the rate of change of moles of species i per unit volume.

Equations (3.24) and (3.21) can be combined to give:

$$\begin{aligned} &\dot{Q} + \dot{P}V + \dot{m}_1 h_1 \\ &= V\left(\sum[\dot{X}_i]\hat{h}_i + \dot{T}\sum[X_i]C_{p,i}(T)\right) + \dot{V}\sum[X_i]\hat{h}_i \end{aligned} \tag{3.26}$$

Rearrange Equation (3.27) and combine with Equation (3.25), the following equation can be obtained

$$\dot{T} = \frac{\frac{\dot{Q}}{V} + \frac{\dot{m}_1 h}{V} - \frac{\dot{V}}{V}\left([X_i]\hat{h}_i\right) - \sum[\dot{X}_i]\hat{h}_i + \frac{P\sum[\dot{X}_i]}{\sum[X_i]}}{\sum[X_i]C_{p,i}(T) - \frac{P}{T}} \tag{3.27}$$

3.5.2 Compression Phase

During the compression phase the pressure will rise rapidly and the process has been assumed as an adiabatic process, which means all of the compression work is transferred to the in-cylinder gas as an increase in internal energy. Also if the compression is very slow the maximum pressure will be approximately the compression-ratio times the inlet pressure since the gas temperature will be maintained at a constant level. However, the heat transfer can be added into modelling for the consideration of polytropic process [109].

Applying the first law of thermodynamics and the definition formula for the enthalpy, we have:

$$\frac{d(mu)}{dt} = \dot{Q} - \dot{W} \tag{3.28}$$

and

$$\frac{d(mh)}{dt} = \dot{Q} + \dot{P}V \tag{3.29}$$

During this stage, the rate of change of concentration for species i is only related to the cylinder volume so that:

$$[\dot{X}_i] = \frac{d}{dt}\left(\frac{N_i}{V}\right) = \frac{\dot{N}_i}{V} - \frac{\dot{V}N_i}{V^2} = -\frac{\dot{V}N_i}{V^2} \tag{3.30}$$

The calculation for temperature rate can be given as:

$$\dot{T} = \frac{\frac{\dot{Q}}{V} - \frac{\dot{V}}{V}\left([X_i]\hat{h}_i\right) - \sum[\dot{X}_i]\hat{h}_i + \frac{P\sum[\dot{X}_i]}{\sum[X_i]}}{\sum[X_i]C_{p,i}(T) - \frac{P}{T}} \tag{3.31}$$

3.5.3 Combustion Phase

During this phase a constant volume combustion process is assumed on the basis of the fact the HCCI combustion duration is very shot [113], so that $\dot{V} = 0$ and the rate of change of concentration for species i, will be given by:

$$[\dot{X}_i] = \frac{d}{dt}\left(\frac{N_i}{V}\right) = \frac{\dot{N}_i}{V} - \frac{\dot{V}N_i}{V^2} = \frac{\dot{N}_i}{V} = w_i \tag{3.31}$$

During the combustion process w_i could be determined through the use of a combustion chemistry mechanism which is assumed to depend directly on both concentration and temperature using well-known Arrhenius-type relations [37, 114]. Treating the chemical reaction as a two-step process, that

is, the reaction generates CO first and the CO then combines with O_2 to generate CO_2:

$$C_3H_8 + 3.5O_2 + 18.8N_2 \rightarrow 3CO + 4H_2O + 18.8N_2 \tag{3.32}$$

and

$$CO + 0.5O_2 \rightarrow CO_2 \tag{3.33}$$

The reaction rates for C_3H_8 oxidation and CO oxidation are given in [107] as:

$$w_{C_3H_8} = 4.83e^9 \exp\left(\frac{-15098}{T}\right)\left[X_{C_3H_8}\right]^{0.1}\left[X_{O_2}\right]^{1.65} \tag{3.34}$$

and

$$\begin{aligned} w_{CO,ox} = {} & 2.24e^{12} \exp\left(\frac{-20130}{T}\right)\left[X_{CO}\right]\left[X_{H_2O}\right]^{0.5}\left[X_{O_2}\right]^{0.25} \\ & - 5e^8 \exp\left(\frac{-20130}{T}\right)\left[X_{CO_2}\right] \end{aligned} \tag{3.35}$$

The temperature rate will then be given as:

$$\dot{T} = \frac{\frac{\dot{Q}}{V} - \sum[\dot{X}_i]\hat{h}_i + \frac{P\sum[\dot{X}_i]}{\sum[X_i]}}{\sum[X_i]C_{p,i}(T) - \frac{P}{T}} \tag{3.36}$$

3.5.4 Expansion Phase

This phase occurs from the end of combustion to the opening of the exhaust valve and is characterised by polytropic expansion. The temperature rate can once again be obtained from equation 3.29 and 3.31.

3.5.5 Exhaust Phase

During this phase, the exhaust valve is open. It is assumed that the conditions within the exhaust manifold remain constant at atmospheric pressure. The first law of thermodynamics gives:

$$\frac{d(mu)}{dt} = \dot{Q} - \dot{W} - \dot{m}_E h \tag{3.37}$$

The temperature rate can therefore be obtained from:

$$\dot{T} = \frac{\frac{\dot{Q}}{V} - \frac{\dot{m}_E h}{V} - \frac{\dot{V}}{V}\left([X_i]\hat{h}_i\right) - \sum[\dot{X}_i]\hat{h}_i + \frac{P\sum[\dot{X}_i]}{\sum[X_i]}}{\sum[X_i]C_{p,i}(T) - \frac{P}{T}} \tag{3.38}$$

3.6 SIMULATION STUDY

The processes described above have been implemented in SIMULINK as a simulation model for computer aided analysis. The schematic block diagram for the SIMULINK implementation is shown in Figure 3-5. The simulation program consists of three main function blocks:

1. Air/Fuel Mixture Calculation: The model takes in the in-cylinder pressure/temperature and species reaction rates and outputs the species concentrations.
2. Thermodynamics sub-model calculates the in-cylinder temperature, in-cylinder pressure and simulates the heat loss during the engine cycle and valve operations.
3. Two-Step combustion sub-model adopts the simplified Arrhenius-type combustion model to calculate the species reaction rates. There is no threshold as knock limitation or temperature trigger inside the model. The ignition happens naturally and only determined by in-cylinder gas temperature, pressure and species concentrations.

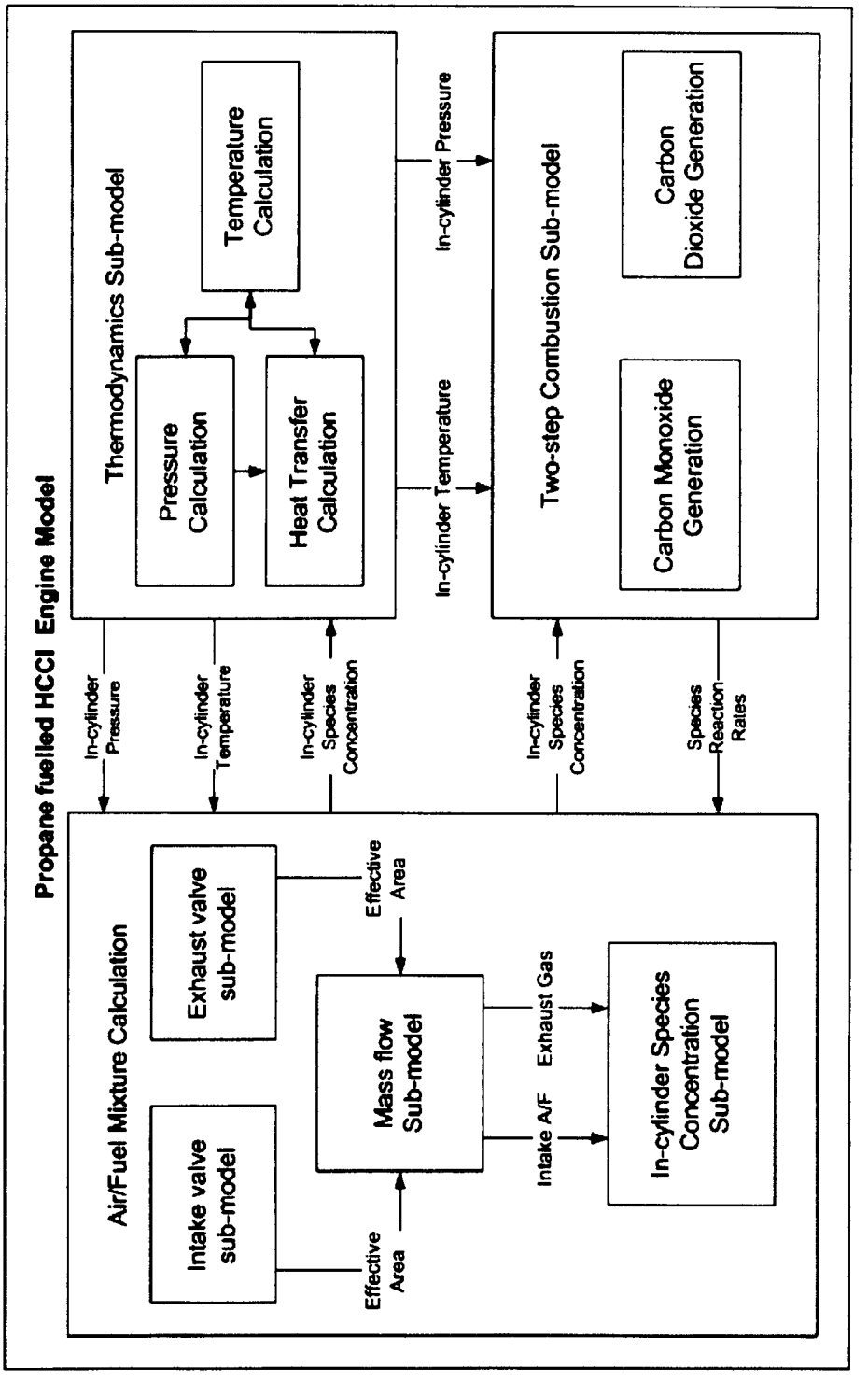

Figure 3-5 Block diagram for the simulation model

A set of simulation studies has been carried out, which is concentrating on the analysis of ignition process and combustion duration. Since the two step chemical kinetics is applied, the reactions are dominated by propane oxidation and carbon monoxide oxidation. Figure 3-6 to figure 3-10 show the typical HCCI engine cycle simulation.

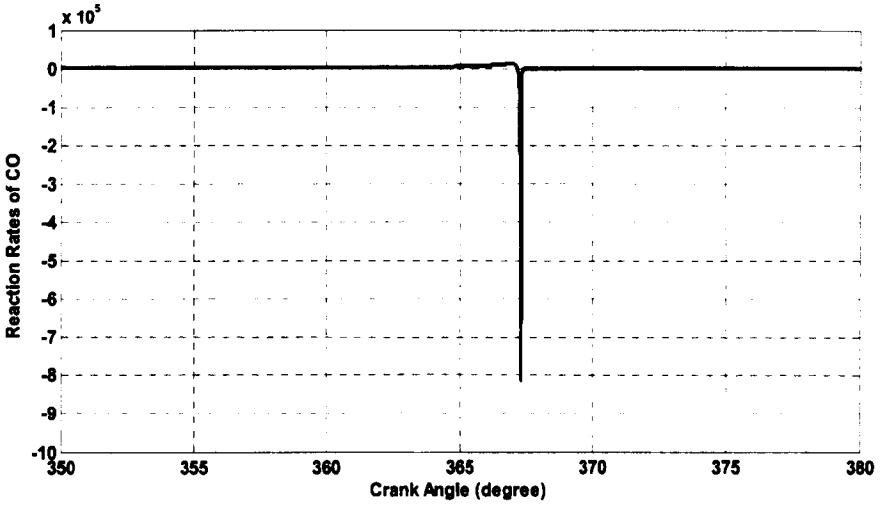

Figure 3-6 Reaction rates of carbon monoxide

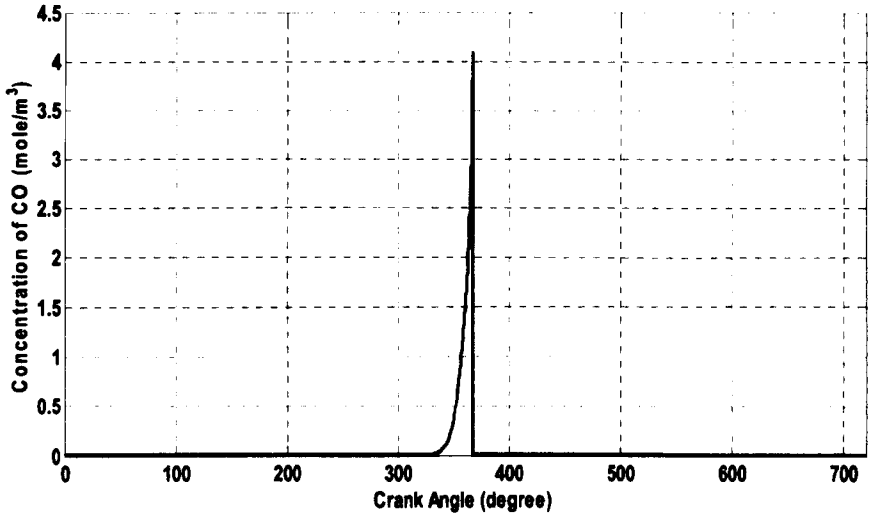

Figure 3-7 Concentration of carbon monoxide

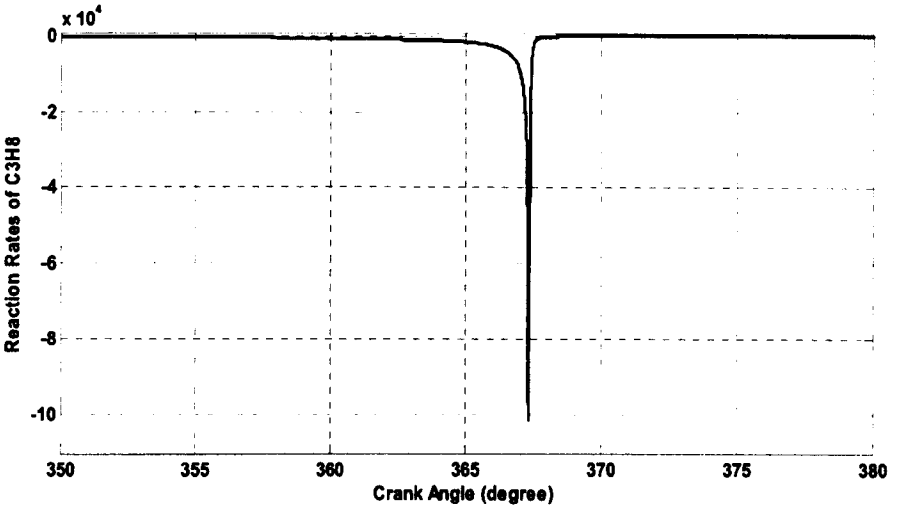

Figure 3-8 Reaction rates of propane

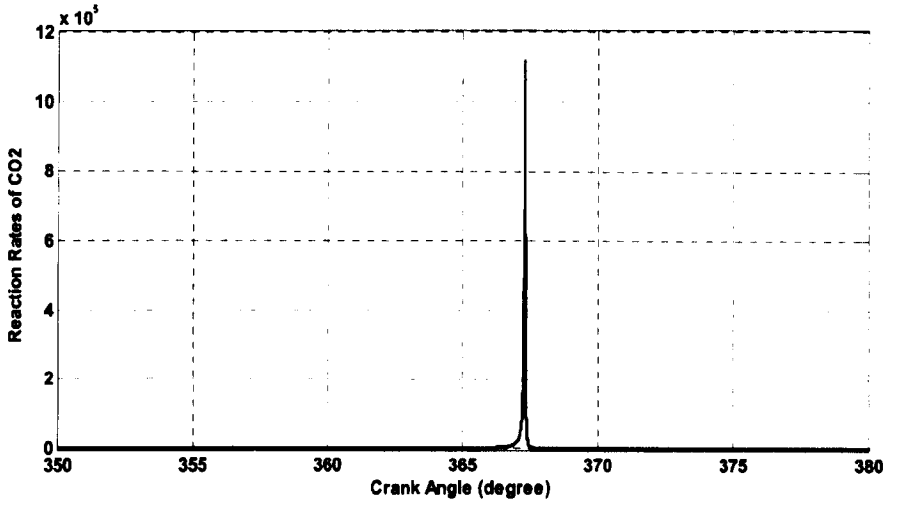

Figure 3-9 Reaction rates of carbon dioxide

Figure 3-6 and Figure 3-7 show the simulation results of oxidation rates and in-cylinder concentrations for carbon monoxide separately. The positive /negative value of reaction rates indicates that the generation rates are greater/less than oxidation rates. Either positive or negative reaction rates are

leading to the final products of the combustion, which includes: water and carbon dioxide. From the results, it is noticeable that the oxidation process starts slowly before the piston reaches TDC, where oxidation rates and concentrations of carbon monoxide both slightly increase. That increase indicates only small amount of carbon monoxide has been generated from the oxidation of propane, and the positive rates indicate the oxidation of propane dominates the chemical reactions during the pre-combustion period. When the concentration of carbon monoxide reaches a certain level together with the heat release from the reactions, the auto-ignition happens. Followed by the ignition, the oxidation of carbon monoxide dominates the chemical process resulting in drastic heat release and thus, accelerates the oxidation of propane sharply until the oxidation completed. The same phenomena is also observed in Figure 3-8 and Figure 3-9, which represent the results of the reaction rates of propane and carbon dioxide separately.

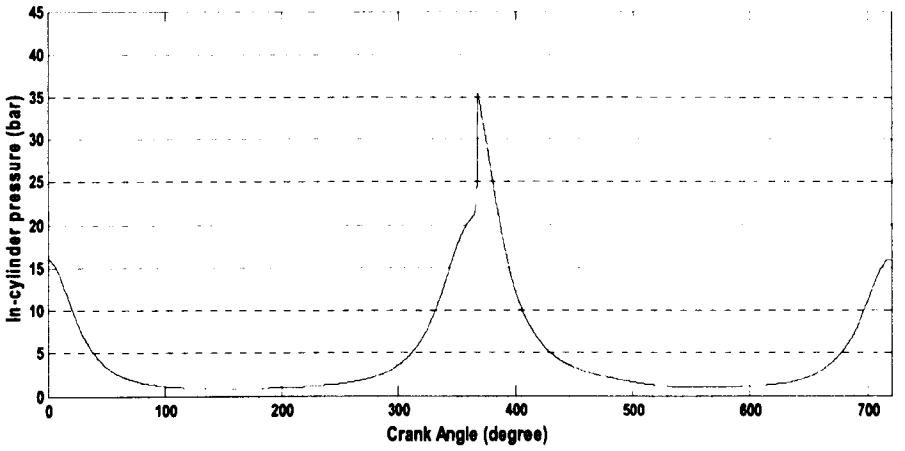

Figure 3-10 in-cylinder pressure history of a completed engine cycle

The result shown in Figure 3-10 is to simulate the in-cylinder pressure history for one completed engine cycle. Since the NVO scheme adopted, the early closing exhaust valve results part of combustion products from

previous engine cycle trapped inside cylinder with a higher initial pressure at the beginning of the engine cycle.

3.7 MODEL VALIDATION AND DISCUSSION

In order to validate the model, the simulation results have been compared against in-cylinder pressure histories obtained from a propane fuelled single cylinder HCCI research engine. Simulations have been carried out for a variety of different inlet temperatures and exhaust valve timing points within the experimental window of the HCCI research engine. Table 3-1 lists the relevant engine parameters and Table 3-2 lists the engine operation variants for simulations.

Table 3-1 Engine parameters

Parameter	Value	Unit
Engine speed	1500	RPM
Bore	80	mm
Stroke	88.9	mm
Connecting rod	160	mm
Clearance volume	38,892	cm^3
Inlet timing	146	MOP CAD

Table 3-2 Engine operation condition

	Inlet Temperature	Exhaust MOP	IMEP
Case 1	371	142	3.62
Case 2	369	146	3.32
Case 3	369	150	3.09

Case 4	377	154	2.89
Case 5	385	158	2.49
Case 6	388	162	2.37
Case 7	398	166	2.10
Case 8	400	170	1.88

The comparisons between the simulations and experimental results obtained are presented in Figures 3-11 to 3-18 inclusive. The comparison has focussed on the ability of the model to predict the crank angle at which auto-ignition occurs, the corresponding in-cylinder peak pressure reached and the pressure rise rate.

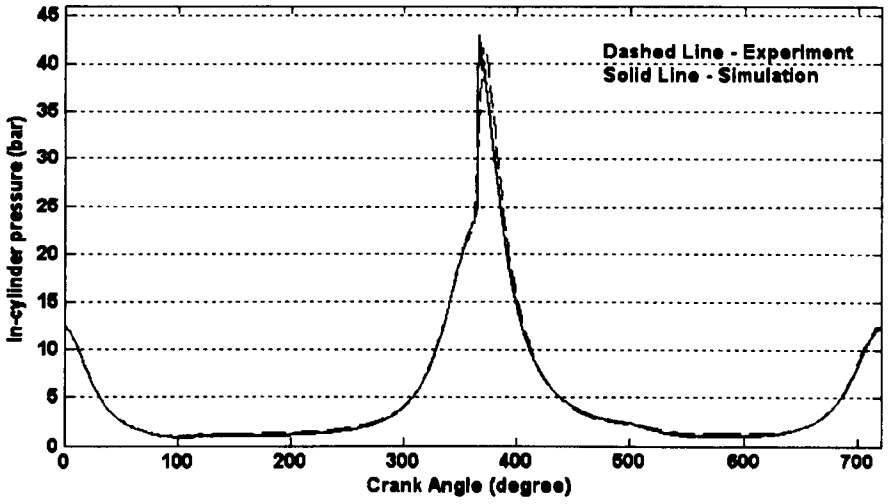

Figure 3-11 Case 1: in-cylinder pressure comparison, Exhaust MOP 142

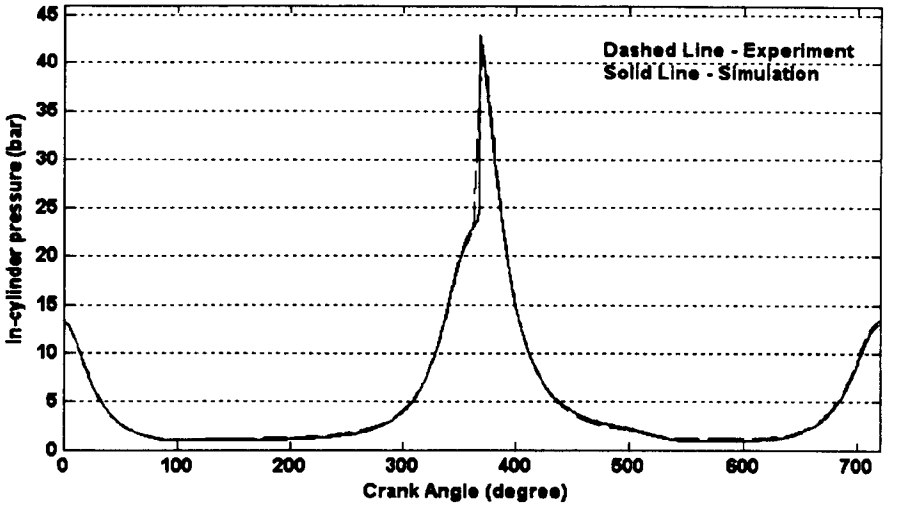

Figure 3-12 Case 2: in-cylinder pressure comparison, Exhaust MOP 146

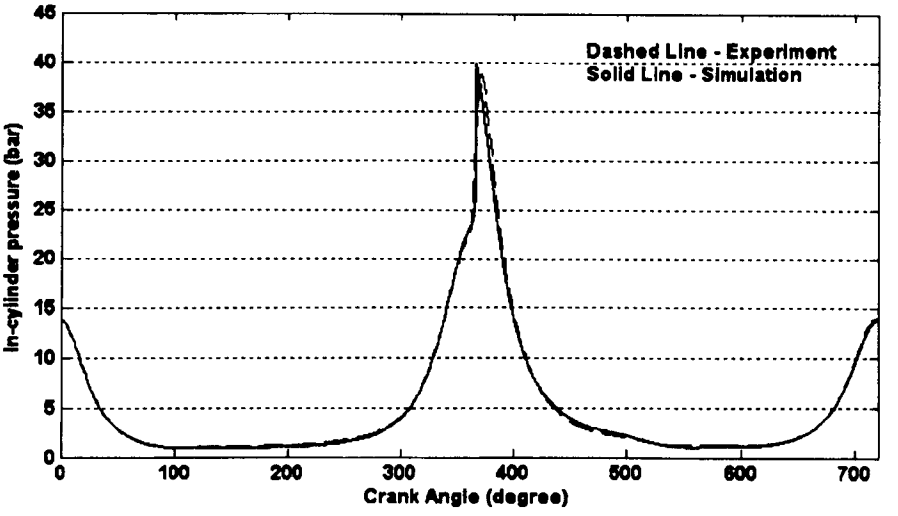

Figure 3-13 Case 3: in-cylinder pressure comparison, Exhaust MOP 150

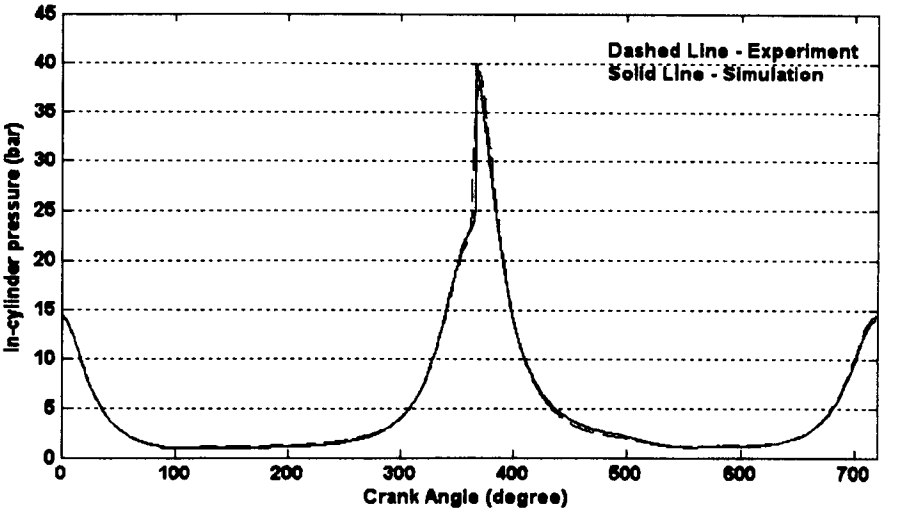

Figure 3-14 Case 4: in-cylinder pressure comparison, Exhaust MOP 154

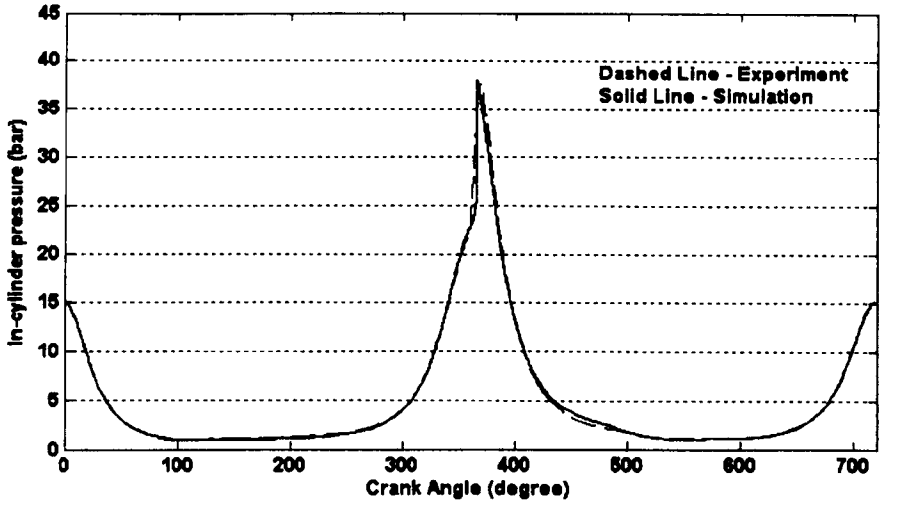

Figure 3-15 Case 5: in-cylinder pressure comparison, Exhaust MOP 158

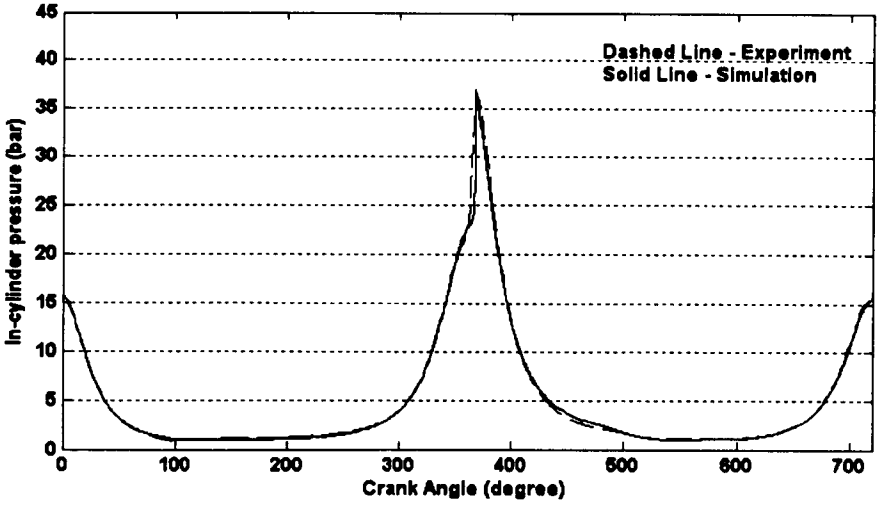

Figure 3-16 Case 6: in-cylinder pressure comparison, Exhaust MOP 162

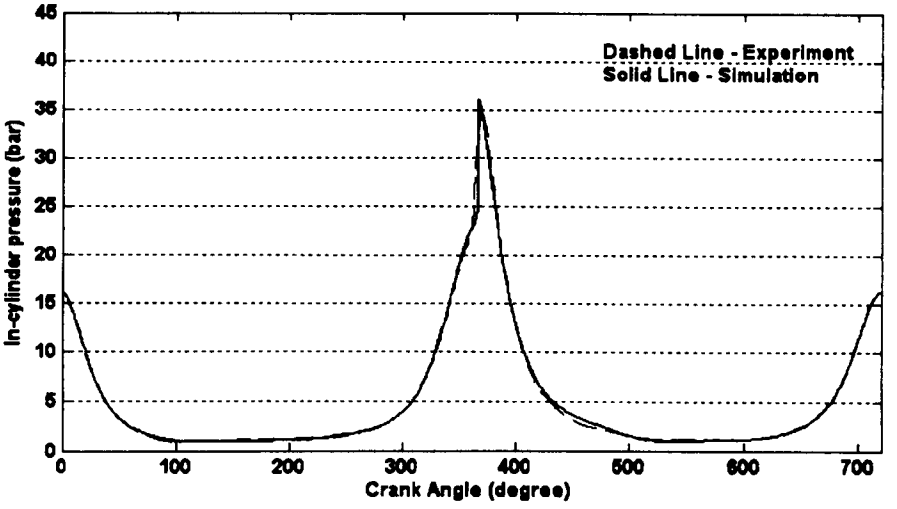

Figure 3-17 Case 7: in-cylinder pressure comparison, Exhaust MOP 166

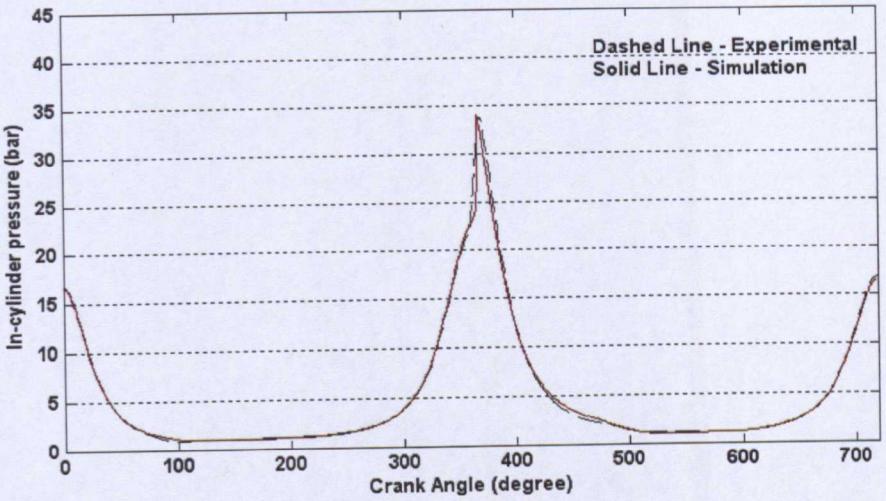

Figure 3-18 Case 8: in-cylinder pressure comparison, Exhaust MOP 170

The results show good general agreement over the complete pressure cycle. The critical comparisons focus on the ability of the model to predict the instant of ignition and the peak pressure rise during combustion. These are highlighted in Figure 3-19 and 3-20, from which it can be observed that the model gives good prediction of the magnitude of the peak pressure rise and also successfully follows the general trend in the pressure variation caused by the change in operating conditions.

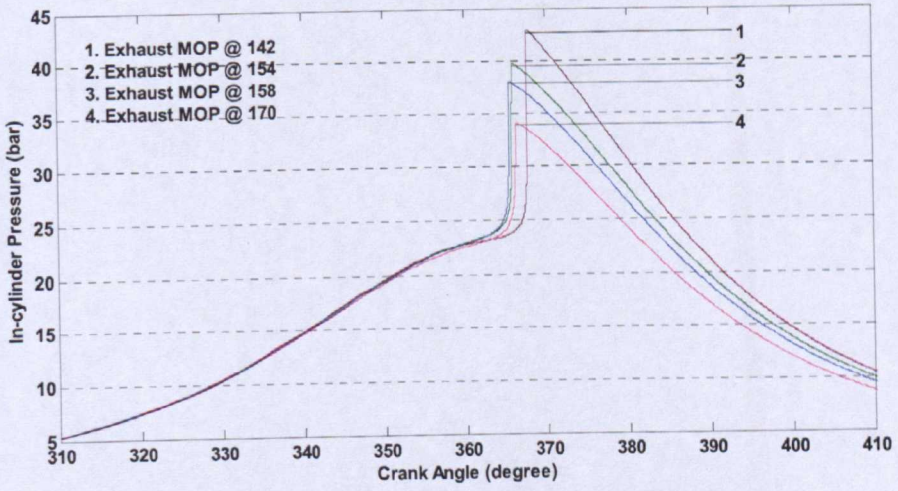

Figure 3-19 Highlighted combustion phase-simulations

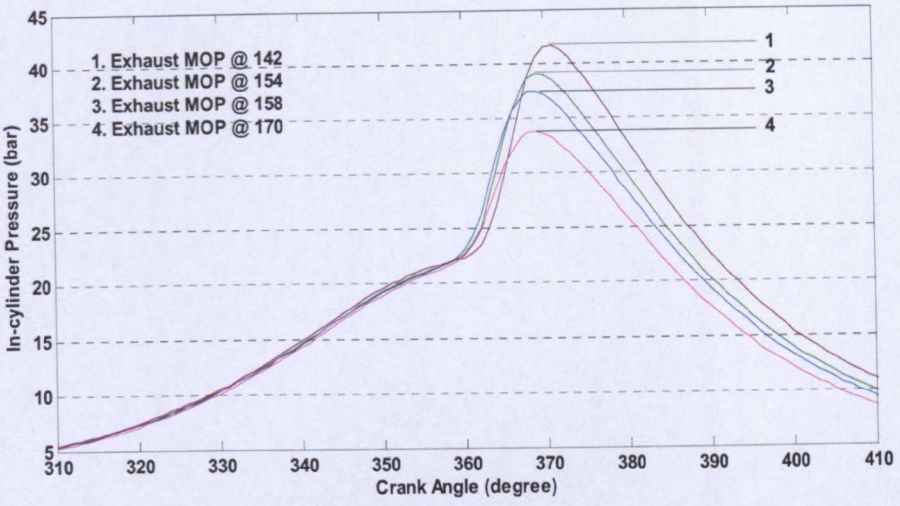

Figure 3-20 Highlighted combustion phase-experiments

However, the model shows a notably sharper rise to peak pressure than that observed in experiments which is attributed to the use a single zone combustion model in the simulation. In the combustion process it has been assumed that all fuel burns simultaneously throughout the entire cylinder volume, resulting in a higher rate of heat release and slight over-prediction of the peak pressure compared to the experimental results. In reality, the temperature of the mixture is not perfectly uniform within the cylinder which causes a more gradual change during the combustion phase [115] and also a small proportion of the mixture may not be burned during the combustion.

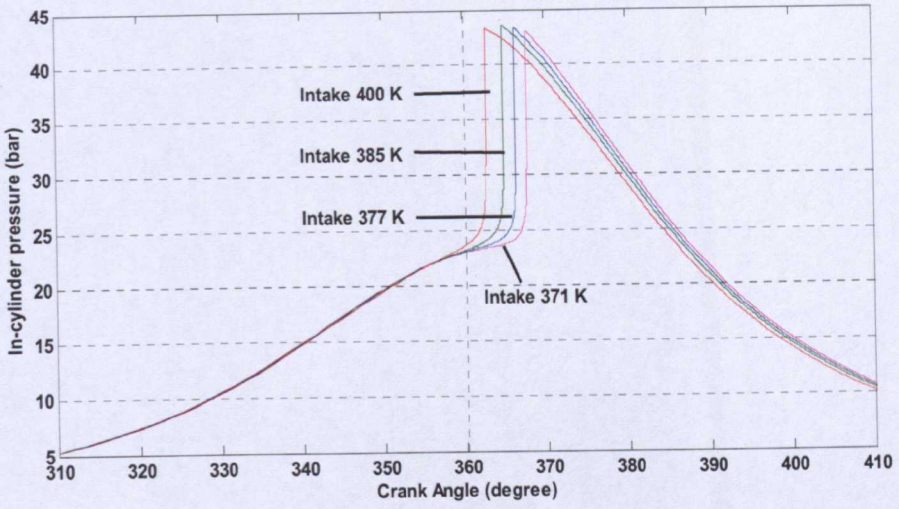

Figure 3-21 Predicted in-cylinder pressure for exhaust MOP 142^0 BTDC

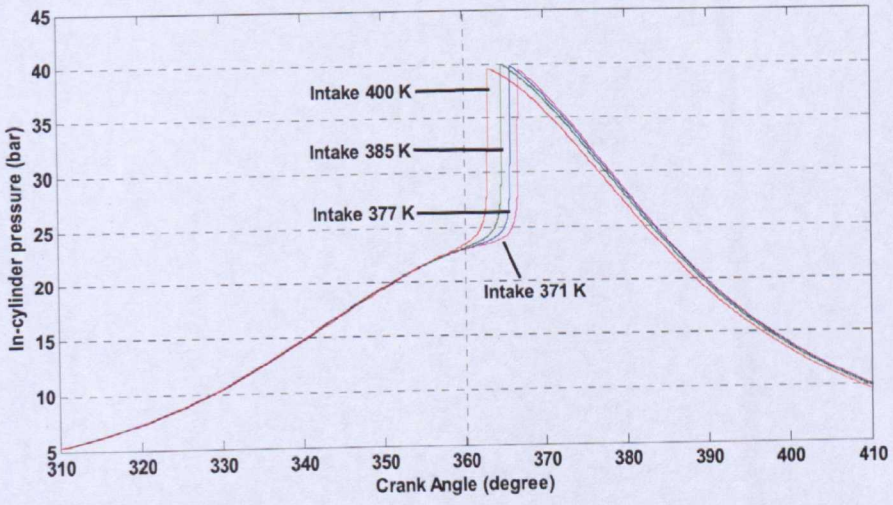

Figure 3-22 Predicted in-cylinder pressure for exhaust MOP 154^0 BTDC

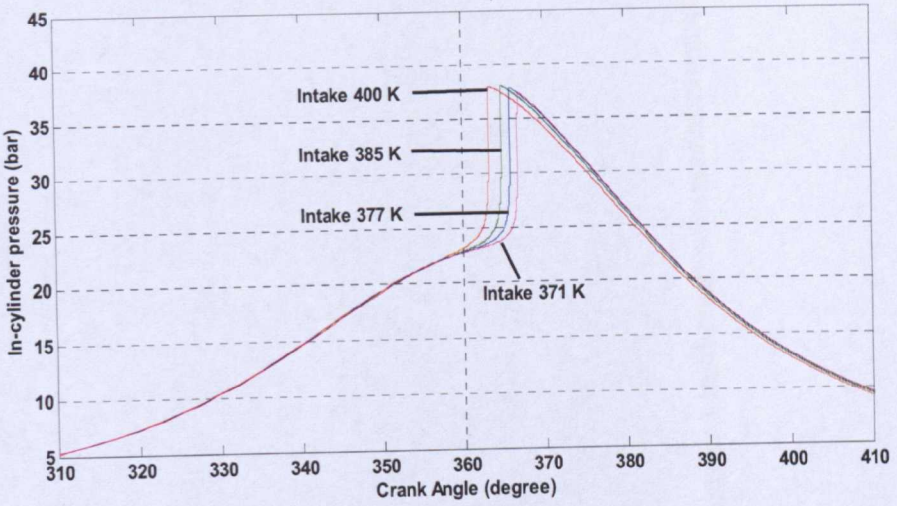

Figure 3-23 Predicted in-cylinder pressure for exhaust MOP 158^0 BTDC

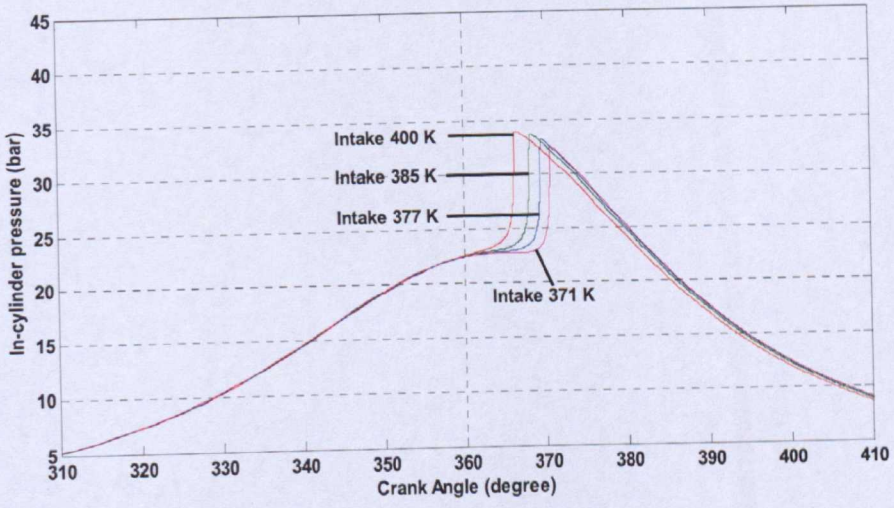

Figure 3-24 Predicted in-cylinder pressure for exhaust MOP 170^0 BTDC

Further analysis has been conducted in order to identify the trend in ignition timing associated with both intake temperature and MOP whilst the remaining parameters are held constant. The simulation results for a range of intake temperatures with four values of exhaust MOP are shown in Figure 3-

21 to Figure 3-24 and for a range of MOP with four values of intake temperature are shown in Figure 3-25 to Figure 3-28.

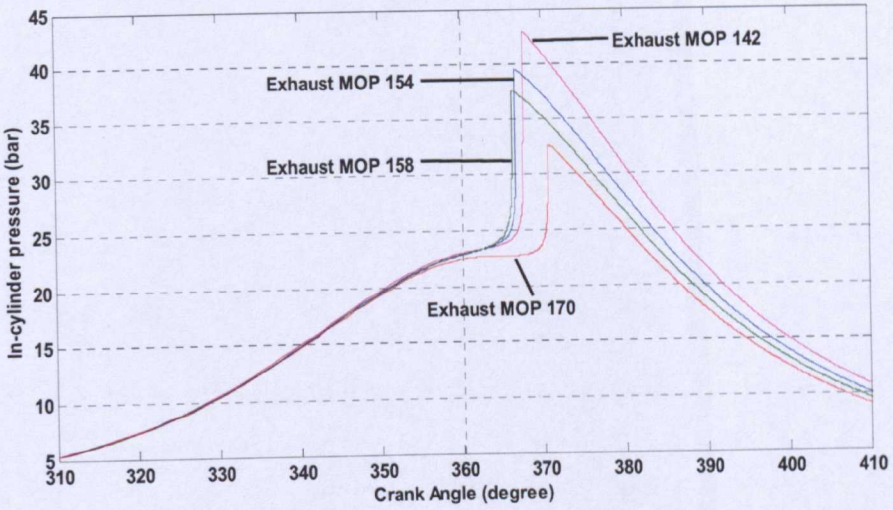

Figure 3-25 Predicted in-cylinder pressures for intake temperature 371K

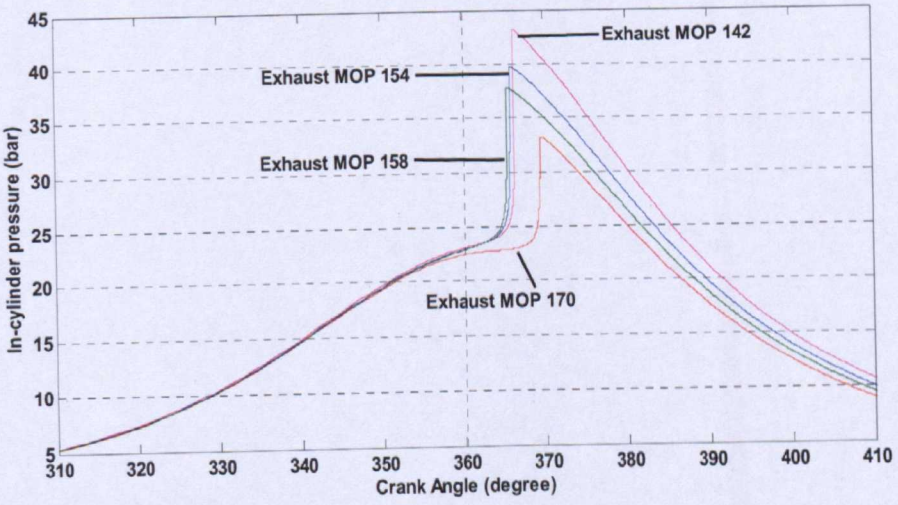

Figure 3-26 Predicted in-cylinder pressures for intake temperature 377K

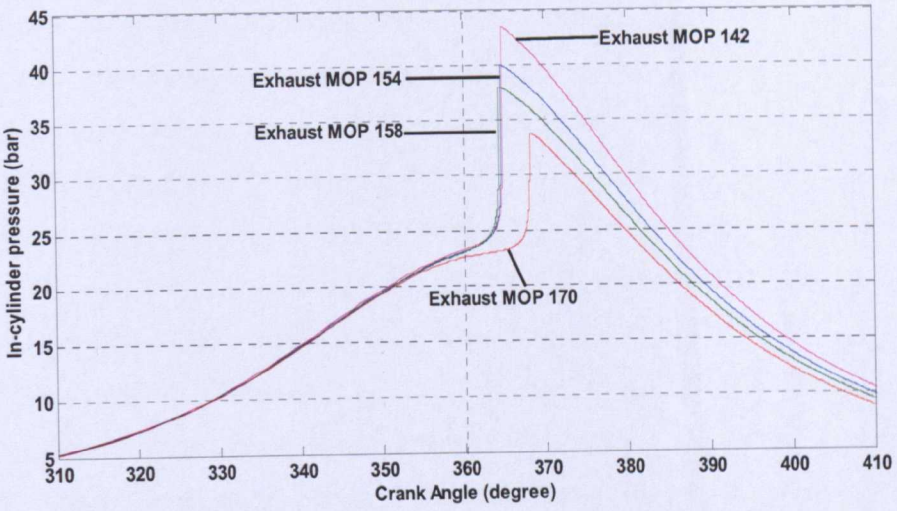

Figure 3-27 Predicted in-cylinder pressures for intake temperature 385K

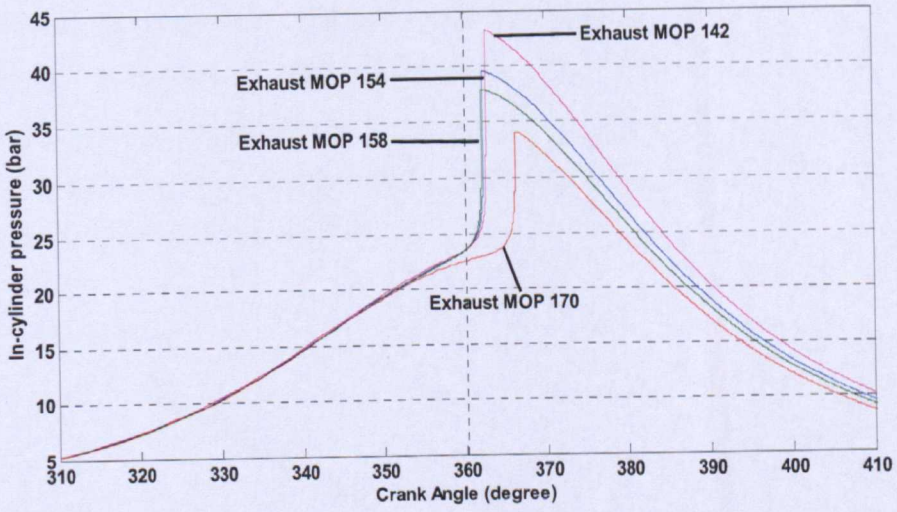

Figure 3-28 Predicted in-cylinder pressures for intake temperature 400K

Figure 3-21 to Figure 3-24 show that the predicted ignition timing is significantly affected by both the intake temperature and exhaust MOP. A higher intake temperature results in an earlier ignition time as expected, because a higher temperature will bring more internal energy into the cylinder. However, an earlier exhaust MOP (corresponding to a larger MOP crank angle value) causes the retardation in the ignition timing. These two

effects have had a cancelling effect on the experimental results shown in Figure 3-20 because for the test conditions used, an increase in intake temperature was accompanied by an earlier exhaust MOP (Cases 1 and 8 in Table 3-2). Figure 3-21 to Figure 3-24 also shows that there is only a modest rise in peak pressure and a very small change in peak temperature as the intake temperature is increased. In contrast, Figure 25 and 28 show that the exhaust MOP has a much greater influence on these parameters. A later exhaust MOP (corresponding to a smaller MOP value) results in a significantly higher in-cylinder pressure and temperature under the condition of constant intake temperature. The tendency is in consistency with findings in previous modelling studies using commercial thermodynamic engine simulation codes and experiments [113, 116], because a later exhaust MOP reduces the proportion of trapped exhaust gases which in turn leads to a greater proportion of fuel intake at the same intake temperature. We conclude that the changes in the maximum in-cylinder pressure that were observed in the experimental results can be attributed mainly to the changes in exhaust MOP that took place.

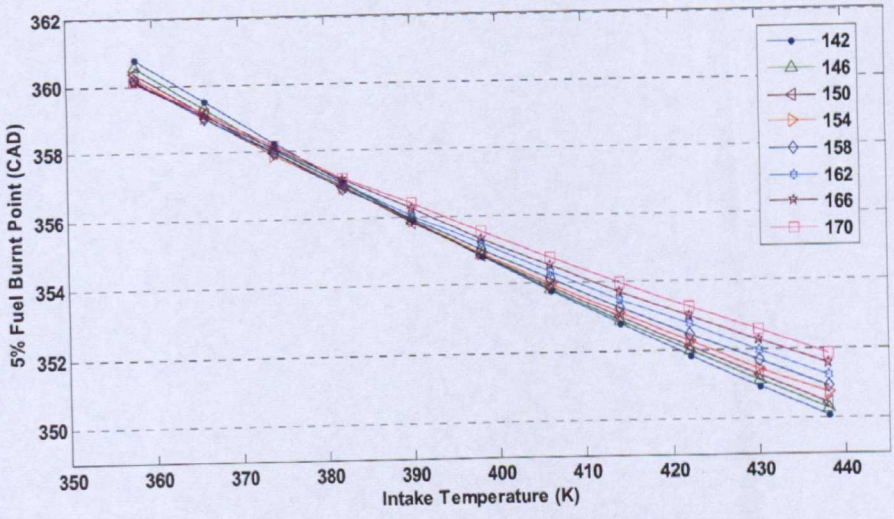

Figure 3-29 Predicted 5% fuel burnt points with different intake temperature, exhaust MOPs and fixed inlet MOP 146

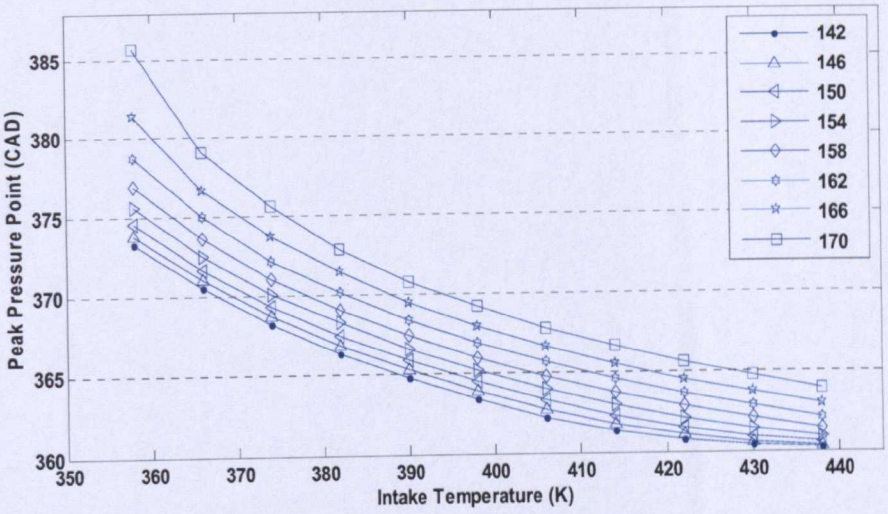

Figure 3-30 Predicted peak pressure points with different intake temperature, exhaust MOPs and fixed inlet MOP 146

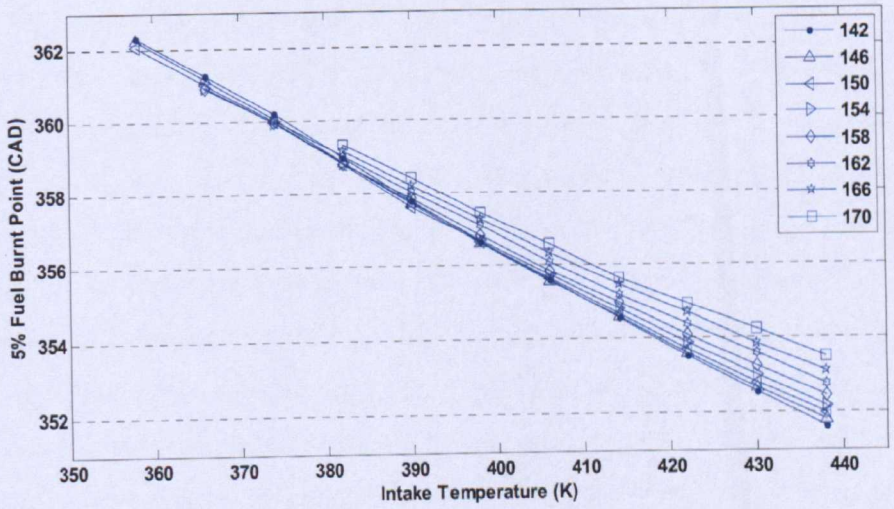

Figure 3-31 Predicted 5% fuel burnt points with different intake temperature, exhaust MOPs and fixed inlet MOP 130

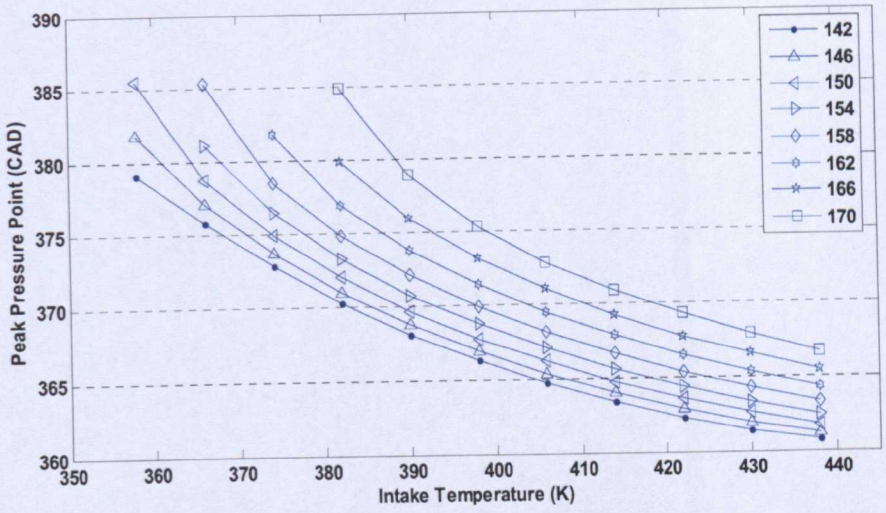

Figure 3-32 Predicted peak pressure points with different intake temperature, exhaust MOPs and fixed inlet MOP 130

The observed influences of exhaust MOP and intake temperatures on the ignition timing (5% fuel burn point [116]) and peak in-cylinder pressure are shown more comprehensively in Figure 3-29 to Figure 3-32. The results shown in Figure 3-29 and 3-30 are operated with a fixed inlet MOP at 146 (ATDC) and Figure 3-31 and 3-32 show the simulation results with a early inlet MOP at 130 (ATDC). The ignition timing is more sensitive to the intake temperature changes when a later exhaust MOP is chosen but the cross-over of the curves indicates that it is possible to obtain similar ignition timing for different exhaust MOPs by using a combination of selected intake MOPs and intake temperatures. This has important implications for the design of a control system for HCCI. In contrast, no such cross-over occurs in the peak pressure crank angle point, so that exhaust MOP is predicted to influence the peak pressure point over the whole range of intake MOP and intake temperatures investigated, influencing the rate of rise of in-cylinder pressure and temperature.

3.8 SUMMARY

A mathematical model for a propane fuelled HCCI engine using an NVO scheme has been developed adopting a simplified description of chemical kinetics and the model is implemented in SIMULINK. An extensive simulation study of HCCI engine behaviour has been conducted. The model has been evaluated and validated by comparing the simulation results with a series of experiment data obtained from a single cylinder HCCI research engine. Representative examples have been presented which are associated with two engine parameters variations: the inlet temperature and exhaust valve timing. The comparisons have demonstrated that the model can correctly predict the in-cylinder pressure, auto-ignition timing and combustion characteristics. The simplifications inherent in the model are not critical to the successful prediction of trend of ignition timing and work output variation – two of the most challenging problems of HCCI engines. Furthermore, the reduced complexity of the simulation offers the prospect of achieving simulation speeds that will allow real time predictions so that the model can be used as a practical engineering tool and a valuable testing facility in the development of suitable control strategies.

Chapter 4

GASOLINE FUELLED HCCI ENGINE MODELLING FOR CONTROL

As for the propane fuelled HCCI combustion, chemical kinetics plays the major role in the auto-ignition and fuel oxidation processes that characterise gasoline HCCI combustion: Unlike other engine types, diffusion and turbulence are of moderate importance compared with chemistry. This is because the gas mixture in the cylinder prior to auto-ignition is close to homogeneous. Besides this, ignition is initiated by other means than a spark and, hence, no turbulence dependent flame propagation occurs [106]. It can be concluded that realistic modelling of the gasoline HCCI engine is necessary to obtain satisfactory predictions for the moment of auto-ignition, the rate of heat release and the pressure evolution.

Unfortunately, a large number of species participate in an even greater number of elemental reactions during the oxidation of hydrocarbons typically found in gasoline fuel. Including all these species and reactions in a

detailed reaction mechanism and implementing this in a modelling code (including fluid mechanics) leads to unacceptably long calculation times. Some research groups are working on reducing the size of the reaction mechanism as much as possible while maintaining it as realistic as possible. The method is achieved by including the most relevant intermediate species and reaction branches in the reduced mechanism [106, 117]. Recently, Westbrook *et al* [118] reported the HCCI combustion can be described by a single-step combustion model and Kim *et al* [119] developed numerical combustion model to explore the chemical kinetics of HCCI process by using genetic algorithms (GAs) to identify and optimise the parameters. All of these methods indicate that the gasoline HCCI combustion is able to be simulated by a simplified chemical process and GAs as an optimization tool is able to optimise the parameters for numerically predicting in combustion simulation.

The aim of this chapter is to develop an accurate, simple and intuitive model of the gasoline HCCI process. The goal is real-timely capture most control relevant behaviours of HCCI process, which include: combustion timing, in-cylinder pressure evolution and work output. Specifically, the model presented in this chapter is the overall model that carried over from Chapter 3. The model is based on the first law of thermodynamics analysis and the premixed reactant at fixed equivalence ratio.

Given the accuracy, intuition and simplicity of Wiebe function, it has been integrated into the model to describe the combustion process. GAs has been applied in order to identify the unknown parameters in the segment of the combustion process. Subsequent validation with variety engine operations demonstrate that the model is capable of reproducing the engine cycles of gasoline HCCI process. Furthermore, the model is able to provide an

efficient simulation platform for evaluation of control strategy developed, and possibly, fault detection.

4.1 STRUCTURE OF THE MODEL

The gasoline HCCI test engine being modelled achieves HCCI process in the same way as the propane fuelled HCCI engine by negative valve overlap scheme (Figure 3-1). The process can be partitioned into seven stages which are as follows:

1. EGR expansion phase - commencing from TDC, the cylinder volume is expanded to the IVO.
2. Induction phase - between the two points where intake valves open and close. The pre-mixed fuel and air charge is drawn into the cylinder and mixed with the reactants and residual product gases present in the cylinder.
3. Compression phase – the period between the instant when the intake valve is closed to the moment of combustion. During this phase, the contents in the cylinder are compressed to the point where the auto-ignition occurs.
4. Combustion phase – including the ignition threshold and combustion process.
5. Expansion phase (power stroke) – the cylinder volume is expanded to exhaust valve open.
6. Exhaust phase – the period between exhaust valve open and the instant of the exhaust valve close.
7. EGR Compression – in this period, the residual combustion products are trapped in the cylinder by an early exhaust valve closure and then compressed to TDC.

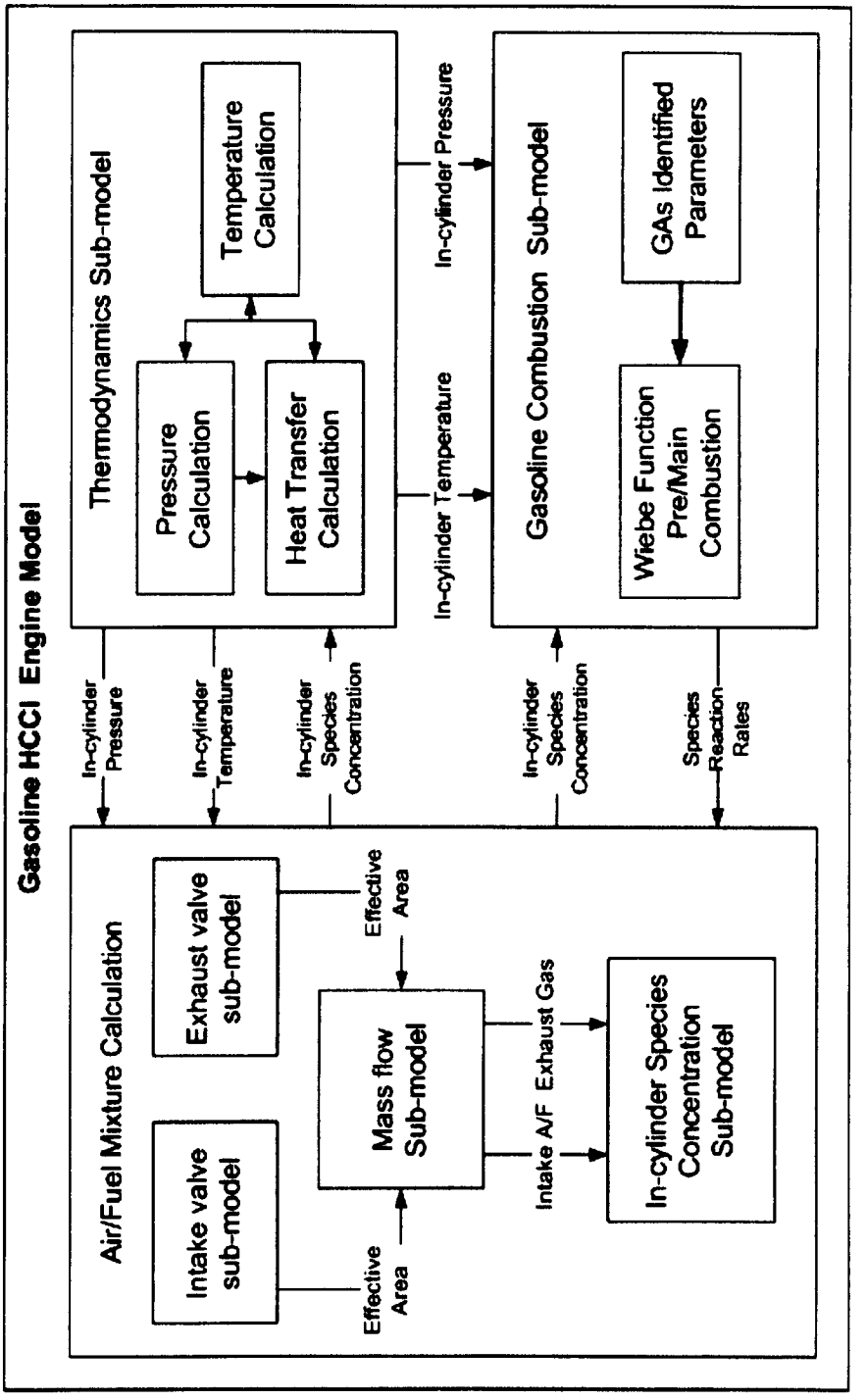

Figure 4-1 Schematic of gasoline fuelled HCCI engine model

After replacing the combustion sub-model in propane fuelled HCCI engine model developed in Chapter 3, the model is potentially capable of serving as a real-time simulation platform for gasoline NVO HCCI engine. The change required is fairly minor, since differences in fuels only involve the chemical reaction equation and some parameters in the combustion model. Specifically, the reaction in Equation 3.32 to 3.35 must be replaced by the valid reaction for the fuel being modelled. The schematic of the model is shown in Figure 4-1.

4.2 GASOLINE AUTO-IGNITION MODELLING BY USING WIEBE FUNCTION

4.2.1 GASOLINE AUTO-IGNITION

Auto-ignition in a gasoline-air mixture is generally defined as a rapid chemical reaction, which is not caused by an external ignition source such as a spark, a flame or a hot surface. It is widely accepted that auto-ignition is a chain reaction. The following equations are given by Heywood [108] to describe the auto-ignition process and defined ignition occurrence.

$$\tau_{id} = AP^{-n} \exp\left(\frac{E_A}{RT}\right) \tag{4.1}$$

where τ_{id} is the ignition delay, which defined as the time between the start of injection and the start of detectable heat release.

A and n are constants that dependent on the fuel from experiments.

E_A is an apparent activation energy

A common expansion of above Arrehenius function is given in equation 4.2 to indicate the auto-ignition occurrence.

$$\int_{t_i}^{t_i+\tau_{id}} \left(\frac{1}{\tau}\right) dt = 1 \tag{4.2}$$

where τ is the ignition delay at the conditions pertaining at time t.

t_i is the time of injection or the time of IVO [107].

Generally, gasoline auto-ignition is proposed with two particular types [88]: Single stage ignition (main combustion): High temperature auto-ignition precedes extremely rapid combustion of the air/fuel mixture. Cool flames (pre-combustion): Result in some hydrocarbons when the mixture is raised to 600 to 700 K. The general range of the threshold temperature is between 950-1100K [106, 113] for gasoline auto-ignition. The auto-ignition for gasoline HCCI process is very similar with the auto-ignition of end gas [120], which is described as the auto-ignition process is generally due to compression of the end-gas by expansion of the burned part of the charge. This raises the gas's temperature and pressure to the point where the end gas auto-ignites.

4.2.2 GASOLINE HCCI COMBUSTION MODELLING BY WIEBE FUNCTION

Followed by the discussion in previous section, the auto-ignition of gasoline HCCI process is similar with other compression-ignition combustion processes. Hence, using Wiebe function to model the gasoline HCCI combustion is the simplest and most convenient way. A common mass fraction burned profile is often represented by the Wiebe function:

$$X_{mb} = 1 - \exp\left(-a\left(\frac{\theta - \theta_i}{\Delta\theta}\right)\right)^{m+1} \tag{4.3}$$

where X_{m_b} is the mass of fuel burned.

θ_i is the crank angle of the ignition points.

$\Delta\theta$ is the combustion duration.

a and m are the adjustable shape parameters for Wiebe function.

One extensively used model developed by Watson *et al.* [121] is used in total diesel system simulations. It is based on the description of compression-ignition combustion – a rapid premixed burning phase followed by a slower mixing controlled burning phase. These two parts are weighted with a phase proportionality factor β and are given by:

$$X_{\mathrm{mb}} = \beta \cdot f_1 + (1-\beta)\cdot f_2 \tag{4.4}$$

where $f_1 = 1-\left(1-\tau^{c_{p1}}\right)^{c_{p2}}$, $f_2 = 1-\exp\left(-c_{d1}\right)^{c_{d2}}$

It has been reported by Qin *et al.* [88] that the heat release correlation includes two parts: the first part describes a low temperature heat release process leading to auto-ignition, and the second part describes the high temperature combustion process, and establishing these correlations is crucial in modelling the process. Considering HCCI combustion has both the characteristics of SI combustion and compressed combustion – uniform mixture and compressed-ignition combustion, there is no flame propagation in the cylinder and the charge is ignited and burned almost simultaneously. Hence, a simplified Watson Model as given by equation 4.4 may be suitable for describing HCCI combustion by omitting the diffusion burning phase namely, the phase proportionality factor β has been taken as 1 to indicate the main combustion process (above 10% - 15% mass fraction burned).

$$X_{mb} = f_1 = 1-\left(1-\tau^{c_{p1}}\right)^{c_{p2}} \tag{4.5}$$

As discussed above, the start of pre-combustion process is corresponded to the auto-ignition timing and the ignition temperature. The process is

characterised by slow reaction rates and small rate of heat release. It is an accumulating process of energy and active radicals. In this stage, temperature will increase not only from change of volume, but energy release from oxidation reactions. In the same time, some radicals appear during the chain propagation and branching reactions [88, 106, 108]. In Qin's report [88], the mass fraction burned profile has been given as:

$$X_{mb} = A + B\exp(-\frac{\theta}{C}) \tag{4.6}$$

where θ is the current crank angle.

A, B, C can be described by engine speed, n, and mass fraction of residual gas in the cylinder f_{rg} as following:

$$\ln A = a_1 + b_1 / n^{1.5} + c_1 / f_{rg}^{\ 2} \tag{4.7}$$

$$B = a_2 + b_2 \cdot n^2 + c_2 / f_{rg}^{\ 2} \tag{4.8}$$

$$C = a_3 + b_3 \cdot n^{2.5} + c_3 \cdot f_{rg}^{\ 3} \tag{4.9}$$

where the constants a, b and c have been given in table 4-1 [88] that were generalised for the V6 HCCI research engine in Tianjin University:

Table 4-1 Constants list for equation 4.7 to 4.9

Parameter	i	Value
a_i	1	-7.8946
	2	1021019.3
	3	-31700260
b_i	1	0.00344
	2	4.15745e-8
	3	62.054
c_i	1	-3.4486
	2	-2.4334e-8

3	4.5184e-10

Since the pre-combustion and main combustion threshold has been discussed above. In the model, the segment of combustion is modelled by Wiebe function with an ignition temperature threshold. During the combustion process, the combustion rate w_i can be determined by applying Weibe function for approximations. When the chemical reaction is treated as a simple instantaneous process, we have

$$\frac{d\alpha}{d\eta} = a(m+1)(\frac{\theta-\theta_i}{\Delta\theta})^m \exp[-a(\frac{\theta-\theta_i}{\Delta\theta})^{m+1}] \tag{4.10}$$

$$\alpha = \frac{Xm_b}{Xm_0} \tag{4.11}$$

$$\eta = \frac{\theta-\theta_i}{\Delta\theta} \tag{4.12}$$

where X_{m_0} is the mass of fuel.

θ_i is the crank angle of the ignition points.

$\Delta\theta$ is the combustion duration.

The combustion speed can be expressed as follows:

$$\frac{dm_b}{dt} = \frac{m_0}{\Delta\theta}\frac{d\theta}{dt}\frac{d\alpha}{d\eta} \tag{4.13}$$

Re-writting the equation 4.13 and converting the units of combustion speed rates from kg/s^2 to $mole/m^3\,s^2$, the equation 4.14 is derived:

$$w_i = \frac{[X]_{CH_y} V_i \dot{\theta} a(m+1)(\frac{\theta-\theta_i}{\Delta\theta})^m \exp[-a(\frac{\theta-\theta_i}{\Delta\theta})^{m+1}]}{V\Delta\theta} \tag{4.14}$$

where $[X]_{CH_y}$, θ_i, V_i are the concentration of fuel, crank angle and cylinder volume at the point where combustion begins.

4.3 PARAMETER IDENTIFICATION USING GENETIC ALGORITHMS

Wiebe function to describe the HCCI combustion process can lead to a much simpler mathematical model. However, the parameters in the equation are unknown and it is difficult to determine all the parameters by analytic or trial-and-error method. Genetic Algorithms has been chosen as a tool for identification those unknown parameters of the model. As well known, GAs is a search technique used in computing to find exact or approximate solutions to optimization and search problems. Also, as a numerical method, the solutions obtained by GAs are not mathematically oriented and the GA possesses an inherent robustness according to the design problem specifications. GAs is stochastic search methods that mimic the metaphor of natural biological evolution. The algorithms operate on a population which is composed of potential solutions by applying the principle of survival of the fittest of produce better and better approximations to a solution. At each generation, a new set of approximations is created by the process of selection individuals according to their level of fitness in the problem domain and breeding them together [122]. This process leads to the evolutions of the population, which are better suited to their environment than the individuals that they were created from, just as in natural adaptation. The property settings of the GAs are shown in table 4-2:

Table 4-2 GA generation properties list

Name of GA properties	Value of the GA properties
Number of generations	200
Number of individuals per	20

subpopulations	
Generation gap	0.9
Fitness Assignment	Rank-base fitness assignment
Selection	Stochastic uniform
Elite count	2
Crossover fraction	0.8
Mutation	Gaussian
Mutation rate	1.0

As an optimization method, GAs has the advantage that it is able to reach an optimal solution without benefit of explicit knowledge about the problem area. The only existing criterion to evaluate the quality of an individual is the fitness value of this individual. Hence, the evaluation function should provide the required information to GAs. Evaluation functions of many forms can be used in a GAs, subject to the minimal requirement that the function can map the population into a partially ordered set. As stated, the evaluation function is independent to the GAs but greatly dependent on the problem itself. After a number of different fitness functions are studied, it has been found that one particular fitness function gives the algorithm a good convergence and leads to more accurate solutions, which is the sum of absolute values of difference between the in-cylinder pressure histories from simulations and experiments. The fitness function is shown in equation 4.15 and the process for parameter identification using Genetic Algorithms is shown in Figure 4-2.

$$Sum = \min[abs(W_1 \times \sum_{1}^{2}(P_{sim} - P_{exp})_i + W_2 \times \sum_{3}^{5}(P_{sim} - P_{exp})_i + W_3 \times \sum_{6}^{7}(P_{sim} - P_{exp})_i)] \quad (4.15)$$

where i is the engine process stage.

P_{sim} is the simulated in-cylinder pressure.

P_{exp} is the experimental in-cylinder pressure data.

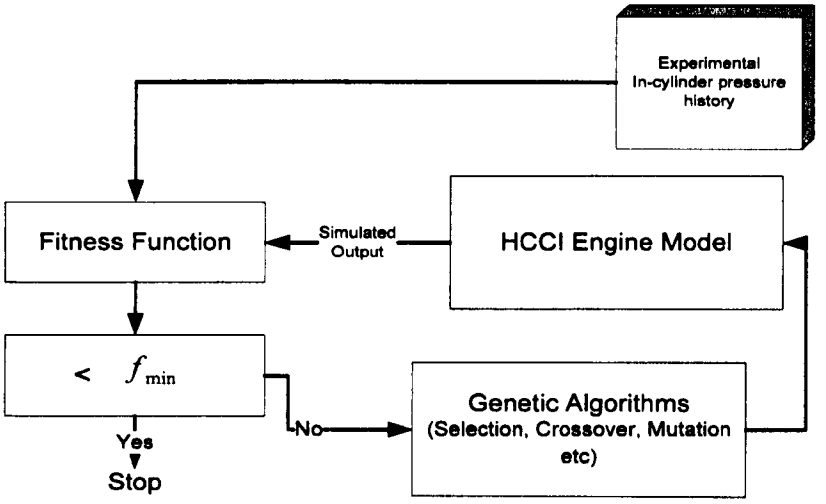

Figure 4-2 Process for parameter identification using GA for HCCI gasoline engine modelling

Referred back to equation 4.14, a set of initial simulation studies was conducted to identify which the parameters need to be identified or can be optimised by GAs. Figure 4-3 and 4-4 show the model predicted in-cylinder pressure with different combustion durations and ignition temperatures. It is observed that the longest combustion duration results a lowest peak pressure and latest ignition timing. Referred back to the equations 4.13 and 4.14, the phenomena can be explanted that the increasing of combustion duration leads to the decreasing of reactants concentrations, and thus the decreasing of reaction rates. The auto-ignition timing has been delayed caused by the lower reaction rates during pre-combustion period. Another trend can be found in

Figure 4-4, the lowest ignition temperature results a highest peak pressure, fastest pressure rates and earliest ignition timing. Within the combustion process, the concentration of reactants keep decreasing, however, since the early ignition occurs before the piston reaches TDC, the cylinder volume keep decreasing. These two effects have had a cancelling effect, thus compared with later ignition, the early ignition results in a higher reaction rates towards higher pressure rates and peak value.

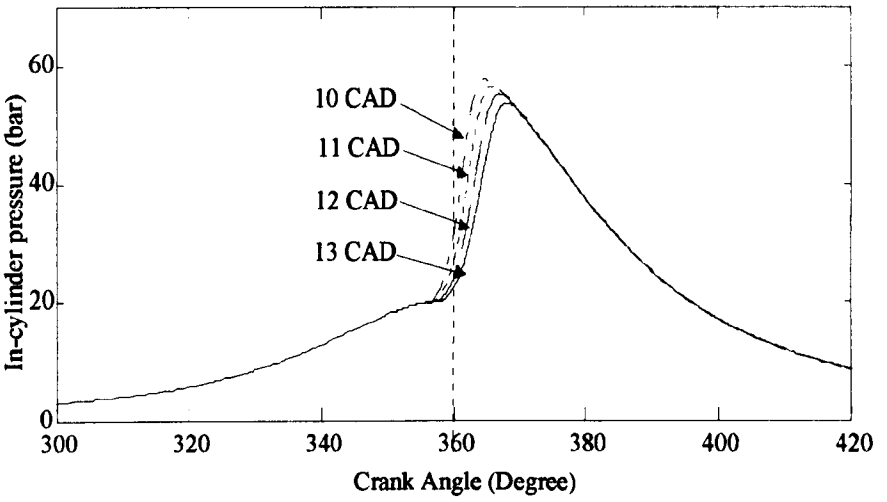

Figure 4-3 Simulation study of the efforts with different combustion durations

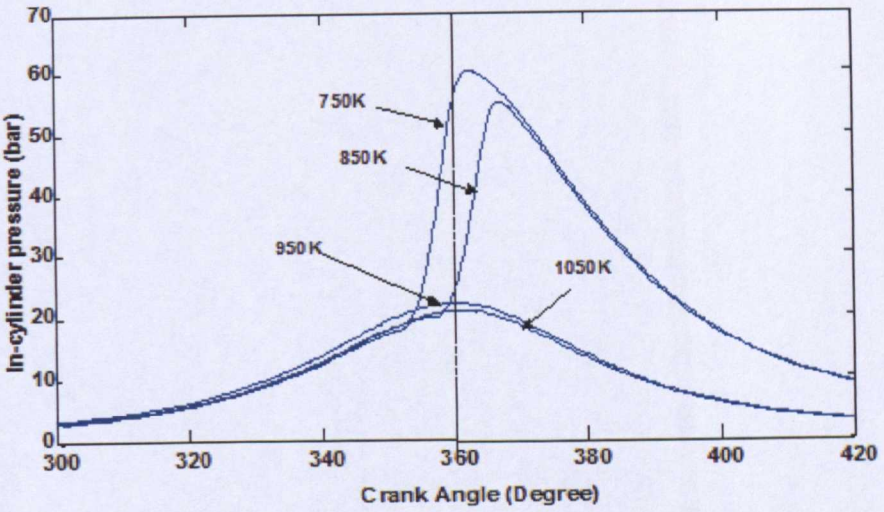

Figure 4-4 Simulation study of the efforts with different ignition temperature

After the initial study, eight parameters were recognised to be identified at least. The parameters are listed in table 4-3:

Table 4-3 Parameters to be identified

Parameters	Description
T_0	Initial temperature
T_{igLow}	Ignition threshold
$\Delta\theta$	Combustion duration
α	Weibe function parameter
m	Weibe function parameter
$ComRatio_{low}$	Adjustable parameter for slow reaction
H_{inlet}	Heat transfer rate when the intake valve operation
H_{outlet}	Heat transfer rate when the exhaust valve operation

4.4 Model Validation and Discussion

The in-cylinder pressure cycles have been compared against results obtained from a gasoline V6 test HCCI engine. The relevant engine parameters are listed in table 4-4. Simulations studies have been carried out for a variety of different engine speeds, inlet temperatures and inlet/exhaust valve timings within the experimental window of the V6 HCCI engine. The simulation conditions for six test examples are presented in table 4-5.

Table 4-4 Test engine parameters

Description	Value
Bore	89.02 mm
Stroke	79.59 mm
Connecting rod	138.10 mm
Compress Ratio	11.3
γ	1.0

Table 4-5 Engine operation conditions

Case number	IVO (aTDC)	EVC (bTDC)	Inlet Temperature(K)	Engine speed
Case 1	56	98	343	1500
Case 2	90	80	342	1500
Case 3	57	98	348	2000
Case 4	95	71	347	2000

Case 5	57	97	353	2500
Case 6	90	74	351	2500

The comparisons between the simulation and experimental results obtained are presented in Figure 4-5 to 4-10, and Table 4-6 listed the GA identified parameters for the model in different cases. The comparison is focussed on the ability of the model to predict the crank angle at which auto-ignition occurs, the corresponding in-cylinder peak pressure reached and the pressure cycle.

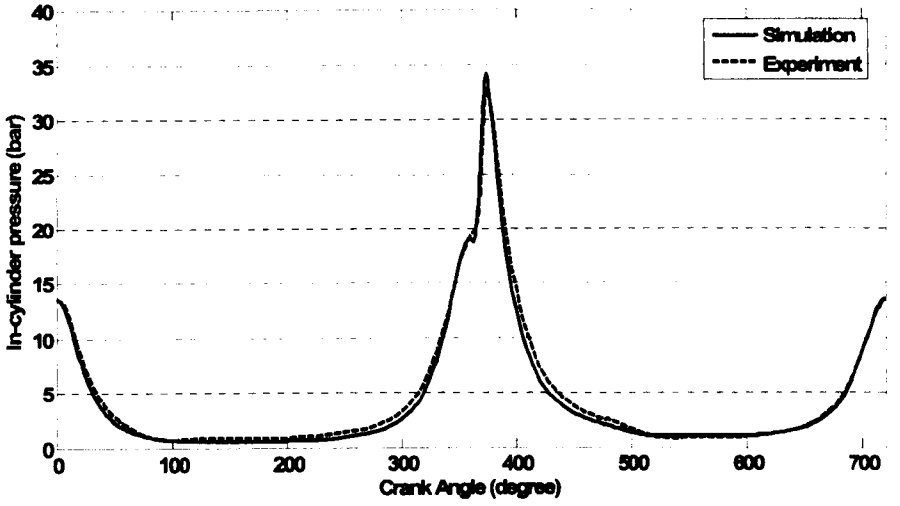

Figure 4-5 Case 1- In-cylinder pressure histories of simulation and experiment

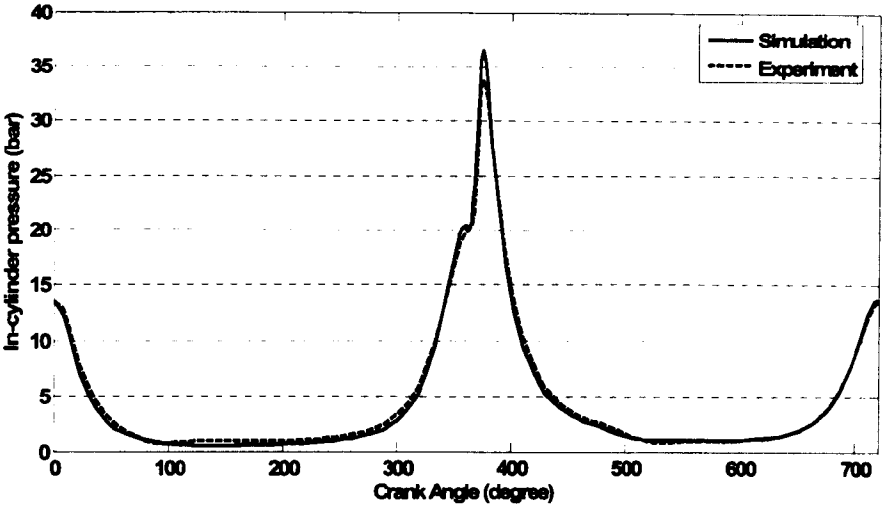

Figure 4-6 Case 2- In-cylinder pressure histories of simulation and experiment

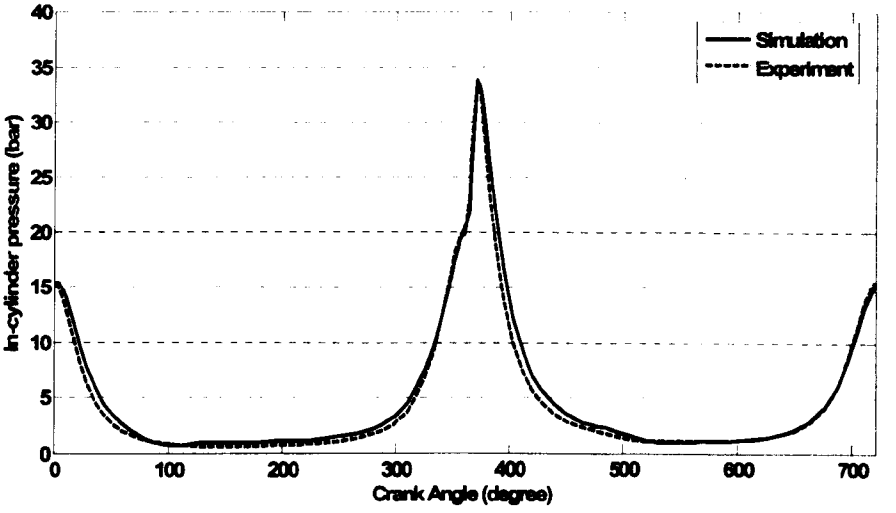

Figure 4-7 Case 3- In-cylinder pressure histories of simulation and experiment

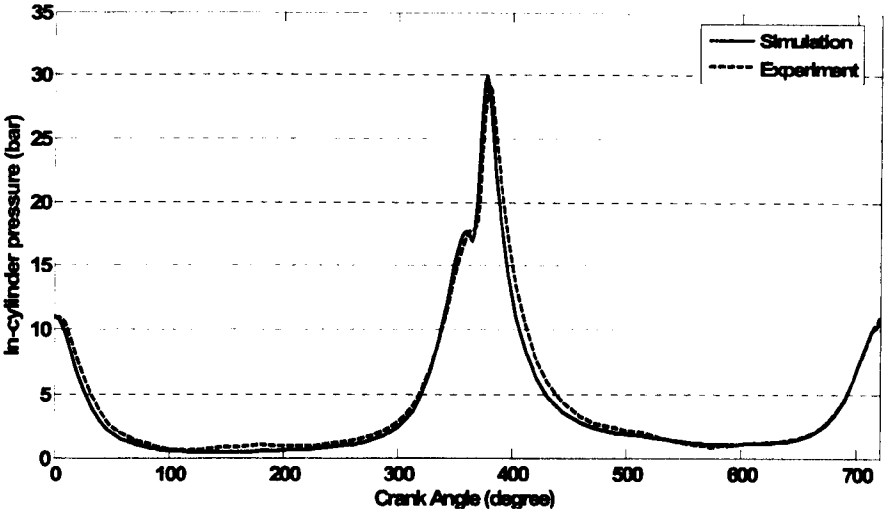

Figure 4-8 Case 4- In-cylinder pressure histories of simulation and experiment

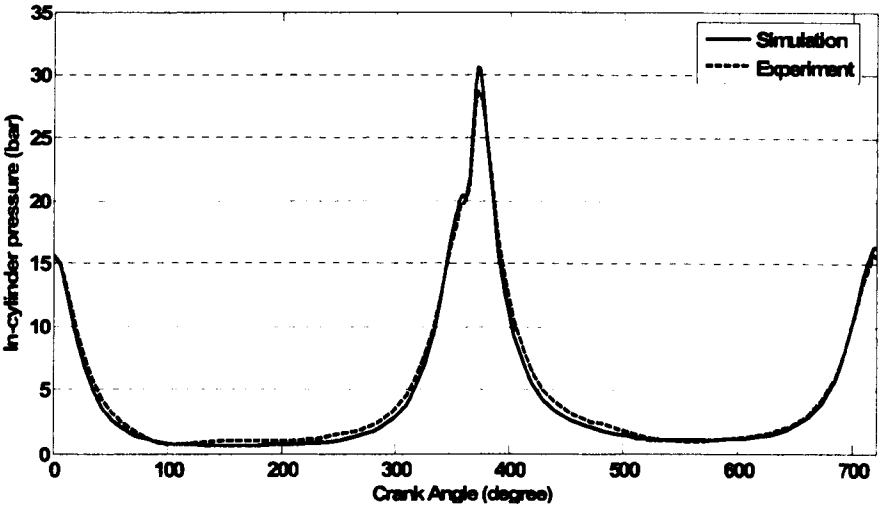

Figure 4-9 Case 5- In In-cylinder pressure histories of simulation and experiment

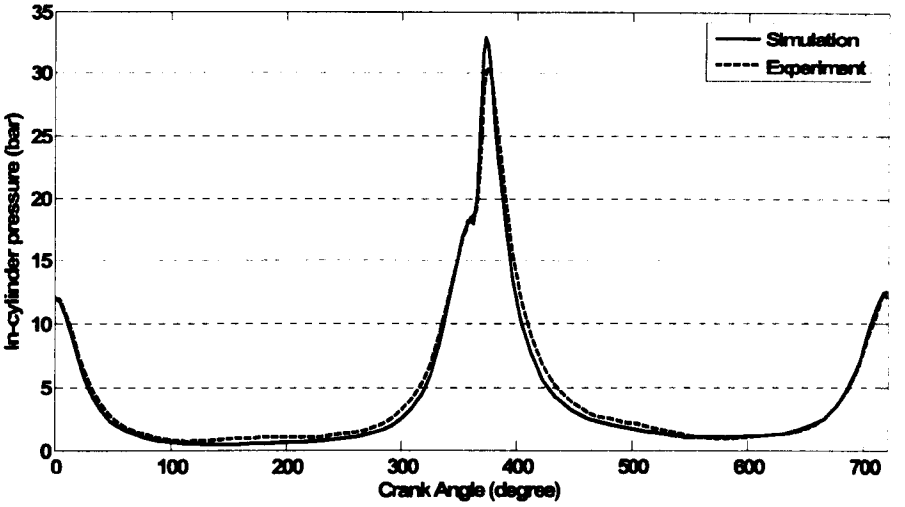

Figure 4-10 Case 6- In-cylinder pressure histories of simulation and experiment

Table 4-6 GA identified parameters for case 1- 6

Parameters	Case 1	Case 2	Case 3	Case 4	Case 5	Case 6
T_0	845.21	876.90	798.30	824.60	857.21	833.95
T_{igLow}	921.98	898.39	932.08	955.27	943.60	950.85
$\Delta\theta$	14.26	13.77	11.32	12.89	14.30	13.85
α	0.98	1.23	0.96	0.87	1.32	1.34
m	1.42	1.89	2.32	1.42	2.21	2.42
$ComRatio$	0.07	0.06	0.06	0.06	0.07	0.07
H_{inlet}	1.78	1.98	2.28	1.11	1.58	1.11
H_{outlet}	2.12	1.72	2.52	2.39	2.42	2.39
$Error_{aver.}$	4.32%	3.79%	4.56%	4.34%	4.10%	4.33%

In general, the results show fair agreement over the complete pressure cycle and the pressure history profiles predicted by simulation match closely with the measurements. As Table 4-6 shown, the average error, which is

calculated upon the basis of 720 CAD in one completed engine cycle, is less than 5% in each case. The critical comparisons focus on that the model can predict the instant of ignition and the peak pressure rise during combustion using. It can be observed that the model gives good generalisation of the magnitude of the peak pressure rise and also successfully follows the general trend in the pressure variation with the different operating conditions. However, because it is assumed that all fuel burns simultaneously throughout the entire cylinder volume in the model, the assumption results the model predictions are slight sharper rise to the peak pressure and also the slightly over-prediction of peak pressure compared with experimental results. The difference in the rate of pressure rising is also related to the simplified one-zone gas model that cannot take into account of in-cylinder temperature and mixture distributions. Another assumption is that the fuel in the cylinder will be consumed completely at the chemical stochiometric condition, but it is not the case in HCCI combustion experiments. In reality, the temperature and mixture are not perfectly uniform within the cylinder which causes a more gradual change during the combustion phase and also a small proportion of the mixture may not be burned during the combustion.

More validations have been conducted in order to exam the capability of the model using GAs identified parameters to predict HCCI behaviours. The experiments data have been obtained from the same V6 HCCI engine, which covers a certain range of HCCI operations: the engine speed is set up in the range between 1500 to 2500 rpm; the range of IVO is from 55 to 95 CAD (aTDC), which is modulated with the range of EVC from 61 to 97 CAD (bTDC). The detailed operation conditions are listed in Appendix A and shown in Figure 4-11 and 4-12.

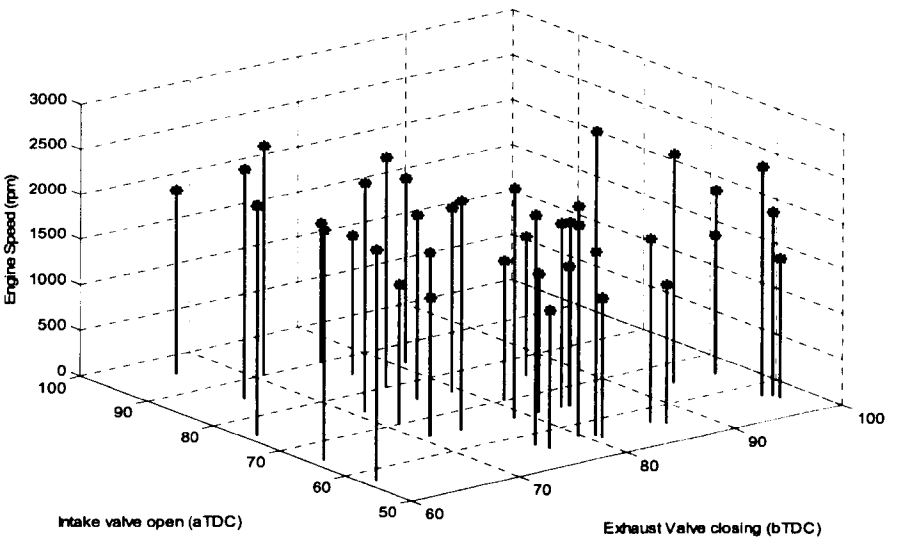

Figure 4-11 Experiments setup for GAs model validations

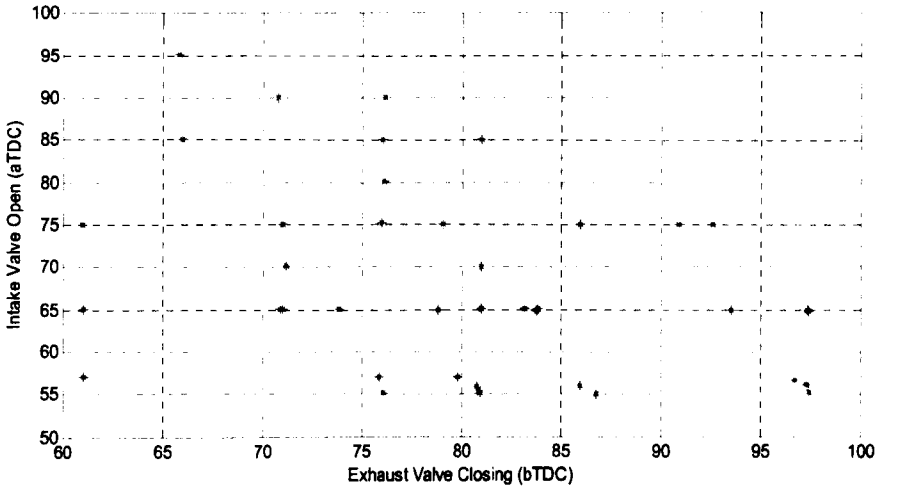

Figure 4-12 Valve timing setup of experiments

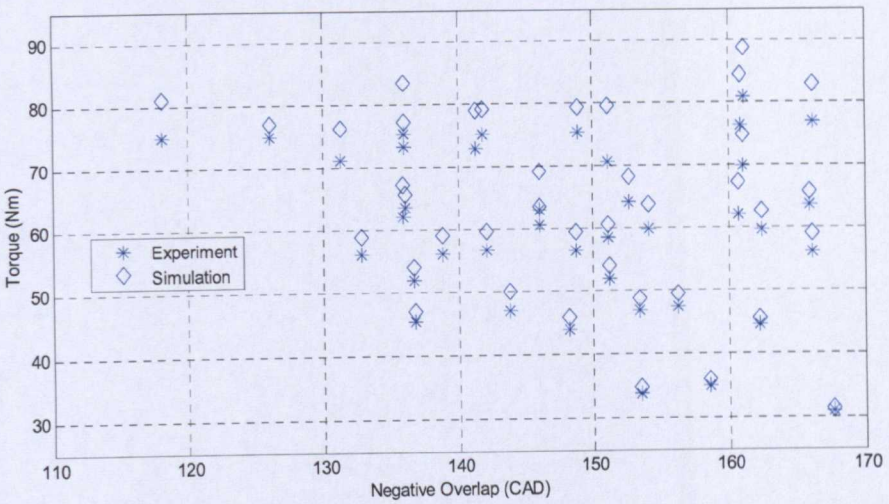

Figure 4-13 Torque comparison of simulation and experiments

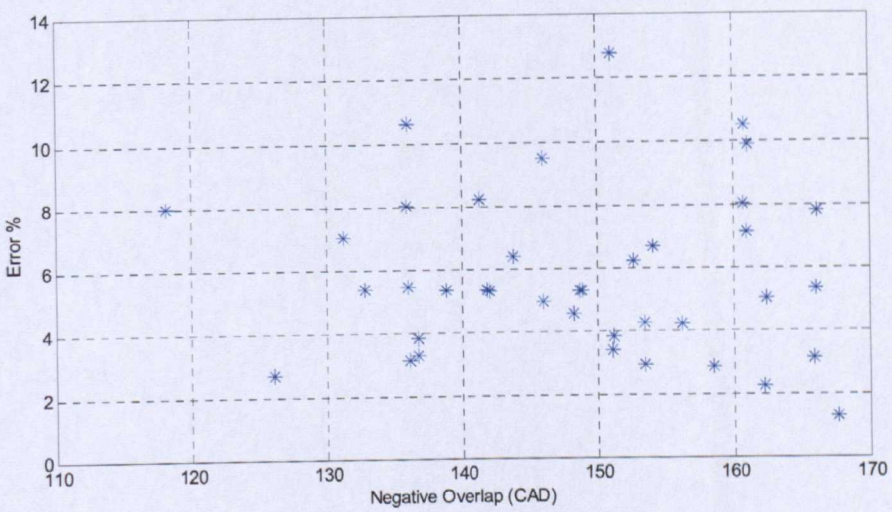

Figure 4-14 Torque errors distributions

The validation results is shown in Figure 4-13, where the Y-axis is engine torque output and the X-axis is the negative overlap that are equal to the sum of IVO (aTDC) and EVC (bTDC). The errors distribution diagram is shown in Figure 4-14. It is can be seen clearly that the average error of these 39 validation examples is around 6%, which is fairly good for this simplified

model. The interesting trend can be found from the results: all the simulations are over-predicted and the errors are increasing followed by the increase of engine torque output. The maximum error is above 12%, in which case, the relevant parameters have to be re-identified. And the minimum error is below 2% where the minimum torque output occurred. The error distributions indicate that the GAs model may need to be refined, specially, when the higher engine torque output is applied. Also, since the error is increasing while torque output increases, which caused by the larger amount of reactant inducted; and the operations are only conducted with different valve timings and intake temperatures, as the discharge coefficient of intake valve may need to be optimised by GAs

Referring back to Chapter 2, several control methods are introduced, which are widely applied for approaching HCCI combustion. In chapter 3, the affects of tuning exhaust valve timing and varying intake temperature have been investigated. This section is focusing on investigating the phenomena of HCCI process by boosting intake pressure and varying compression ratio, where all the rest parameters are fixed as constants.

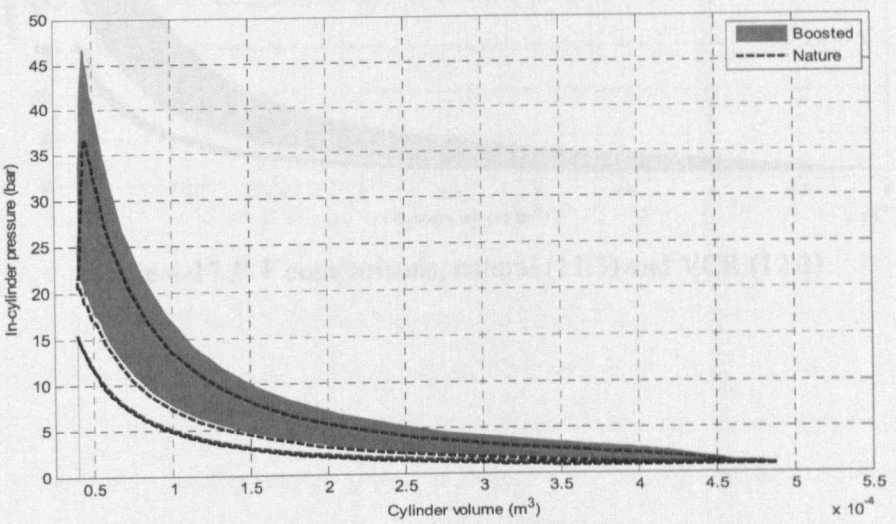

Figure 4-15 *P-V* comparisons, natural and boosted (1.2) intake pressure

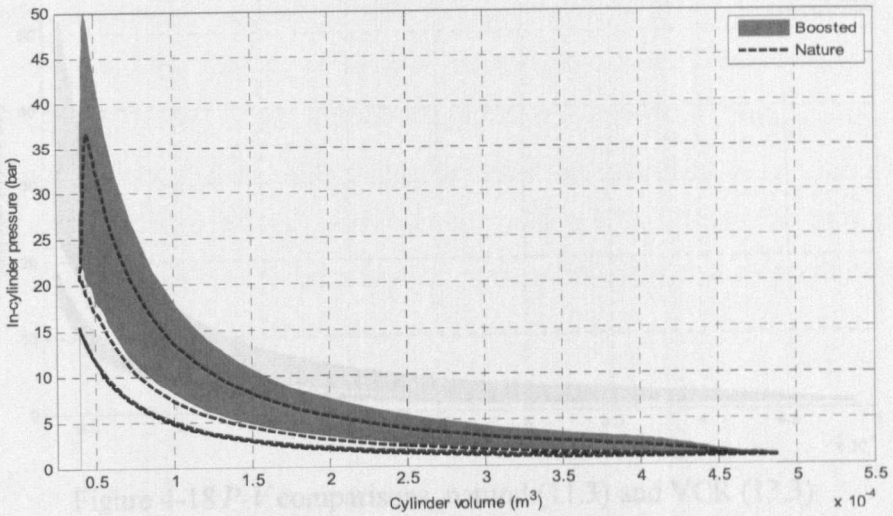

Figure 4-16 *P-V* comparisons, natural and boosted (1.4) intake pressure

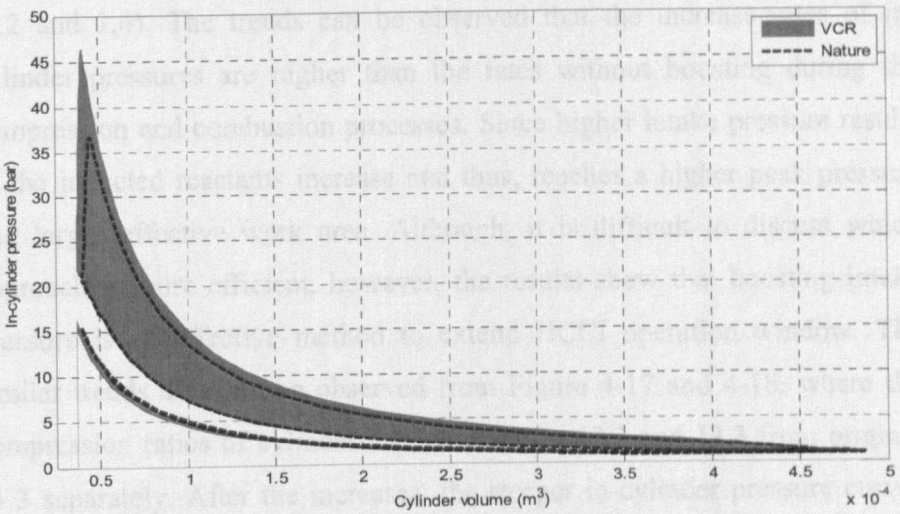

Figure 4-17 *P-V* comparisons, natural (11.3) and VCR (12.3)

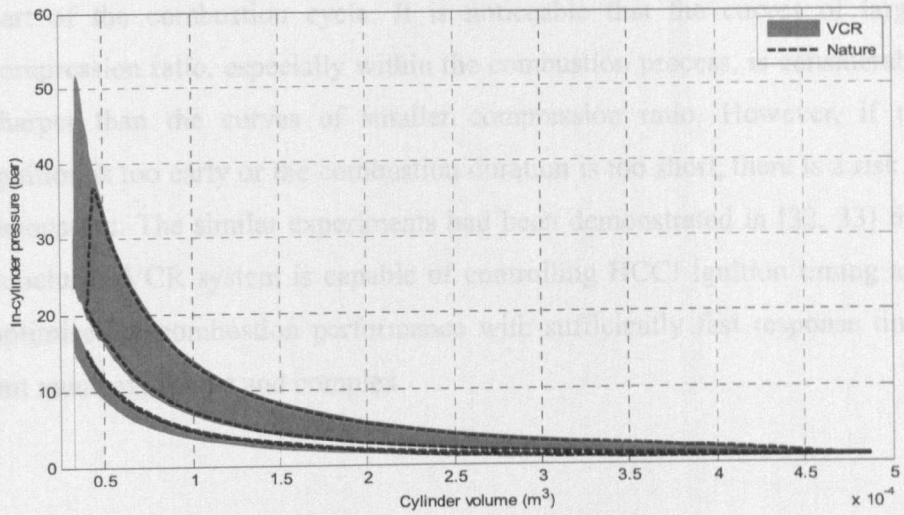

Figure 4-18 *P-V* comparisons, natural (11.3) and VCR (13.3)

The *P-V* diagrams shown in Figure 4-15 and 4-16 represent the comparisons of in-cylinder pressure evolutions with and without intake pressure boosting (1.2 and 1.4). The trends can be observed that the increase rates of in-cylinder pressures are higher than the rates without boosting during the compression and combustion processes. Since higher intake pressure results in the inducted reactants increase and thus, reaches a higher peak pressure and larger effective work area. Although, it is difficult to discuss which approach is more efficient, however, the results show that boosting intake pressure is an effective method to extend HCCI operation window. The similar trends also can be observed from Figure 4-17 and 4-18, where the compression ratios of cylinder are increased to 12.3 and 13.3 from original 11.3 separately. After the increases, the steeper in-cylinder pressure curves indicate the higher increase rates during the compression and combustion processes; also result in advanced ignitions and higher peak pressures that are because there is the similar amount of energy is being released in a smaller volume of combustion chamber, which accounts for the sharper rise in temperature and pressure, and also results in a larger torque output and positive work area as there is more energy being released in a more efficient

part of the combustion cycle. It is noticeable that the curves of larger compression ratio, especially within the combustion process, is considerable sharper than the curves of smaller compression ratio. However, if the ignition is too early or the combustion duration is too short, there is a risk of detonation. The similar experiments had been demonstrated in [32, 33] that concludes VCR system is capable of controlling HCCI ignition timing and optimise the combustion performance with sufficiently fast response time, but much expensive and complex.

4.5 SUMMARY

The mathematical model for a gasoline V6 HCCI engine with a NVO scheme has been developed and implemented by SIMULINK. Utilising Wiebe function to describe the combustion process, the simulation time consuming is sufficiently reduced. The genetic algorithms have been used to identify and optimise the parameters, which are assumed or unknown. The model simulated results have been compared with a series of experiment data obtained from the V6 HCCI test engine. The representative examples have been presented which are associated with four engine parameters variations: the engine speed, the inlet temperature, the inlet valve and exhaust valve timing. The comparisons have demonstrated that the model can simulate the in-cylinder pressure and auto-ignition timing – two of the most challenging problems of HCCI engines. Boosting intake pressure and varying compression ratio, two effective HCCI control methods, have been deployed into the model and the influences of the HCCI processes have been studied. Considering the simple structure and the capability on HCCI behaviours perdition, the model can be used as a practical engineering tool and a valuable test bed in the development of suitable control strategies.

Chapter 5

DEVELOPMENT OF ENGINE AND VEHICLE DYNAMIC MODELS

The simulation models, which are represented in Chapter 3 and Chapter 4, capture the most relevant aspects for control purpose - in-cylinder pressure evolution, work output and combustion process via simplified kinetics - with a level of fidelity matching experimental measurements. The inherent simple structure may offer real-time predictions by the models, which is very helpful in gaining intuition and desirable for providing an accurate virtual test-bed for control.

Followed by the development of the models, the key characteristic of negative valve overlap HCCI will be discussed in this chapter, which is the residual gas coupling between subsequent engine cycles. The cyclic modelling approaches represented in this chapter show the capability of the simple model to capture this coupling during transient and steady state, and also the self-stabilising nature of HCCI process.

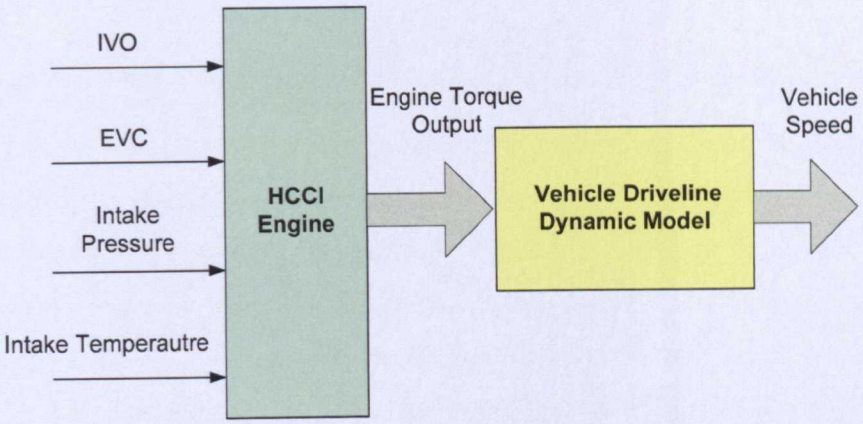

Figure 5-1 Block diagram of the extended HCCI engine - vehicle dynamics model

In this chapter the engine model is extended with a vehicle driveline dynamics model for HCCI control strategy investigation. The system diagram is shown in Figure 5-1. The vehicle driveline model, which is based on Mangan's work [123], describes the relationships among engine torque, torque converter, transmission gear box, final drive differential, brakes and drive wheels to overcome the running resistances and generate vehicle speed output. For the modelled vehicle driven by the HCCI engine, four variables affect the engine torque output, which are the timing of Inlet Valve Opens (IVO), the timing of Exhaust Valve Closes (EVC), the pressure of the intake mixture and the temperature of the intake mixture. The investigation has been carried out on how the four control variables influence the vehicle dynamics, which is open-loop control system study in nature. Some boundary conditions are obtained that can be used as the guidelines in controller design. Finally, closed-loop controls for IVO and EVC timing have been conducted by fixing the intake mixture pressure and temperature

5.1 CYCLE-TO-CYCLE MODELLING APPROACH

5.1.1 MATHEMATIC MODEL FOR INITIAL VALUE REFERENCE

Modelling for the HCCI engine that adopts negative valve overlap scheme, the general model structure has been discussed in Chapter 3 and the procedure schematic can be found in Figure 3-1. In order to simulate the residual gas coupling, the model has been slightly modified and some assumptions have been made to generate the relevant mathematic models. The first assumption is made as the EGR compression stage occurs isentropically, the residual gas temperature is directly related to the exhaust temperature from the previous cycle. The thermodynamic stage of the system prior to and following the stage may be related with the following isentropic relations for an ideal gas:

$$T_{7,1,n} = \left(\frac{V_{6,7,n-1}}{V_{7,1,n}} \right)^{\gamma-1} \cdot T_{6,7,n-1} \tag{5.1}$$

And

$$P_{7,1,n} = \left(\frac{V_{6,7,n-1}}{V_{7,1,n}} \right)^{\gamma} \cdot P_{6,7,n-1} \tag{5.2}$$

where n is referred to n^{th} engine cycle.

γ is the specific heat ratio.

$T_{7,1}$, $P_{7,1}$, $V_{7,1}$ are referred to the in-cylinder temperature, pressure and the displayed cylinder volume at the beginning of the engine cycle (TDC) respectively.

$T_{6,7}$, $P_{6,7}$, $V_{6,7}$ are referred to the in-cylinder temperature, pressure and the displayed cylinder volume at the exhaust valves closure respectively.

The EGR expansion stage exhaust stage is also assumed to be isentropic, hence, we have:

$$T_{1,2,n} = \left(\frac{V_{7,1,n}}{V_{1,2,n}}\right)^{\gamma-1} \cdot T_{7,1,n} \tag{5.3}$$

and

$$P_{1,2,n} = \left(\frac{V_{7,1,n}}{V_{1,2,n}}\right)^{\gamma} \cdot P_{7,1,n} \tag{5.4}$$

where $T_{1,2}$, $P_{1,2}$, $V_{1,2}$ are referred to the in-cylinder temperature, pressure and the displayed cylinder volume at the beginning of intake valve opining respectively.

The inducted gas composition is formulated as the ratio of the moles of residual products N_{Re} to the moles of inducted reactant charge N_{I}:

$$\alpha = \frac{N_{\mathrm{Re}}}{N_{\mathrm{I}}} \tag{5.5}$$

The mixing fresh air/fuel reactant and residual product species during the intake process for lean or stoichiometric propane HCCI can be represented as:

$$\begin{aligned} &\alpha\left(3\phi CO_2 + 4\phi H_2O + 18.8N_2 + 5(1-\phi)O_2\right. \\ &\left.+ \left(\phi C_3H_8 + 5O_2 + 18.8N_2\right)\right) = \\ &\phi C_3H_8 + 5(\alpha(1-\phi)+1)O_2 + 18.8(1+\alpha)N_2 \\ &+ 3\alpha\phi CO_2 + 4\alpha\phi H_2O \end{aligned} \tag{5.6}$$

where ϕ is the equivalence ratio, which is defined as the ratio of moles of fuel to the amount required for the complete combustion of both fuel and oxygen, such that the reactant mixture is $\phi C_3H_8 + 5O_2 + 18.8N_2$.

And for variant fuels, *i.e.* gasoline, the coefficients can be modified as the reaction equations. Also ϕ is corresponding to the actual air/fuel ratio, α is corresponding to the actual internal EGR ratio.

The assumption of intake process has been made as an adiabatic constant pressure process, where the first law of thermodynamics can be applied to modify the equation 3.21 as following:

$$\frac{d(mh)}{dt} = \dot{m}_1 h_1 \tag{5.7}$$

The fresh reactant intake mass flow rate through the intake is $\dot{m}_1$ with corresponding enthalpies in the intake, h_1. When this equation is integrated from the beginning to the end of the intake process with the assumption that manifold conditions do not vary during intake process, the resulting expression for the n^{th} engine cycle at the point of intake valve closure is:

$$\sum_{species\ in-cylinder} N_{i,2,3,n}\hat{h}_i(T_{2,3,n}) = \sum_{residual\ products} N_{i,6,7,n-1}\hat{h}_i(T_{2,3,n}) + \sum_{intake\ reactants} N_{i,1,n-1}\hat{h}_i(T_1) \tag{5.8}$$

5.1.2 Simulation Results and Discussion

As the assumptions are discussed, the additional models have been implemented by SIMULINK and added into the system for referring the initial value of residual gas from previous cycle to current engine cycle. The subsequent investigations has been continuing, which focus on the model inherent has the ability to predict cycle-to-cycle coupling, specially, the transient state of engine when the variety valve timing references are applied

and the affect of the modulation of the gas composition of fresh reactants and residual products.

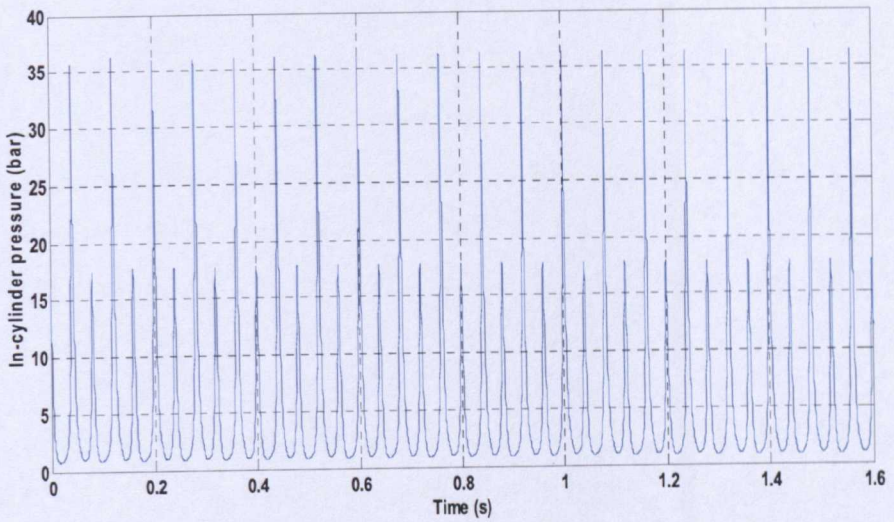

Figure 5-2 Typical cycle-to-cycle simulation

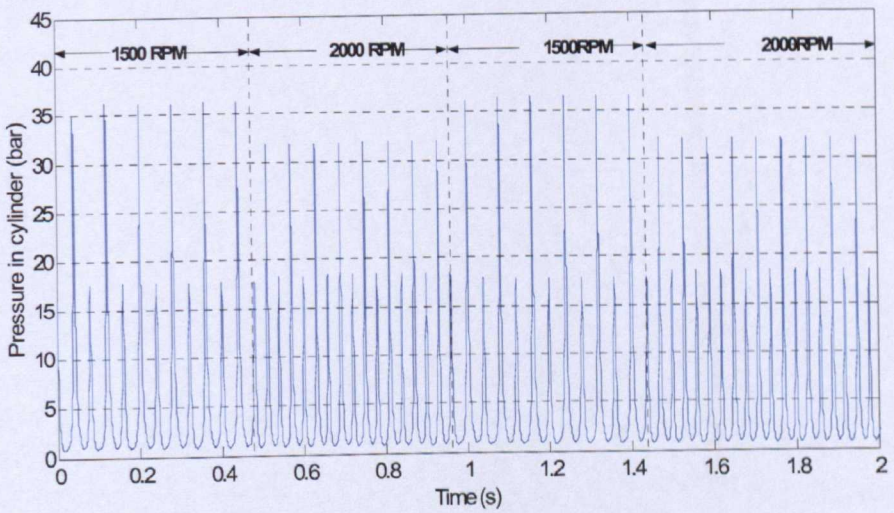

Figure 5-3 Engine speed variants test

Figure 5-2 shows a typical cycle-to-cycle simulation results. The simulation commenced with the first cycle using estimated initial in-cylinder conditions whilst subsequent cycles followed the conditions inherited from the previous

cycle. The cyclic coupling of the HCCI process has been simulated by the model with the cycle behaviour becoming steady after only one cycle.

The investigation has been carried on with varying the engine operation speed for testing the capability of the model to response with engine speed variants. A simulation example is shown in Figure 5-3. By varying engine speed with fixed valve operation timing, the simulation model starts with engine speed setting up to 1500 rpm and then increasing the engine speed to 2000 rpm. Since the valves timing is fixed and the opening/closure duration of the valves is also fixed (the valve lift profile is fixed against crank angle), the higher engine speed results in a smaller amount reactant inducted into the cylinder and a lower in-cylinder pressure. The simulation result clearly shows that the model captures the cycle-to-cycle coupling correctly and predicts the trend of pressure evolutions successfully against different engine speed operations.

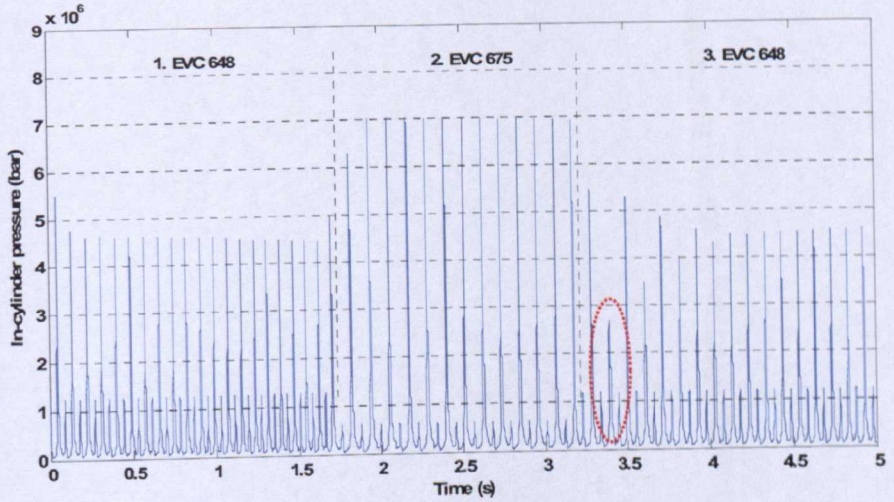

Figure 5-4 EVC timing variants test

More simulation studies have been completed for investigating the affect of the modulation of in-cylinder gas composition. The example shown in Figure

5-4 is for the simulation testing of varying exhaust valve timing against a fixed engine speed. The engine simulation starts with setting up the exhaust valve closing time to 648 CAD, then varying it to 675 CAD and changing back to initial setup at 648 CAD. The engine fitting with NVO scheme is used to varying intake and exhaust valve profiles to achieve HCCI combustion. The residual products are trapped by varying the exhaust valves closing timing when the valve lift profile has been fixed. For later exhaust valve closing, the amount of combustion products trapped in the cylinder is decreased, results in lower pressure rising during the EGR compression and causes an increase in the amount of fuel and air inducted, which will result in a higher pressure rising during the combustion process. So through modulation of the EVC timing, the relative amounts of reactants and residual combustion products can be changed. It is clearly to see from the Figure 5-4, the model simulates the cyclic in-cylinder pressure and captures the transients during the valve timing changing. However it's notably, there are few of in-cylinder pressure cycle are not stabilised when the exhaust valve timing is referred back to 648 CAD. The dashed circle in the figure indicates a later ignition/combustion process, it may caused by when the EVC moving forward for 675 CAD to 648 CAD, the relevant more low temperature products are trapped in the cylinder, diluting the combustion and resulting in the internal energy may not be able to maintain the HCCI ignition timing stable. Since the later ignition occurred, the combustion may not be stoichiometric, portions of unburned reactants will be pulled out cylinder through the exhaust process and the rest portions will be trapped in the cylinder and mixed with combustion products going to next engine cycle. That results in a relevant higher pressure rise in next engine cycle since the small amount unburned fuel will increase the reactants concentration. After several of engine cycles the combustion is stabilised without changing the operation. That also indicates another important factor of HCCI combustion - self-stabilizing nature of HCCI adopting negative valve overlap scheme.

Figure 5-5 shows an example of cyclic reaction timing revolutions against two EVC timing variants. It's clear to see from the Figure that the combustion timing and duration both are going to be stabilised after few of unstable cycle, which may be caused by the errors of initial conditions setup.

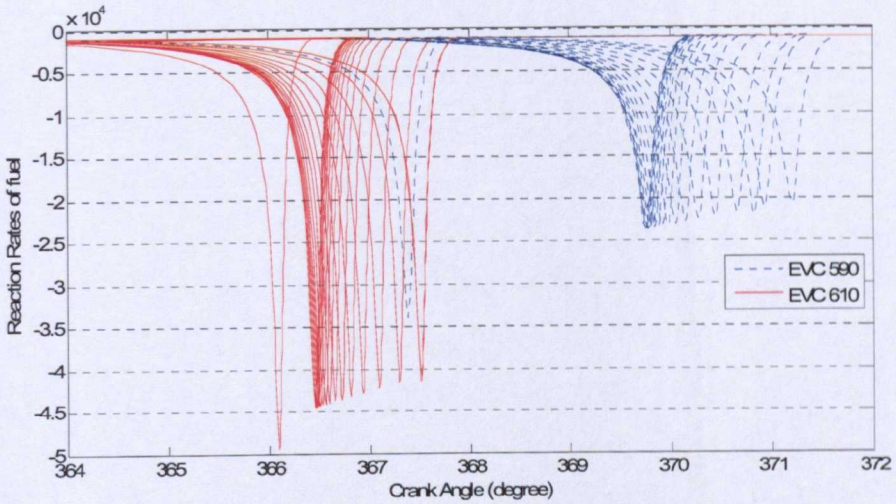

Figure 5-5 Cyclic reaction evolutions of two EVC variants

The results indicate the key insight from the modelling work, which is that the combustion timing can be predicted with these simple and intuitive models - the simplified two-stage Arrhenius/Wiebe function models. The dependence of combustion timing on the in-cylinder temperature, reactant concentrations and final valve closure is evident from equation 3.33, 3.34 and 4.14. These relations capture the fact that the combustion timing will occur earlier for any of the following behaviours: increased reactant concentrations (fuel and air), increased mixture temperature or increased compression. This dependence on both temperature and reactant concentrations is especially important for HCCI adopting NVO scheme, where trapped exhaust species from the previous cycle both dilute and increase the temperature of the reactant species. Since the dilution of reactants delays the onset of combustion, but the increase in reactant

temperature advances the onset of combustion. Hence, as residual mass fraction increases (*i.e.* as dilution increases) the reactant concentration decreases while the initial mixture temperature increases. This leads to very little change in combustion timing for varying amounts of dilution, giving the system a self-stabilizing characteristic.

5.2 EXTENSION OF THE HCCI ENGINE MODEL FOR CONTROL DEVELOPMENT

The insights discussed above and in previous chapter provide valuable clues about how to approach the control problem. Since the cycle-to-cycle model shows its capability to predict the HCCI behaviours during the steady state and transient against different engine operations and also its inherent simple structure can offer the model to simulate one completed engine cycle within 0.03 seconds on a PC. The time consuming of the simulation is nearly fast enough for real-time simulation, hence the model provides a useful tool for a model based controller design and also an off-line engine test platform to verify the control strategies developed. The HCCI process model has then been extended by combining a simplified driveline model [123] in order to investigate the control strategies.

5.2.1 DESCRIPTIONS OF VEHICLE DRIVELINE

Before introducing the modelling work, it's important to give a basic introduction to vehicular driveline system. A complete driveline model would be capable of six degrees of freedom, which includes roll, pitch, yaw, longitudinal, lateral and vertical [123]. However in this thesis, the driveline is only modelled with one degree of freedom, longitudinal motion. This is because the model is only required to provide a longitudinal acceleration

estimate. And it will also ensure that the model is kept as simple as possible for real-time control strategy development. Figure 5-6 depicts the driveline model for a rear driven vehicle fitting with an auto-transmission. The main parts of the driveline system includes: engine, torque converter, auto-transmission, drive shafts and wheels.

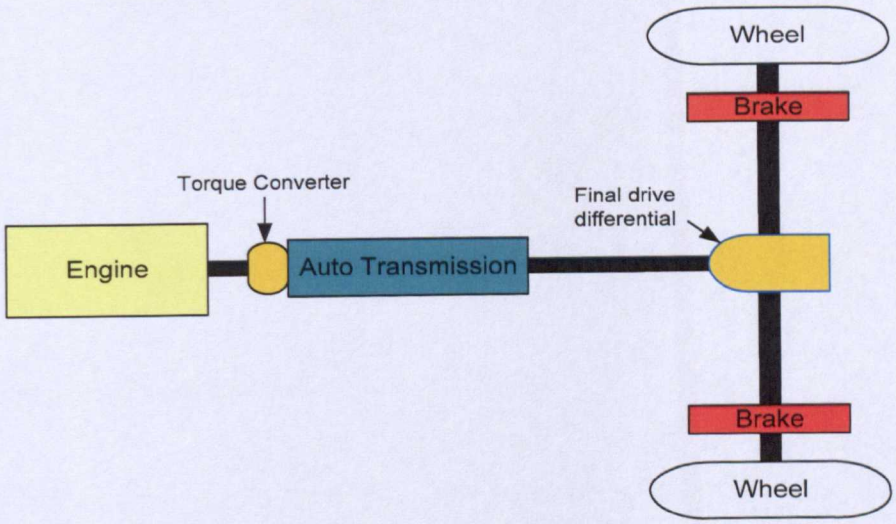

Figure 5-6 A typical driveline system fitting auto-transmission

ENGINE

The HCCI engine models are integrated into the driveline model to simulate the force produced by engine. As Figure 5-7 shows the inputs of engine model is valve timing, air/fuel ratio and engine speed that is converted from vehicle speed as the feedback of system output. The force, which required by driveline model, is estimated in torque, hence the in-cylinder pressure history output from engine model is converted to torque output as the input of driveline model.

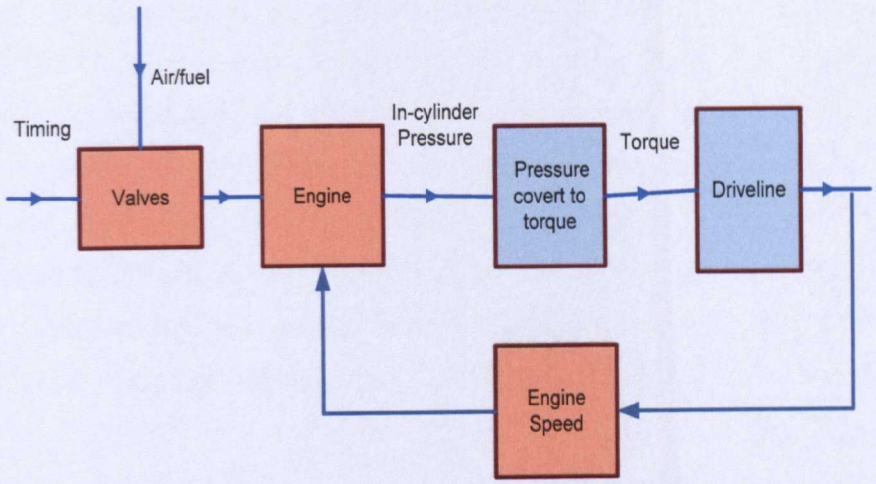

Figure 5-7 Schematic of system inputs and outputs

TORQUE CONVERTER

As the connection between the engine and the auto-transmission, torque converter is a type of fluid coupling that allows the engine to spin somewhat independently of the transmission. In general, torque converter operates in the following manner. The housing of the torque converter is bolted to the flywheel of the engine, so it turns at whatever speed the engine is running at. The fins that make up the pump of the torque converter are attached to the housing, so they also turn at the same speed as the engine. The pump inside a torque converter is a type of centrifugal pump. As it spins, fluid is flung to the outside. As fluid is flung to the outside, a vacuum is created that draws more fluid in at the centre. The fluid then enters the blades of the turbine, which is connected to the transmission. The turbine causes the transmission to spin, which basically moves the vehicle. The blades of the turbine are curved. This means that the fluid, which enters the turbine from the outside, has to change direction before it exits the centre of the turbine. It is this directional change that causes the turbine to spin. The fluid exits the turbine at the centre, moving in a different direction than when it entered. The fluid

exits the turbine moving opposite the direction that the pump (and engine) is turning. If the fluid were allowed to hit the pump, it would slow the engine down and wasting power. This is why a torque converter has a stator. The stator resides in the very centre of the torque converter. Its job is to redirect the fluid returning from the turbine before it hits the pump again. This dramatically increases the efficiency of the torque converter [124]. Figure 5-8 shows the main sections of the torque converter. And the typical torque multiplication for a torque converter can be seen in Figure 5-9.

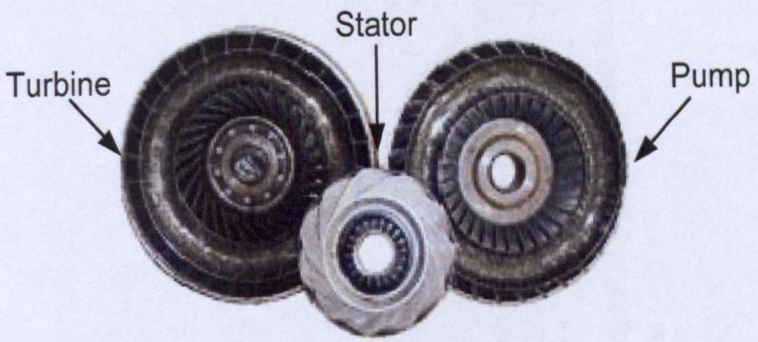

Figure 5-8 Torque converter components

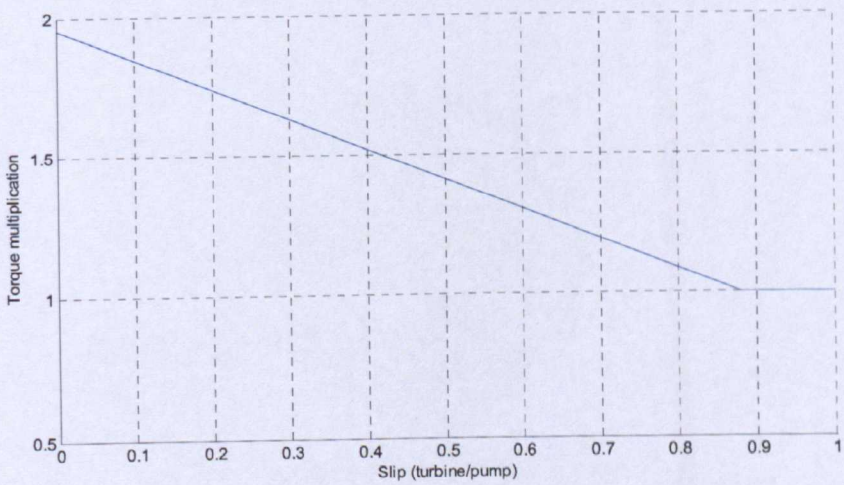

Figure 5-9 Typical torque multiplication characteristics

AUTO-TRANSMISSION

The transmission is used to allow the engine to operate at a small range of speeds whilst providing a wide range of output speeds. Generally, the transmission uses gears to make more effective use of the engine's torque, and to keep the engine operating at an appropriate speed. There two main types of transmissions – manual and automatic. In the thesis, an auto-transmission is fitted with the modelled vehicle driveline. The key difference between manual and automatic transmission is that the manual transmission locks and unlocks different sets of gears to the output shaft to achieve the various gear ratios, while in an auto-transmission; the same set of gears produces all of the different gear ratios. The planetary gear set is the device that makes this possible in an auto-transmission. As Figure 5-10 shown, the planetary gear set has three main components: the sun gear, the planet gears (and its carrier) and the ring gear. Each of these three components can be the input, the output or can be held stationary. Table 5-1 shows the typical gear combinations [124].

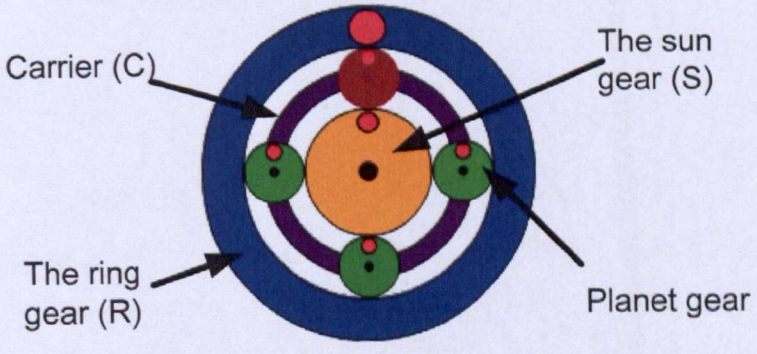

Figure 5-10 the planetary gear set

Table 5-1 Planetary gear combinations [124]

Input	Output	Stationary	Calculation	Gear Ratio
Sun (S)	Planet Carrier (C)	Ring (R)	1+R/S	3.4:1
Planet Carrier (C)	Ring (R)	Sun (S)	1/(1+S/R)	0.71:1
Sun (S)	Ring (R)	Planet Carrier (C)	-R/S	-2.4:1

By locking any two of the three components together will lock up the whole device at 1:1 gear reduction. The first gear ratio listed above is a reduction and the output speed is slower than the input speed. The second is an overdrive; the output speed is faster than the input speed. The last is a reduction again and the output direction is reversed. Thus this one set of gears can produce all of these different gear ratios without having engage or disengage any other gears. The auto-transmission in the modelled driveline is adopted a 5-speed automatic gearbox, the detailed gear ratios are listed in Table 5-3.

FINAL DRIVE

Known as the differential, final drive plays as the role to transfer power from the propeller shaft to the drive shafts and then onto the wheels. The differential has a gear ratio that increases the torque from the transmission, so called the final drive ratio or differential ratio, which is listed in Table 5-3. The main functionality of differential can be describe as following: when the vehicle is travelling in a straight line both wheels will rotate at the same speed; when the vehicle is travelling around a corner the outside wheel will rotate quicker, because it has further to travel. When the outside wheel

rotates quicker the gear arrangement in the differential will make the other drive shaft start to turn backwards. This action will not cause the wheel to turn in the opposite direction and the opposite rotation will just slow the inside wheel down slightly.

5.2.2 MATHEMATIC MODELS OF THE VEHICLE DRIVELINE

The vehicle acceleration can be described by using Newton's second law with the following equation:

$$a = \frac{F}{m} \tag{5.8}$$

where F is the resulting vehicle driving force.

m is the total mass of the vehicle. In the driveline model, the vehicle mass is assumed as a constant.

The driving force is calculated by:

$$F = F_{\text{drive}} - F_{\text{R}} \tag{5.9}$$

where F_{drive} is vehicle drive force powered by the engine.

F_{R} is the resistance force, which includes two main opposing forces, they are running resistance and brake force.

Followed by above basic mathematic equations, Mangan [123] developed a group equation to model the driveline system in 2004. The model is composed by following equation:

$$F_{\text{Drive}} = \frac{T_{\text{e}} \times \mu \times i_{\text{t}} \times i_{\text{d}}}{r} \tag{5.10}$$

$$F_{\text{Brake}} = b_{\text{p}} \times k_{\text{b}} \tag{5.11}$$

$$F_{\text{Roll}} = f \times m \times g \times \cos(\theta) \tag{5.12}$$

$$F_{\text{Air}} = 0.5 \times \sigma \times C_{\text{w}} \times A \times v^2 \tag{5.13}$$

$$F_{\text{Hill}} = f \times m \times g \times \sin(\theta) \tag{5.14}$$

$$a = \frac{F_{\text{Drive}} - F_{\text{Brake}} - F_{\text{Roll}} - F_{\text{Air}} - F_{\text{Hill}}}{m} \tag{5.15}$$

where F_{Brake} represents the break line force.

F_{Roll} represents the rolling resistance, which is the product of the deformation processes at the contact patch between the tyre and road surface.

F_{Air} represents the aerodynamic drag.

F_{Hill} represents the climbing resistance (with a positive operation sign) and downgrade force (with a negative operational sign).

a represents the vehicle acceleration.

b_{p} is the brake line pressure;

θ represents the longitudinal road gradient.

μ is found using the torque converter characteristic chart available from the torque converters manufacturer.

The other parameters are given in Table 5-1.

Table 5-2 Jaguar XKR Vehicle Model Parameter Values

Parameter	Description	Units
a	Vehicle acceleration	m/s^2
T_{e}	Estimated engine torque	N.m
i_{d}	Final drive gear ratio	3.06
r	Tyre radius	0.306
b_{p}	Brake line pressure	Bar

k_b	Brake coefficient	253.5
f	Coefficient of rolling resistance	0.01
m	Vehicle mass	Approx 1950 kg
g	Gravity	9.81 m/s^2
θ	Longitudinal road gradient	Radians
σ	Air density	1.202kg/m^2
C_w	Drag coefficient	0.36
A	Vehicle front area	2.2m^2
v	Vehicle velocity	m/s

The gear box auto switching scheme is simplified and modelled in this section as well, where it assumes the gear position changes finish instantly. The gear box auto switching scheme is given in Table 5-2

Table 5-3 Simplified gear box auto switching scheme

Vehicle Velocity		Auto Switch Gear Box	
Velocity (mile/hour)	Velocity (m/s)	Position	Gear Ratio
[0 ~ 5]	[0 ~ 2.2345]	1st	3.59
(5 ~ 15]	(2.2345 ~ 6.7035]	2nd	2.19
(15 ~ 30]	(6.7035 ~ 13.4070]	3rd	1.41
(30 ~ 45]	(13.4070 ~ 20.1105]	4th	1
(45 ~ 100]	(20.1105 ~ 44.6900]	5th	0.83

5.2.3 MATHEMATIC MODEL OF ENGINE TORQUE

In order to calculate the driving force, pressure evolutions for the gas in the cylinder over the operating cycles of the engine is used to calculate the work transfer from the gas to the piston. The indicated work per engine cycle is obtained by integrating around the *P-V* curve to obtain the area enclosed on the Figure 5-11:

$$W = \oint P \cdot dV \tag{5.16}$$

where W is the work output from the cylinders.

P represents the cylinder pressure.

V represents the piston displaced volume.

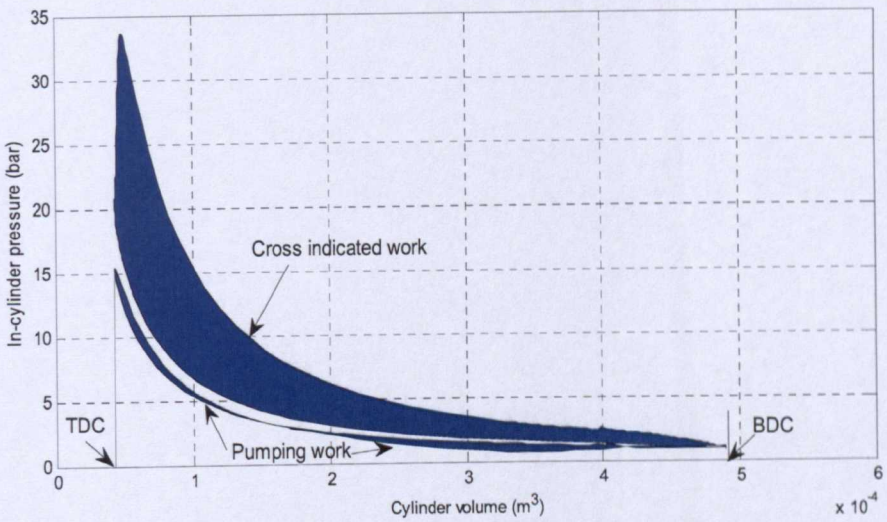

Figure 5-11 Typical P-V diagrams of a HCCI engine cycle

Regarding to the engine work output, the indicated work are usually defined as follows: the gross indicated work is that the work delivered to the piston over the compression and expansion strokes; the net indicated work is that the work delivered to the piston over the entire four-stroke cycle. And also the work transfer between the piston and cylinder gases during the intake and exhaust stokes is defined as pumping work. In this thesis, the work per cycle of the four-stroke cycle engine is defined as gross indicated output. Since the indicated quantities are used primarily to identify the impact of the compression, combustion and expansion processes on engine performance. And it represents the sum of the useful work available at the shaft and the work required to overcome all the engine losses[108]. The equation for engine power, which is related to the indicated work per cycle, is given as:

$$P_{ower} = \frac{W \cdot n}{2} \tag{5.17}$$

where P_{ower} represents the engine power output.

n represents the engine speed.

The torque exerted by the engine can be given as

$$T_e = \frac{P_{ower}}{2 \cdot \pi \cdot n} \tag{5.18}$$

where T_e represent the engine torque output

$$n = \frac{60 \cdot v \cdot i}{2 \cdot \pi \cdot r} \tag{5.19}$$

where v represents the vehicle velocity.

i is the transmission ratio between the vehicle wheel to the engine shaft.

r is the vehicle tyre radius (m).

It should be noticed that there are two different sampling time system in the model. The unit of the sampling time for engine simulation is per crank angle or per second. The calculation of torque output is based on per cycle, while the equations 5.16 and 5.18 are applied. For generating a cycle based calculation, a trigger/enable system has been added into the SIMULINK model that is shown in Figure 5-12.

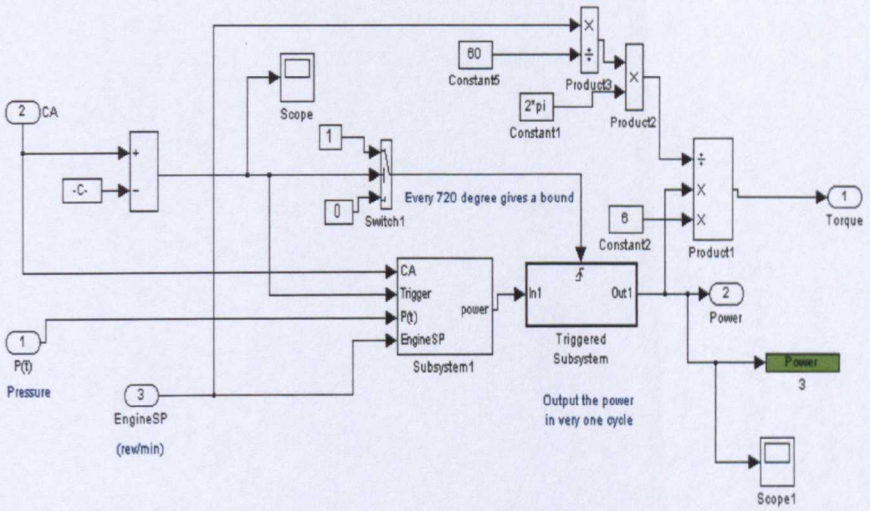

Figure 5-12 Block diagram of pressure to torque conversion in SIMULINK

5.3 SIMULATION RESULTS AND DISCUSSIONS

Followed by the discussion above, the mathematic models have been implemented by SIMULINK and the HCCI engine model is integrated into the model to simulate the driving force generation. Figure 5-13 shows the block diagram of model structure in SIMULINK. The simulation studies are conducted in two steps. The first step is open-loop test in order to exam the system working properly and the responses from different sampling time based model are coupled correctly. After that the closed-loop testing is carried out. A range of IVO and EVC valve timing strategies have been investigated and relevant PID controllers have been developed for vehicle cruise control.

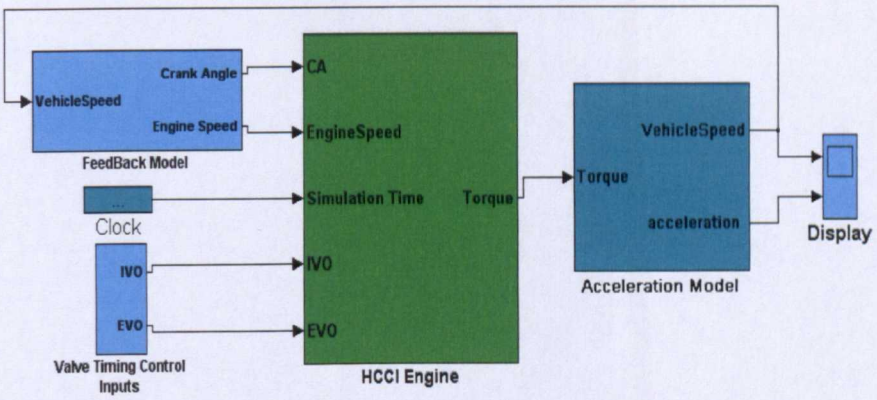

Figure 5-13 System diagram in SIMULINK

5.3.1 OPEN-LOOP TEST

Initial open loop control simulation tests have been conducted to verify the completed driveline model, which requires the capability of the model to response the variables changing. Figure 5-14 and 5-15 show an example of the simulation results for open-loop test. The model was first tested in open loop with the IVO set at 78 CAD (equalise to MOP 148 ATDC) and EVC at 648 CAD (equalise to MOP 142 BTDC). And the valves opening durations and valve lift profile are both fixed with crank angle. The affects from valve timing operating have been discussed in this chapter early.

As Figure 5-14 shown, the simulation starts with the vehicle speed at 8m/s and slowly accelerates through two gear changes, finally reaches a steady speed of just under 30m/s. The relevant engine behaviours are shown in Figure 5-15. It can be observed that against the engine speed increases/decreases, the engine torque output and in-cylinder pressure decreases/increases. This trend is caused by two main reasons:

1. As the discussion in early this chapter, the fixed valve lift profile will results in a shorter intake opening period and a smaller amount of inducted fresh reactants.

2. With the engine speed increasing the vehicle velocity increases. This increasing causes the increase of resistance force.

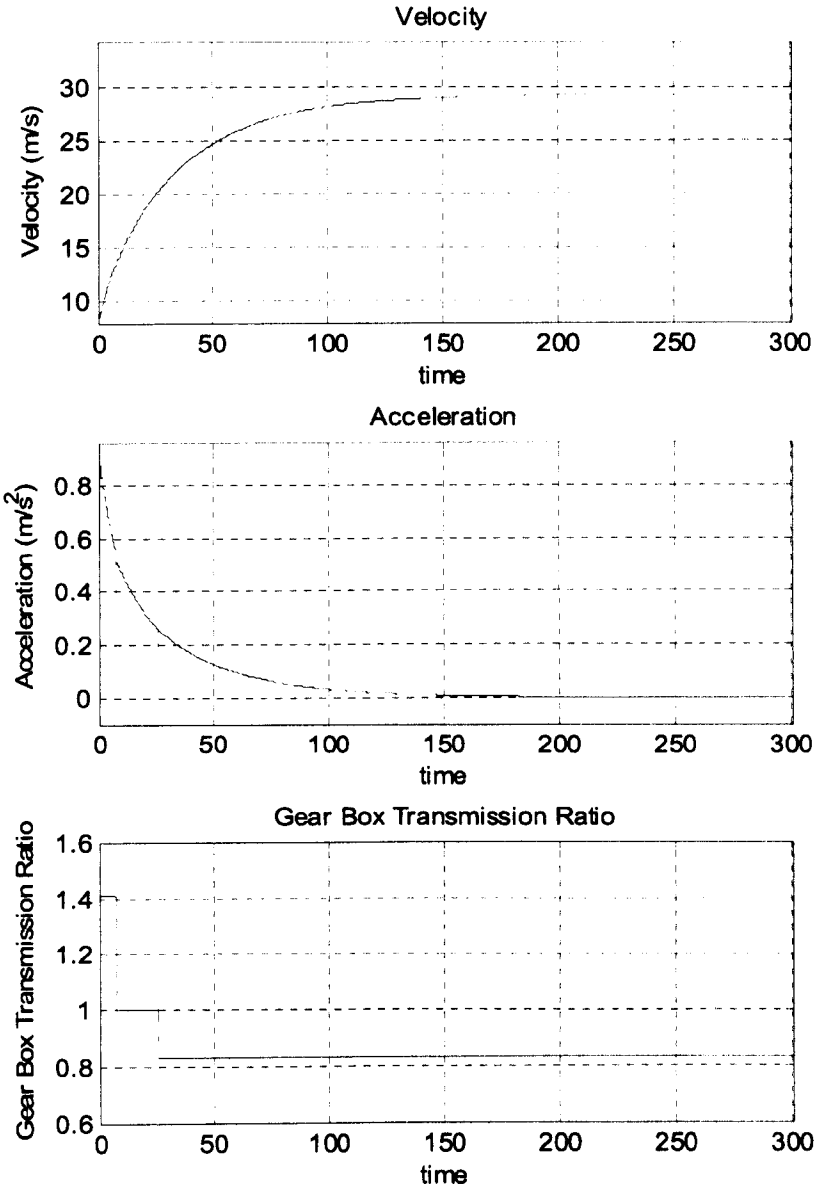

Figure 5-14 Open-loop testing result A - driveline

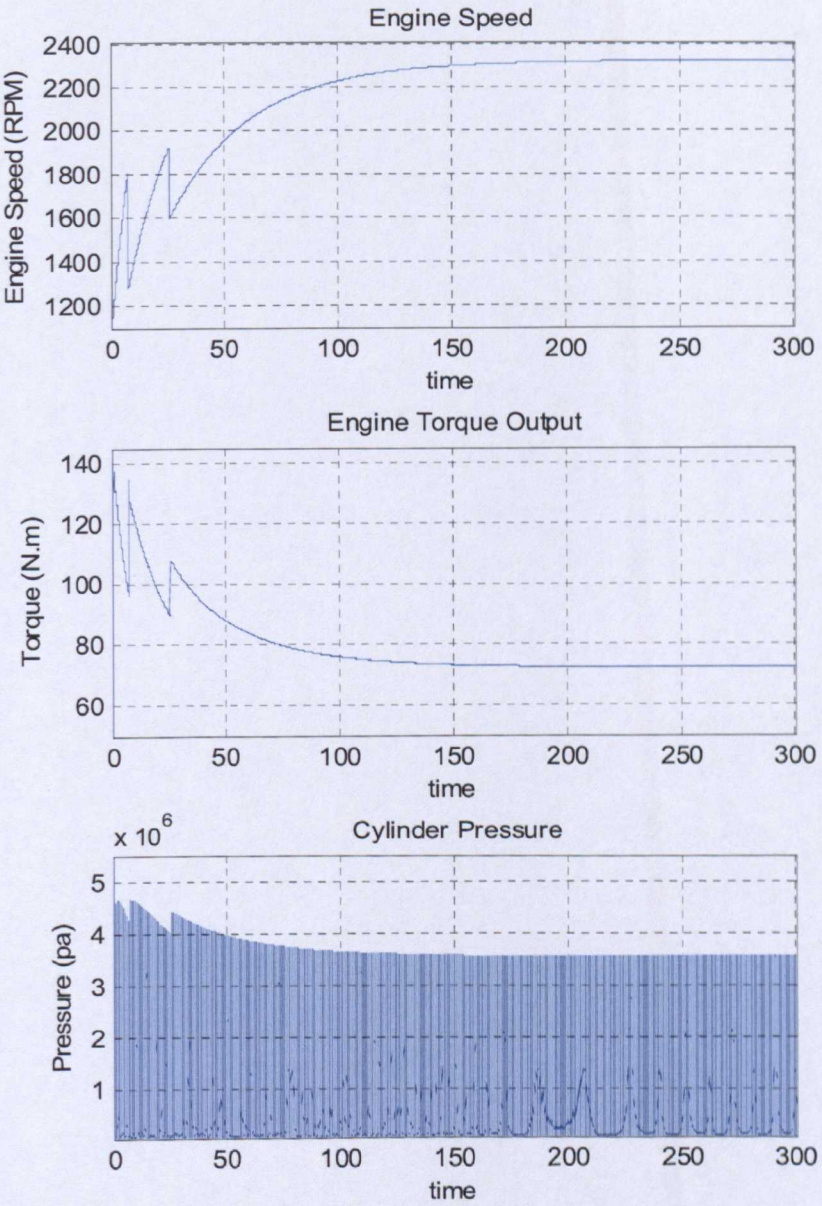

Figure 5-15 Open-loop testing result B – engine

The open loop test demonstrates the capability that the model can capture the dynamic responses of vehicle driveline when the operating changes. Together with the successful prediction on the in-cylinder pressure histories, the model can be trusted as a test platform for control strategy developments.

5.3.2 CLOSED-LOOP TEST

As the discussion in the previous section, by adopting with NVO, the HCCI combustion can be achieved by closing the exhaust valve early to trap hot combustion products. However, this phenomenon only occurs when the valve timing strategies are applied to modulate the composition of residual gases and fresh reactants properly. Hence, before applying the control strategies, the studies are carried out for investigating the boundary conditions of valve timing operation. Based on the extended HCCI driveline model described in previous section, two simulation experiments have been performed to identify the possible IVO and EVC range for achieving HCCI at two different engine speeds – 1077 rpm and 1685 rpm. This work is co-operated with Wei *et al* [125]. The results are summarised in Figure 5-16 and 5-17.

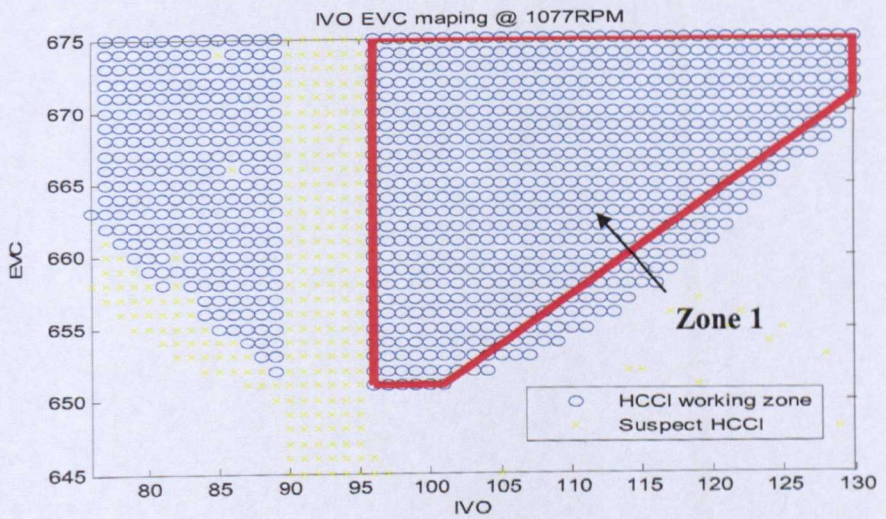

Figure 5-16 Investigation of range of valve timing for HCCI engine – A

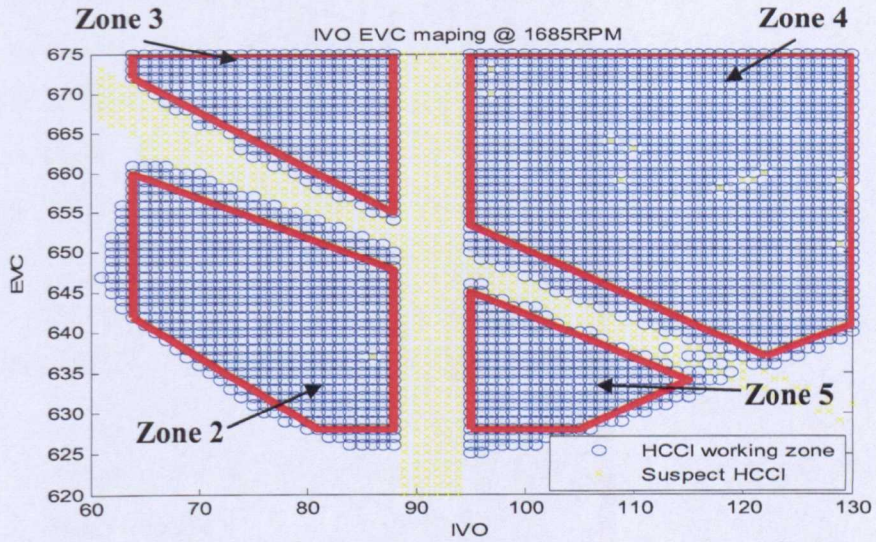

Figure 5-17 Investigation of range of valve timing for HCCI engine - B

The framed zones are the positive HCCI working zone, that is, HCCI can be maintained; other marked zones are unreliable HCCI area, that is, HCCI may or may not happen in those zones. It is found that the HCCI working zone for IVO and EVC is enlarged while the engine speed is increased. In order to simplify our study of control strategy, Zone 1 has been adopted for setting the initial point of the PID control when engine speed is lower than 1685 rpm, alternatively the Zones 2, 3, 4 and 5 are adopted for the engine speed over 1685 rpm.

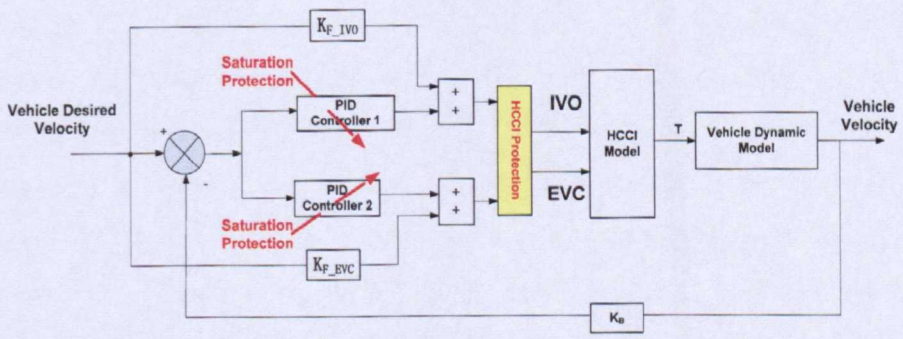

Figure 5-18 System diagram of the PID controller for valve tuning

Within the working zones introduced above, two PID plus feed-forward controllers are employed for tuning IVO and EVC. The purpose of the control actions is to simulate a simple vehicle cruise control system. The functionality of the system is to minimise the difference between the measured and the desired vehicle velocity. As the system structure diagram shown in Figure 5-18, the simplified saturation protections have been employed into the system in order to prevent the saturation of integral control actions, It works according to the following rules:

1. When IVO or EVC are inside of the working zone, the PID controller acts normally.
2. When IVO or EVC hit at the minimum boundary, then only the positive error will be accumulated into the integrator.
3. When IVO or EVC hit at the maximum boundary, then only the negative error will be accumulated into the integrator.

For validate the functionality of the controller, the simulation tests have been set up with two different conditions. In the first test, a step change in the desired velocity has been applied, where the desired velocity is set up from 27 m/s (60 mph) to 29 m/s (70 mph). The simulation results in Figures 5-19 and 5-20 show that the PID control of IVO and EVC can make the vehicle to maintain in the desired velocity, the vehicle settle down to the new desired velocity in about 200 seconds. The long period of time for tuning is mainly caused the limited engine power. In the second test, a road condition disturbance is applied by running the vehicle uphill with a gradient from a flat road. In the test, the vehicle was simulated to be driven by the HCCI engine from a horizontal flat road which is 2000 meter long and then into a road with +0.8 degree longitudinal gradient, where the vehicle running resistance is increased as approaching the uphill road. The results are shown in Figures 5-12 and 5-22. It is observed that the vehicle conquers the

additional resistance force by tuning IVO and EVC to increase the torque outputs.

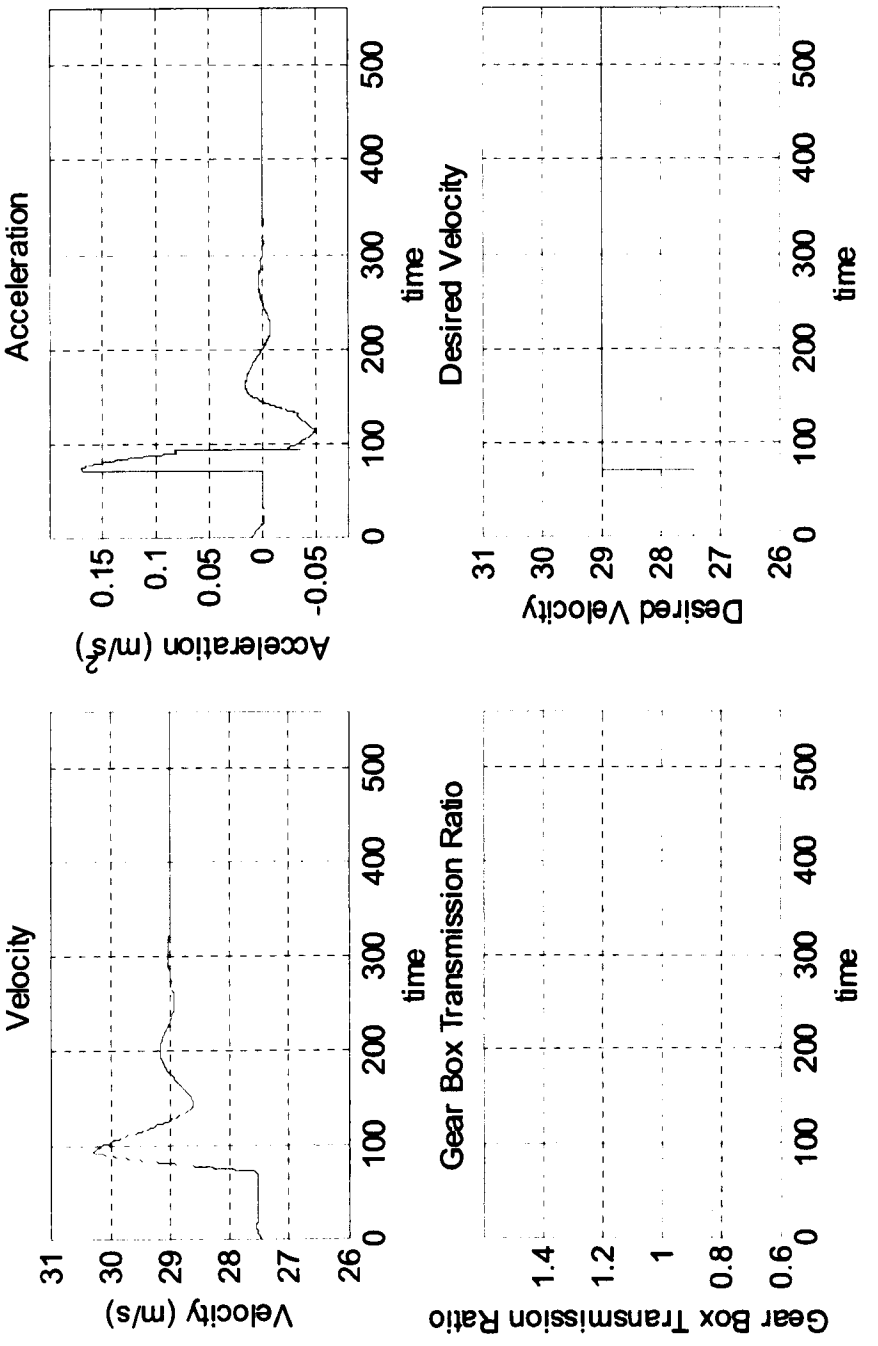

Figure 5-19 Step change in desired velocity, Part A

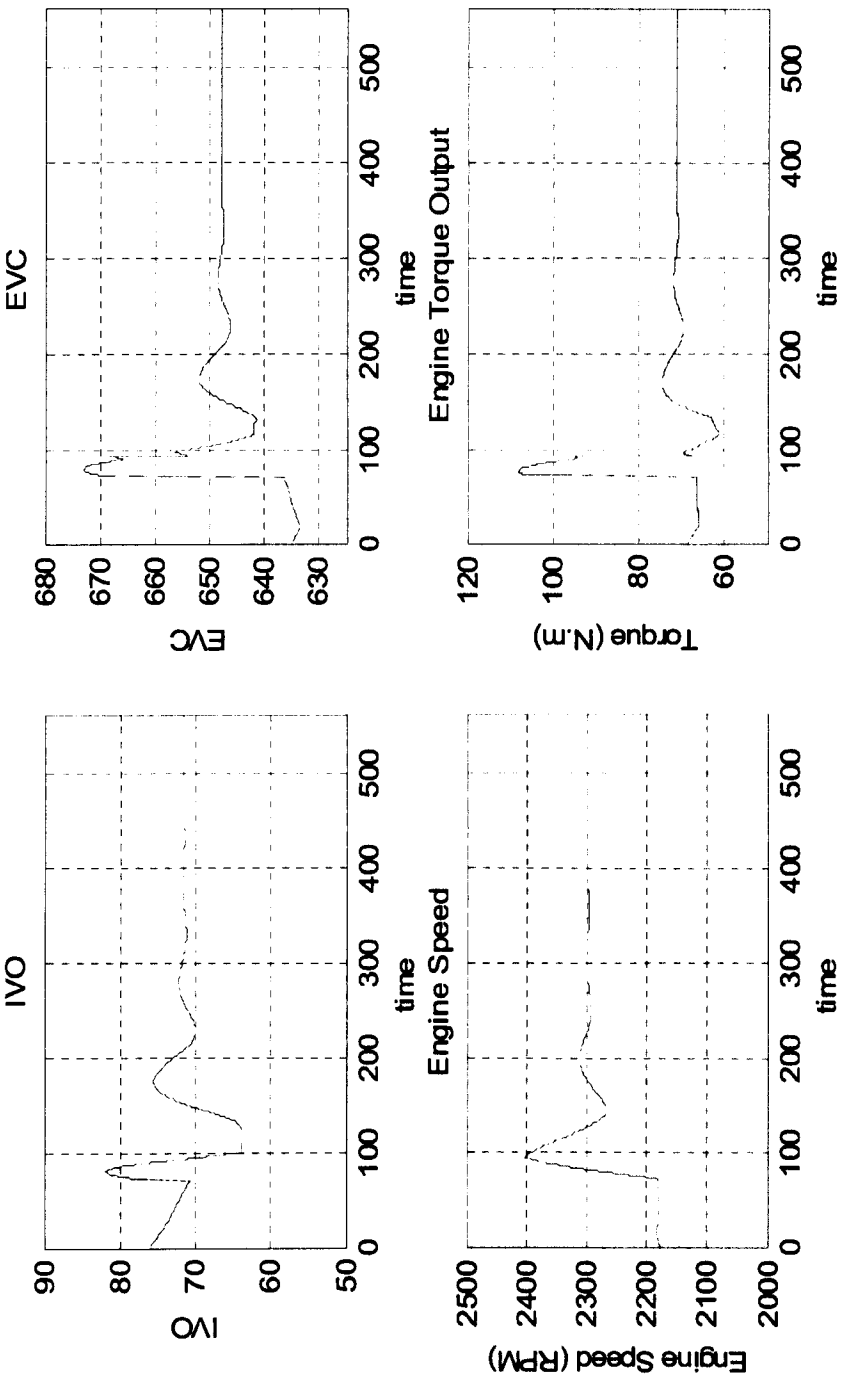

Figure 5-20 Step change in desired velocity, Part B

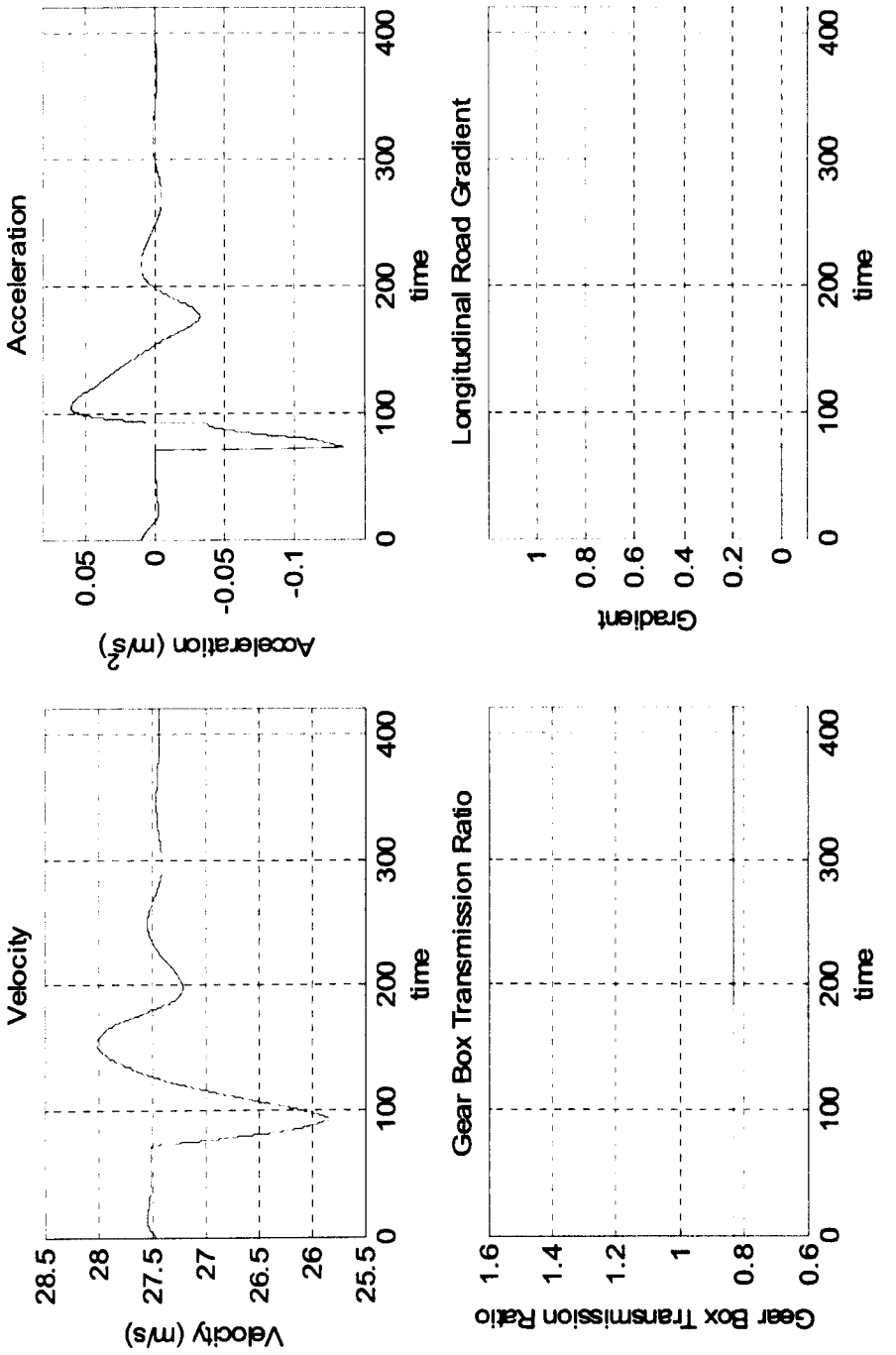

Figure 5-21 Road disturbance test, Part A

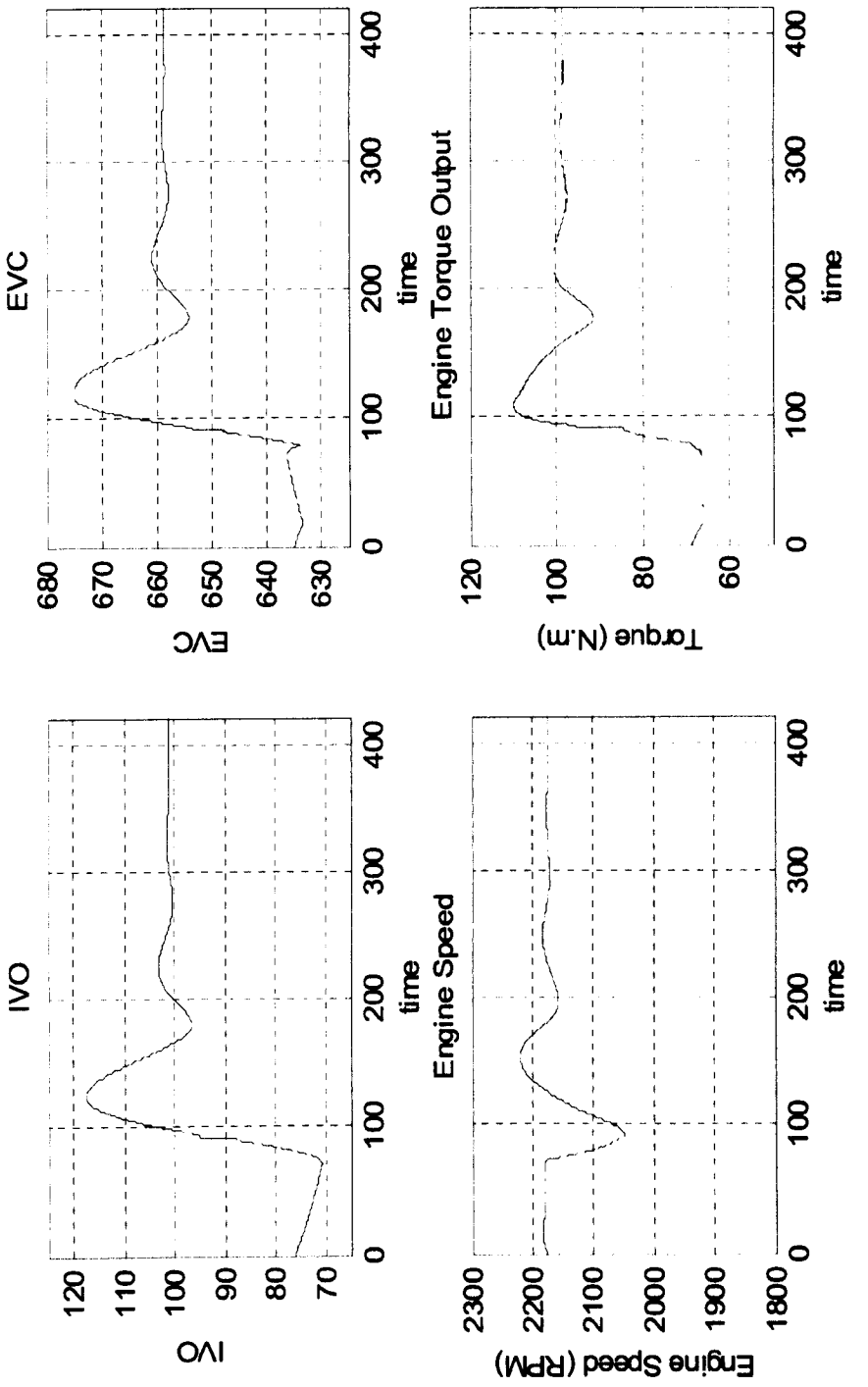

Figure 5-22 Road disturbance test, Part B

In summary, the vehicle speeds and relevant engine torque outputs are controlled as desired by regulating IVO and EVC timing of the engine while HCCI processes are maintained. These initial simulation studies for control demonstrate that the HCCI engine model presented in this chapter provides a convenient and cost-effective off-line test bed and on-line implementation for hardware-in-loop simulation which is essential for HCCI control system development.

Concurrently, however, it is noticeable that the valve tunings take a relative long period of time for stabilising the vehicle speed. The possible reasons and solutions are summarized as follows:

1. HCCI engine is difficult to control where a heavy load is applied. In the simulation, the vehicle is based on the specifications of Jaguar XKR, which is weighted as 1.9 ton and the vehicle speed is set up to 29 m/s. Both of these result in the considerable increase of resistance force.

2. HCCI engine is difficult to a fast control by tuning valve timings only. Other boosting applications are desired for improving the engine performance, such as turbo-charge and variable compression ratio.

3. The control strategy needs to be improved. Further advanced control strategy may be conducted to improve the system performance, *i.e.* torque-based control.

4. Advanced fuel injection technology essentially improves the controllability of HCCI engine, *i.e.* CIDI and multi-injection technology. CIDI allows the use of injected fuel mass as a control

input, which widely extends the controllability of the engine system. Multi-injection technology allows the variety of injection timings, times and fuel to improve HCCI combustion performance.

5.4 SUMMARY

Although the HCCI adopting negative valve overlap is a complex physical process, the simple and intuitive cycle-to-cycle model demonstrate the capability to predict and capture the most important engine behaviours for control developments – cyclic in-cylinder pressure evolution, combustion timing, work output and residual gas coupling. The simulation studies indicate the key insights of nature of the HCCI process can be predicted by the model - modulation of inducted gas composition, the self-stabilise nature of HCCI engine adopting negative valve overlap scheme and the cycle-to-cycle coupling. The investigations of these important characterises are not only the indication that the model can be applied for control strategy testing, but also provide important clues for control strategy design.

The aforementioned model has been extended with a simplified driveline model to simulate the vehicle dynamics, furthermore, a PID controller has been developed and implemented into the model to test the valve timing control strategy. The simulation studies demonstrate that the engine power output can be controlled by tuning the intake and exhaust valve timing. A certain range of intake/exhaust valve timing pairs has been investigated for obtaining the operation boundary condition. The studies also indicate that although the HCCI process can be controlled by tuning the timings of IVO and EVC, more controllable factors must be considered into the controller design for extending the operation window of HCCI engine, such as boosting

the intake pressure, advanced thermal management of the engine, variable compression ratio.

Finally, with run times of about 0.03 seconds/cycle and comparable levels of fidelity, the properties most relevant to control are captured - the simulation model presents a useful virtual test bed for control strategies development. Furthermore, the simulation codes are flexible to be modified for analysing different thermal dynamic processes and energy conversion system.

Chapter 6

CONCLUSIONS AND FUTURE RESEARCH

This chapter summarises the major achievements of the presented research work in the field of HCCI engine modelling development for real-time control purpose. Possible directions for further investigations are also indicated in this chapter.

6.1 CONCLUSIONS

As a promising alternative to conventional IC engines, HCCI engine has great potential to deliver diesel-like combustion efficiency accompanied by significantly lower NO_x emissions. In addition to these benefits, however, there also exist significant control challenges: the lack of a direct combustion initiator and the cycle-to-cycle residual gases coupling. In order to investigate the control strategies for solving the essential control challenges of HCCI engine, the original project specification set by Jaguar Cars Ltd

required a modelling approach that can be used as a test bed for control developments. This thesis represents the research work to achieve the objectives of the project.

At the beginning of the thesis, the project background, motivations, objectives and significance of this research work are all presented. The development of HCCI engine is introduced in Chapter 2, which covers the time period from the earliest concept to the latest demo car. The key technologies of HCCI control are then reviewed, which focus on the field of four-stroke HCCI engine combustion control. A wide variety of numerical modelling approaches for HCCI engine are discussed and categorised according to the variety types and the levels of complexity of the approaches. From the comparisons of different modelling approaches, the studies indicate that it is not necessary that engine model predicts the HCCI combustion in every detailed aspect. It will be sufficient if the model could capture most control relevant behaviours of HCCI process in both steady states and transients. And the model is desired inherent simple structure to reduce the simulation consuming time for control strategy investigation.

Although HCCI combustion is a quite complex process, Chapter 3 shows that a simple and intuitive physical-based model can capture most control relevant HCCI behaviours, such as ignition timing and in-cylinder pressure evolution. The model is evaluated and validated by comparing the simulation results with a series of experiment data obtained from a single cylinder HCCI research engine. An extensive simulation study of HCCI engine behaviour is conducted. Representative examples are presented which are associated with two engine parameters variations: the inlet temperature and exhaust valve timing. The comparisons demonstrate that the model can correctly predict the in-cylinder pressure, auto-ignition timing and combustion characteristics. While the simulation model formulated in Chapter 3 accurately predicts the

trend of ignition timing and work output variation of the propane fuelled HCCI engine by utilising Arrhenius rate approach, it is complicated to model the HCCI process of more complex fuel, *i.e.* gasoline which contains over 100 chemical reactions. For that reason, Wiebe function is selected as an accurate, simple and intuitive model to describe the gasoline HCCI process in Chapter 4. GAs are applied in order to identify the unknown parameters in the segment of the combustion process. The validations demonstrate that simplifications inherent in the model are not critical to the successful reproduce the engine cycle of gasoline HCCI process.

In Chapter 5, the approaches outlined in Chapter 2 and 3 are extended for cycle-to-cycle simulations to investigate the HCCI dynamics behaviours, including: the cyclic in-cylinder pressure evolution, combustion timing, work output and residual gas coupling. The simulation studies indicate the key insights of the nature of HCCI can be predicted by the models - modulation of inducted gas composition, the self-stabilise nature of HCCI engine adopting negative valve overlap scheme and the cycle-to-cycle coupling. The investigations of these important characterises not only indicate that the model can be applied for control strategy testing, but also provide important clues for control strategy design.

A simplified driveline model and a PID controller are developed and integrated into the system to test the valve timing control strategy. The simulation studies demonstrate that the engine power output can be controlled by tuning the intake and exhaust valve timing. A certain range of intake/exhaust valve timing pairs is investigated for obtaining the operation boundary condition. The studies also indicate that although the HCCI process can be controlled by tuning the timings of IVO and EVC, more controllable factors must be considered into the controller design for extending the operation window of HCCI engine, such as boosting the intake

pressure, advanced thermal management of the engine, variable compression ratio.

6.2 FUTURE RESEARCH EFFORTS

HCCI combustion can be operated with variety fuels. In the thesis, Chapter 3 and Chapter 4 present the HCCI engine modelling approaches for propane and gasoline fuelled engine respectively. HCCI diesel engine is a promising strategy to achieve stricter emission target. In future studies, diesel HCCI modelling will be carried out using the same framework as that outlined in Chapter 3 and Chapter 4. The common rail system and multi-injection strategy will be explicitly included. For heavy duty vehicle, ideal solution is to operate the engine in HCCI mode for light-duty and mid-duty; switch back to diesel mode when heavy-duty is required. Hence, the conventional diesel combustion model and relevant strategy are also desired to be included, *i.e.* direct injection, common rail pressure control. Following figures show an example of common rail pressure control by modulating the inlet metering valve (IMV) and high pressure valve (HPV). Figure 7-1 shows the experimental data of two control inputs of common rail system, and Figure 7-2 shows the simulation results.

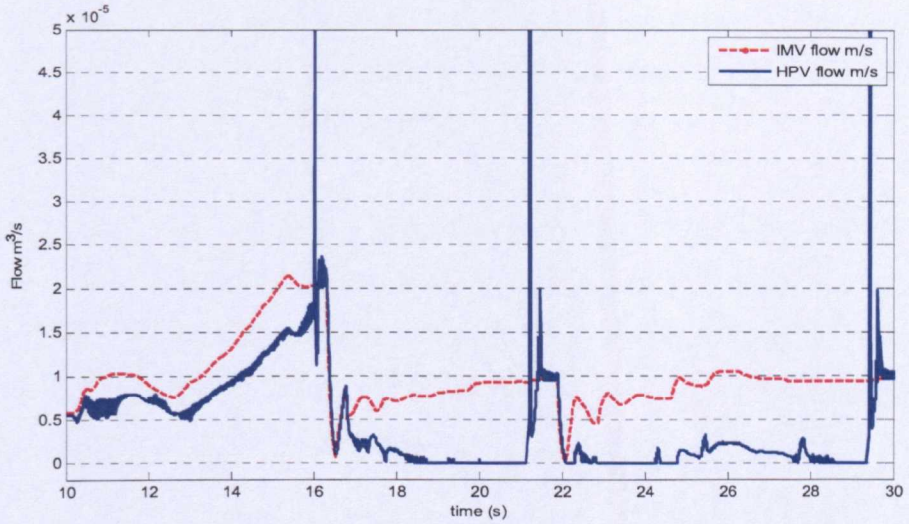

Figure 6-1 Rail control inputs

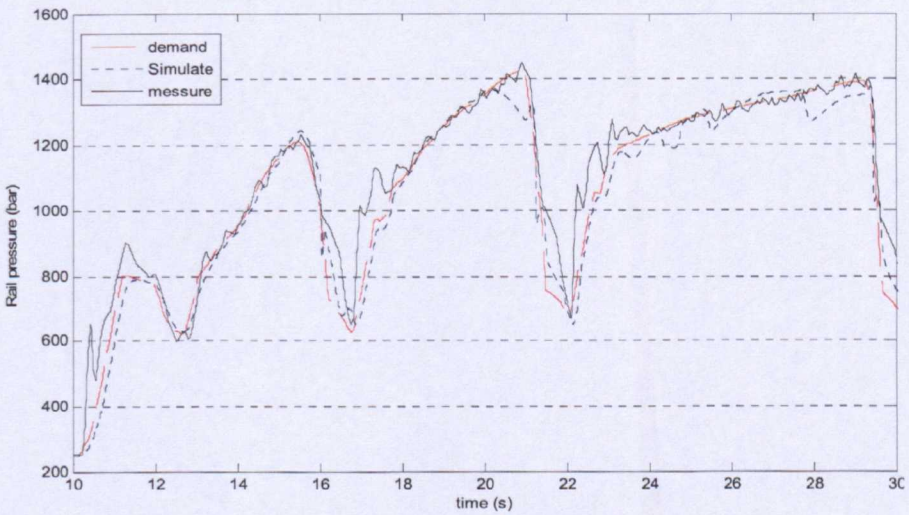

Figure 6-2 Rail pressure demand, simulation and measurement

Apart from the modelling works, Chapter 6 shows that the vehicle model is controlled by a simple PI controller to regulate the valve timings. However the simulation results indicate that more controllable inputs and advanced control strategies are desired to be included for more effective control. For that reason, the nonlinear low-order model will be investigated by splitting the HCCI process into discrete steps, and then, the model will be linearised to synthesise controllers. It is expected that the advanced control strategy,

i.e. torque-based control, can be deployed into the system to control the ignition timing and work output by varying effective compression ratio, intake boosting and valve timing together.

Furthermore, the modelling approach for scroll expander outlined in Appendix is applicable for pneumatic hybrid system design. The next steps involve extending it to the engine model and vehicle model to investigate the feasibility of energy recirculation. Author proposed scroll-type generator will be assessed in a physically based analysis.

Bibliography

1. Department of Transport, *DVLA Annual Report 07-08.* 2008.

2. Heywood, J., *The Performance of Future Ice and Fuel-Cell-Powered Vehicles and Their Potential Fleet Impact* SAE Paper 2004-01-1011, 2004

3. Ellinger, R., Prenninger, P., Meitz, K., Brandstater, W. and Salchenegger, S., *Comparison of Co2 Emission Levels for Internal Combustion Engine and Fuel Cell Automotive Propulsion Systems* SAE PAper 2001-01-3751, 2001.

4. Reynolds, C., and Kandlikar, M., *How Hybrid-electric Vehicles are Different from Conventional Vehicles: the effect of weight and power on fuel consumption.* Environment Reserch, 2007. **2.**

5. Environmental Protection Agency., U., *First Full Hydraulic Hybrid Urban Delivery Vehicle* EPA Announcement 2005.

6. Najt, P., and Foster, D., *Compression-Ignited Homogenous Charge Combustion.* SAE Paper 830264, 1983.

7. Epping, K.A., S., Bechtold, R. and Dec, J., *The Potential of HCCI Combustion for High Efficiency and Low Wmissions.* SAE Paper 2002-01-1923, 2002.

8. Aceves, S., Flowers, D., Martinez-Frias, J. and Smith, J. , *HCCI Combustion: Analysis and Experiments.* SAE Paper 2001-01-2077, 2001.

9. Caton, P., Simon, A., Gerdes, J. and Edwards, C *Residual-effected Homogeneous Charge Compression Ignition at Low Compresion Ratio using Exhaust Re-induction.* International Jounal of Engine Research, 2003. **4.**

10. Koopmans, L., Denbratt, I., Strin, H., Lundgren, S. and Backlund, O. , *Demonstrating a SI-HCCI-SI Mode Change on a Volvo 5- Cylinder Electronic Valve Control Engine* SAE Paper 2003-01-0753, 2003.

11. Hardy, A., Heywood, J. and Kenny, T., *Fuel Economy Benefit and Aftertreatment Requirements of a Naturally Aspirated HCCI - SI Engine System.* SAE Paper 2008-01-2512 2008.

12. Flynn, P., Hunter, G., Durrett, R., Farrell, L. and Akinyemi, W., *Minimum Engine Flame Temperature Impacts on Diesel and Spark-Ignition Engine NO_x Production.* SAE Paper 2000-01-1177, 2000.

13. Onishi, S., Jo, S., Shoda, K., Jo, P. and Kato, S., *Active Thermo-Atmosphere Combustion (ATAC) - a new combustion process of internal combustion engines.* SAE Paper 790501, 1979.

14. Noguchi, M.S., 1979., *A Study on Gasonline Engine Combustion by Observation of Intermediate Reactive Products during Combustion.* SAE Paper 790810, 1979.

15. Thring, R., *Homogeneous-Charge Compression Ignition (HCCI) Engines.* SAE Paper 892068, 1989.

16. Ryan, T., and Callahan, T., *Homogeneous Charge Compression Ignition of Diesel Fuel.* SAE Paper 961160, 1996.

17. Motyl, K., and Rychter, T., *HCCI Engine - a preliminary analysis.* Journal of KONES Internal Combustion Engines, 2003. **10**.

18. Stockinger, M., Schäpertöns, H. and Kuhlmann, P, *Versuche an einem gemischansungenden Verbrennungsmotor mit Selbstzündung (Attempt to a Homogenours Charged Combustion with Self-ignition).* Motortechnisches Zeitschrift, 1992. **53**.

19. Aoyama, T., Hattori, Y., Mizuta, J. and Sato, Y., *An Experimental Study on Premixed-Charge Compression Ignition (PCCI) Gasoline Engine* Sae Paper 960081, 1996.

20. Gentill, R., *Experimental Study on ATAC (Active Thermo-Atmosphere Combustion) in Two-Stroke Gasoline Diesel Engine.* SAE Paper 970363, 1997

21. Kong, S., Marriott, C., Reitz, R. and Christensen, M., *Modeling and Experiments of HCCI Engine Combustion Using Detailed Chemical Kinetics with Multidimensional CFD.* SAE Paper 2001-01-1026, 2001.

22. Zhao, H., Peng, Z., Williams, J. amd Ladommatos, N., *Understanding the Effects of Recycled Burnt Gases on the Controlled Autoignition (CAI) Combustion in Four Stroke Gasoline Engines* SAE Paper 2001-01-3607, 2001.

23. Zhao, H., Li, J., Ma, T. and Ladommatos, N., *Performance and Analysis of a Four-Stroke Multi-Cylinder Gasoline Engine with CAI Combustion.* SAE paper 2002-01-0420, 2002.

24. Morimoto, S., Kawabata, Y., Samurai, T and Amano, T., *Performance and Analysis of a Four-Stroke Multi-Cylinder Gasoline Engine with CAI Combustion.* SAE Paper 2002-01-0420, 2002.

25. Christensen, M., and Johansson, B., *The Effect of Combustion Chamber Geometry on HCCI Operation.* SAE 2002-01-0425, 2002.

26. Christensen, M.a.J., B., *The Effect of In-Cylinder Flow and Turbulence on HCCI Operation.* SAE Paper 2002-01-2864, 2002.

27. Agrell, F., Angstrom, H., Eriksson, B., Wikander, J and Linderyd, J., *Transient control of HCCI through combined intake and exhaust valveactuation.* SAE Paper 2003-01-3172, 2003.

28. Bengtsson, J., Strandh, P., Johansson, R., Tunestal, P. and Johansson, B., *Cycle-to-cycle control of a dual-fuel HCCI engine.* SAE Paper 2004-01-0941, 2004.

29. Haraldsson, G., Tunestal, P., Johansson, B. and Hyvonen, J. , *HCCI Combustion Phasing with Closed-loop Combustion Control using Variable Compression Ratio in a Multi-cylinder Engine.* JSAE Paper 20030126,, 2003.

30. Ishibashi, Y., and Asai, M, *Improving the Exhaust Emissions of Two Stroke Engines by Applying the Activated Radical Combustion.* SAE Paper 960742, 1996.

31. Kimura, S., Aoki, O., Ogawa, H. and Muranaka, S., *New Combustion Concept for Ultra-Clean and High-Efficiency Small DI Diesel Engines.* SAE Paper 1999-01-3681, 1999.

32. Christensen M., H., A. and Johansson, B., *Demonstrating the Multi-Fuel Capability of a Homogeneous Charge Compression Ignition Engine with Variable Compression Ratio.* SAE Paper 1999-01-3679, 1999.

33. Szybist, J., and Bunting, B., *The Effects of Fuel Composition and Compression Ratio on Thermal Efficiency in an HCCI Engine.* SAE Paper 2007-01-4076, 2007.

34. Kaahaaina, B., Simon, J., Caton, A., and Edwards, F.,, *Use of Dynamic Valving to Achieve Residual-Affected Combustion.* SAE Paper 2001-01-0549, 2001.

35. Persson, H., Agrell, M., Olsson, J. and Johansson, B., *The Effect of Intake Temperature on HCCI Operation Using Negative Valve Overlap.* SAE Paper 2004-01-0944, 2004.

36. Department of Energy, U.S., *Homogeneous Charge Compression Ignition (HCCI) Technology - A report to U.S. congress.* 2001.

37. Martinez-Frias, J., Aceves, S., Flowers, D., Smith, J. and Dibble, R.,, *HCCI Engine Control by Thermal Management.* SAE Paper 2000-01-2869, 2000.

38. Haraldsson, G., Hyvonen, J., Tunestal, P. and Johansson, B. , *HCCI Closed-Loop Combustion Control Using Fast Thermal Management.* SAE Paper 2004-01-0943, 2004.

39. Kanoto, Y., Ohmura, T. and Lida, N., *An Investigation of Combustion Control Using EGR for Small and Light HCCI Engine Fuelled With DME* SAE Paper 2007-01-1876, 2007.

40. Konno, M., and Chen, Z., *Ignition Mechanisms of HCCI Combustion Process Fueled with Methane/DME Composite Fuel* SAE Paper 2005-01-0182 2005.

41. Sato, S., Jun, D., Kweon, S., Yamashita, D. and Lida. N., *Basic Research on the Suitable Fuel for HCCI Engine from the Viewpoint of Chemical Reaction* SAE Paper 2005-01-0149 2005.

42. Ohmura, T., *A Study on Combustion Control by Using Internal and External EGR for HCCI Engines Fuelled with DME* SAE Paper 2008-01-1705, 2006.

43. Flowers, D., Aceves, S., Martinez-frias, J., Smith, J., AU, M. Girard, J. and Dibble R., *Operation of a Four-Cylinder 1.9 l Propane-fueled Homogeneous Charge Compression Ignition Engine: Basic Operating Characteristics and Cylinder-to-cylinder Effects.* sAE Paper 2001-01-1895, 2001.

44. Millet, J., Maroteaux, F. and Ravet, F, *Modelling of HCCI Combustion by One-Step Reaction Function: In View of Assisting the Optimization of Engine Management System* SAE Paper 2007-24-0033 2007.

45. Wang, Z., An, X. L., Shuai, S. J., Wang, J. X. and Tian, G.H., *Modeling of HCCI Combustion: From 0D to 3D* SAE Paper 2006-01-1364, 2006.

46. Christensen, M., Johansson, B., AmnJus, P., and Mauss, F., *Supercharged Homogeneous Charge Compression Ignition.* SAE Paper 980787, 1998.

47. Flowers, D., Aceves, S., Smith, J., Torres, J., Girard, J. and Dibble R., *Hcci in a CFR Engine: Experiments and Detailed Kinetic* SAE PAPER 2000-01-0328, 2000.

48. John, D., *A Computational Study of the Effects of Low Fuel Loading and Egr on Heat Release Rates and Combustion Limits in HCCI Engines* SAE Paper 2002-01-1309 2002.

49. Cernansky, N., Zheng, J., Yang, W. and Miller, D., *A Skeletal Chemical Kinetic Model for the Hcci Combustion Process* SAE Paper 2002-01-0423, 2002.

50. Aichlmayr, H., Kittelson, D., and Zachariah, M., Miniature, *Modelling HCCI Combustion in Small Scales with Detailed Homogeneous Gas Phase Chemical Kinetics.* Chemical Engineering Science, 2002. **57**.

51. Bruce G. Bunting, K.P., Chitralkumar Naik, Chen-Pang Chou, Ellen Meeks, *A Comparison of HCCI Ignition Characteristics of Gasoline Fuels Using a Single-Zone Kinetic Model with a Five Component Surrogate Fuel* SAE Paper 2008-01-2399, 2008.

52. Ogink, R., *Computer Modelling of HCCI combustion*, in *Division of Thermo and Fluid Dynamics*. 2004, Chalmers University of Technology: Sweden.

53. Aceves, S., Flowers, D., Westbrook, K., Smith, J., Dibble, R., Christensen, M., Pitz, W. and Johansson, B, *A Multi-Zone Model for Prediction of Hcci Combustion and Emissions* SAE Paper 2000-01-0327, 2000.

54. Fiveland, S., and Assanis, D., *Development of a Two-Zone Hcci Combustion Model Accounting for Boundary Layer Effects* SAE Paper 2001-01-1028, 2001.

55. Jia, M., Xie, M.Z. and Peng, Z., *A Comparative Study of Multi-zone Combustion Models for HCCI Engines* SAE Paper 2008-01-0064 2008.

56. Mehl, M., Tardani, A., Faravelli, T., Ranzi, E., D'Errico, G., Lucchini, T., Onorati, A., Miller, D. and Cernansky, N., *A Multizone Approach to the Detailed Kinetic Modelling of HCCI Combustion* SAE Paper 2007-24-0086, 2007.

57. Easley, W., Agarwal, A., and Lavoie, G.,, *Modeling of HCCI Combustion and Emissions Using Detailed Chemistry.* SAE Paper 2001-01-1029, 2001.

58. Noda, T.a.F., D.,, *A Numerical Study to Control Combustion Duration of Hydrogen-Fueled HCCI by Using Multi-zone Chemical Kinetics Simulation.* SAE Paper 2001-01-0250,, 2001.

59. Lee, D., and Hochgreb, S., *Hydrogen Autoignition at Pressures above the Second Explosion Limit.* International Jounal of Chemical Kinetics, 1998. **30**.

60. Ogink, R., and Golovitchev, V., *An Engine Cycle Simulation Code with a Multi-Zone Combustion Model.* SAE paper 2002-01-1745, 2002.

61. Jia, M., Xie, M., and Peng, Z, *Prediction of Operating Range for a HCCI Engine Based on a Multi-Zone Model.* SAE Paper 2008-01-1663, 2008.

62. Felsch, C., Sloane, T., Han, J., Barths, H. and Lippert A., *Numerical Investigation of Recompression and Fuel Reforming in a SIDI-HCCI Engine* SAE Paper 2007-01-1178, 2007.

63. Amano, T., Morimoto, S., and Kawabata, Y. and 01-1024, *Modeling of the Effect of Air/Fuel Ratio and Temperature Distribution on HCCI Engines.* SAE Paper 2001-01-1024, 2001.

64. Babajimopoulos, A., Assanis, D., and Fiveland, S., *An Approach for Modeling the Effects of Gas Exchange Processes on HCCI Combustion and Its Application in Evaluating Variable Valve Timing Control Strategies.* SAE Paper 2002-01-2829, 2002.

65. Subramanian, S., *Modeling Engine Turbulent Auto-Ignition Using Tabulated Detailed Chemistry* SAE Paper 2007-01-0150 2007

66. Gogan, A., Sunden, B., Lehtiniemi, H. and Mauss., F, *Stochastic Model for the Investigation of the Influence of Turbulent Mixing on Engine Knock* SAE Paper 2004-01-2999, 2004.

67. Wang, Z., *Multi-dimensional Simulation of HCCI Engine using Parallel Computation and Chemical Kinetics.* SAE Paper 2008-01-0966, 2008.

68. Koopmans, L., Ogink, R., Wallesten, J. and Denbratt, I., *Location of the First Auto-Ignition Sites for Two HCCI Systems in a Direct Injection Engine.* SAE paper 2004-01-0564, 2004

69. Hessel, R., Foster, D., Steeper, R., Aceves, S. and Flowers, D., *Pathline Analysis of Full-cycle Four-stroke HCCI Engine Combustion Using CFD and Multi-Zone Modeling*. SAE Paper 2008-01-0048, 2008.

70. Aceves, S., Martinez-Frias, J., Flowers, D., Smith, J. and Dibble, R., *A Decoupled Model of Detailed Fluid Mechanics Followed by Detailed Chemical Kinetics for Prediction of Iso-Octane HCCI Combustion*. SAE paper 2001-01-3612, 2001.

71. Bhave, A., Kraft, M., Mauss, F. and Montorsi, L., *Modelling a Dual-Fuelled, Multi-Cylinder Hcci Engine Using a Pdf-Based Engine Cycle Simulator* SAE Paper 2004-05-061, 2004.

72. Kung, E., and Haworth, D., *Transported Probability Density Function (TPDF) Modeling for Direct-Injection Internal Combustion Engines* SAE Paper 2008-01-0969 2008.

73. Tun, M., Pasternak, M., Mauss, F. and Bensler, H., *A PDF-Based Model for Full Cycle Simulation of Direct Injected Engines* SAE 2008-01-1606, 2008.

74. Zilwa, S., and Steeper, R., *Predicting Emissions from HCCI Engines using LIF Imaging* SAE Paper 2005-01-3747, 2005.

75. Maigaard, P., Mauss, F., and Kraft, M., *Homogeneous Charge Compression Ignition Engine: A Simulation Study on the Effects of Inhomogeneities*. ASME Paper 2000-ICE-275, 2000. **34-2**.

76. Choi, K., Noh, Y. and Du, L., *Reliability-Based Design Optimization with Correlated Input Variables* SAE Paper 2007-01-0551 2007.

77. Tuner, M., and Mauss, F. , *Studying HCCI Combustion and its Cyclic Variations versus Heat Transfer, Mixing and Discretization using a PDF based approach*. SAE 2008-01-1606, 2009-01-1607.

78. Durand, P., Gorokhovski, M. and Borghi, R., *The Pdf-Equation Approach to Diesel Spray Evaporation Computations*. SAE Paper 960632, 1996.

79. Mura, A., and Demounlin, F., *Crul and Intermediate Closures of Micromixing and Their Influence in the context of HCCI Combustion.* Journal of Chemical Physics, 2005. **24**.

80. Curl, R., *Disperse Phase Mixing.* AIChE, 1963. **9**.

81. Agrell, F., Angstrom, H., Eriksson, B. and Wikander, J, *Transient Control of Hcci Through Combined Intake and Exhaust Valve Actuation* SAE Paper 2003-01-3172, 2003.

82. Bengtsson, J., Strandh, P., Johansson, R., Tunestal, P. and Johansson, B., *Multi-Output Control of a Heavy Duty HCCI Engine Using Variable Valve Actuation and Model Predictive Control* SAE Paper 2006-01-0873, 2006.

83. Narayanaswamy, K., and Rutland, C., *Cycle Simulation Diesel Hcci Modelling Studies and Control.* SAE Paper 2004-01-2997, 2004.

84. Hessel, R., and Rutland, C., *A New Approach to Model DI-Diesel HCCI Combustion for Use in Cycle Simulation Studies.* SAE Paper 2005-01-3743, 2005.

85. Xu, H.M., Williams, A., Fu, H., Wallace, S., Richardson, S. and Richardson, M., *Operating Characteristics of a Homogeneous Charge Compression Ignition Engine With Cam Profile Switching-Simulation Study* SAE Paper 2003-01-1859, 2003.

86. Xu, H.M., *Modelling of Hcci Engines: Comparison of Single-Zone, Multi-Zone and Test Data* SAE Paper 2005-01-2110, 2005.

87. Tuner, M., Pasternak, M., Mauss, F. and Bensler, H. , *A PDF-Based Model for Full Cycle Simulation of Direct Injected Engines.* SAE Paper 2008-01-1606, 2008.

88. Qin, J., Xie, H., Zhang, Y. and Zhao, H., *A Combustion Heat Release Correlation for CAI Combustion Simulation in 4-Stroke Gasoline Engines.* sae paper 2005-01-0183, 2005.

89. Ogink, R., and Golovitchev, V., *Applications and Results of a User-Defined, Detailed-Chemistry HCCI Combustion Model in the AVL BOOST Cycle Simulation Code.* International AVL User Meeting, 2003.

90. Wong, Y., and Karim, G., *An Analytical Examination of the Effects of Hydrogen Addition on Cyclic Variations in Homogeneously Charged Compression Ignition Engines.* International Journal Of Hydrogen Energy, 2000.

91. Livengood, J.a.W., P., *Correlation of Autoignition Phenomenon in Internal Combustion Engines and Rapid Compression Machines.* The Combustion Institute, 1955. **5th Symposium (International) on Combustion.**

92. Kong, S., Patel, A., Yin, Q. and Reitz, R., *Numerical Modelling of Diesel Engine Combustion and Emissions Under Hcci-Like Conditions With High Egr Levels* SAE Paper 2003-01-1087, 2003.

93. Kongsereeparp, P., and Checkel, M., *Novel Method of Setting Initial Conditions for Multi-Zone HCCI Combustion Modeling* SAE Paper 2007-01-0674, 2007.

94. Mahrous, A., Potrzebowski, A., Wyszynski, M., Xu, H. M., Tsolakis, A and Luszcz, P., *A 1D Analysis into the Effect of Variable Valve Timing on HCCI Engine Parameters.* SAE Paper 2008-01-2459, 2008.

95. Sloane, T., Han, J., Barths, H. and Lippert, A. , *Numerical Investigation of Recompression and Fuel Reforming in a SIDI-HCCI Engine.* SAE Paper 2007-01-1878, 2007.

96. Su, W., and Huang, H., *A New Reduced Chemical Kinetic Model for Autoignition and Oxidation of Lean n-heptane /air Mixtures in HCCI Engines.* SAE Paper 2005-01-0118, 2005.

97. Winter, H., Kogler, G., Schnessl, E. and Wimmer, A., *Investigations on Combustion and Heat Transfer in a Large Gaseous-Fuelled Engine.* SAE Paper 2003-01-0562, 2003.

98. Iwashiro, Y., Tsurushima, T., Nishijima, Y., Asaumi, Y. and Aoyagi, Y., *Fuel Consumption Improvement and Operation Range Expansion in HCCI By Direct Water Injection* SAE Paper 2002-01-0105, 2002.

99. Iida, S., Kusaka, J. and Daisho, Y., *Numerical Study on Iso-Octane Homogeneous Charge Compression Ignition.* SAE Paper 2003-01-1820, 2003.

100. Kusaka, J., and Daisho, Y., , *Multi-Dimensional Modeling Combined with a Detailed Kinetics*, in *COMODIA 2001.* 2001: Japan.

101. Karim, A., and Liu, C., *A 3D-Simulation with Detailed Chemical Kinetics of Combustion and Quenching in an HCCI Engine* SAE Paper 2008-01-1655, 2008.

102. Toshihiro, O., Xiaofeng, Y., Toru, T., Yasuhiro, U., Shunichi, K. and Hideki, K, *Ignition and Combustion Simulation in HCCI Engines.* SAE Paper 2006-01-1522, 2006.

103. Flowers, D., Aceves, S., Martinez-Frias, J., Hessel, R. and Dibble, R., *Effect of Mixing on Hydrocarbon and Carbon Monoxide Emissions Prediction for Isooctane HCCI Engine Combustion Using a Multi-Zone Detailed Kinetics Solver.* SAE paper 2003-01-1821, 2003.

104. Chen, R., *A CFD Model with Optical Validation on In-cylinder Charge Performances of CAI Engines.* SAE Paper 2008-01-0045, 2008.

105. Shaver, G., Gerdes, J., Jain, P., Caton, P. and Edwards, C. *Modeling for Control of HCCI Engines.* in *American Control Conference.* 2003. Denver.

106. Ogink, R., *Computer modeling of HCCI Combustion.* 2004, Chalmers University of Technology: Sweden.

107. Shaver. G., G.J., Jain. P., Caton. P. and Edwards. C. *Modeling for Control of HCCI Engines.* in *American Control Conference.* 2003. Denver.

108. Heywood, J., *Internal Combustion Engine Fundamentals.* 1988, New York: McGraw-Hill.

109. Jia, N., Wang, J.W., Nuttall, K., Wei, J.L., Xu, H.M., Wyszynski, M.L., Qiao, J. and Richardson, M.J., *HCCI Engine Modeling for Real-Time Implementation and Control Development.* IEEE/ASME Transactions on Mechatronics, 2007. **12**(6).

110. Annand, W. *Heat Transfer in the Cylinders of Reciprocating Internal Combustion Engines.* in *Proc. Instn Mech. Engrs.* 1963.

111. Woschni, G., *A Universally Applicable Equation for the Instantaneous Heat Transfer Coefficient in the Internal Combustion Engine.* SAE paper, No.670931, 1967.

112. Stone, R., *An Introduction to Internal Combustion Engines.* SAE International, 199.

113. Zhao, F.T., Asmus. D., Assanis. J., , *Homogeneous Charge Compression Ignition Engines - Key Research and Development Issues.* SAE International, 1994.

114. Zheng., J., Miller, D. and Cernansky., P., *A Global Reaction Model for the HCCI Combustion Process.* SAE Paper 2004-01-2950, 2004.

115. Xu, H.M., Liu, M., Gharabaghi, S., Richardson, S., Megaritis, T. and Wyszynski, M, *Modelling HCCI Engines: Comparion of Single-zone, Multi-zone and Test Data.* SAE Paper 2005-01-2123, 2005.

116. Yap, D., Karlovsky, J., Megaritis, A., Wyszynski, M. and Xu, H.M., *An Investigation into Propane Homogeneous Charge Compression Ignition (HCCI) Engine Operation with Residual Gas Trapping.* Fuel, 2005. **84**: p. 2372-2379.

117. Saylam, A., Ribaucour, M., Pitz, W. J., and Minetti, R., , *Reduction of large detailed chemical kinetic mechanisms for autoignition using joint analyses of*

reaction rates and sensitivities. International Journal of Chemical Kinetics, 2007. **39**(4).

118. Westbrook, C.a.P., W, *Alternatives for modeling autoignition in homogeneous charge, compression ignition.*, in *International Conference on Num. Comb.* 2002: No. MS052.

119. Kim, S., ITO, K., Yoshihara, D. and Wakisaka, T., *Application of a Genetic Algorithm to the Optimization of Rate Constants in Chemical Kinetic Models for Combustion Simulation of HCCI Engines.* JSME International Journal, 2005. **4**: p. 48.

120. Sheppard, C.G.W., Tolegano, S. and Wooley, R., *On the Nature of Auto-ignition and Knock in HCCI Engines.* SAE paper 2002-01-2831, 2002.

121. Waston, N., Pilley, A.D. and Marzouk, M., *A combustion Correlation for Diesel Engine Simulation.* SAE Paper 800029, 1980.

122. Wei, J.L., Wang, J.H., Wu, Q.H, Oluwande, G. and Boardman, M. *Further Study on Coal Mill Modelling by Machine Learning Based on Onsite Measuments* in *16th ICSE.* 2003. Coventry UK.

123. Mangan, S., *Development of an intelligent road gradient estimation method using vehicle CAN bus data.* 2004, University of Liverpool: Liverpool.

124. Nice, K. *How Torque Converters Work.* [cited 2007; Available from: http://auto.howstuffworks.com/auto-parts/towing/towing-capacity/information/torque-converter.htm.

125. Wei, J.L., Jia, N., Wang, J.H., Nuttall, K., Xu, H.M., Qiao, J. and Richardson, M. *Study of HCCI Engine Model and Control Strategy.* in *Mechatronics Forum 2006.* 2006. USA.

126. Kim, H.J., Ahn, J.M., Park, I. and Rha, P.C., *Scroll Expander for Power Generation from a Low-grade Steam Source.* Power and Energy, 2007. **221**.

127. Zhao Y., L.L., and Shu P., *Thermodynamic Simulation of Scroll Compressor/Expander Module in Automotive Fuel Cell engine.* Automobile Engineering, 2006.

128. Zhao, H., Jiang, X. and Ma, T., *Innovative Air Hybrid Engine Concepts for Next Generation Fuel Efficient Road Vehicles.* 2007- 2010, EPSRC, Ford Motor, Lotus Engineering Ltd: Brunel University.

129. Yang, L., Wang, J., Mangan, S. and Derby, J., Lu, N., *Mathematical Model and Energy Efficiency Analysis of a Scroll-type Air Motor.* IAENG International Journal of Applied Mathematic, 2008. **38**.

130. Xing, L., Jia, N., Shpanin, L. and Wang, J.H. , *An Energy Efficient Pneumatic-Electricity System -- Modelling Study of the Scroll Expender*, in *Mechatronics Forum 2008*. 2008: Ireland.

APPENDIX A
ENGINE OPERATION CONDITIONS

Test Number	IVO aTDC	EVC bTDC	Engine Speed (rpm)	Intake Temperature (K)	Torque (N)
1	55.26	97.41	1519.62	68.09	64.10
2	55.05	86.79	1521.34	64.26	75.06
3	65.01	97.37	1517.70	64.94	59.64
4	65.03	83.85	1519.95	63.48	75.32
5	75.05	90.87	1519.70	64.84	63.66
6	75.04	85.97	1519.88	64.36	69.81
7	85.07	76.03	1520.10	66.11	80.75
8	90.02	76.13	1520.27	67.18	76.83
9	55.21	80.92	1521.19	64.36	63.61
10	55.17	76.10	1521.68	63.34	71.15
11	65.02	80.99	1520.05	63.04	60.57
12	65.02	71.01	1519.74	61.35	75.36
13	70.12	71.18	1519.87	60.97	72.82
14	70.11	80.99	1520.22	62.09	58.55
15	56.14	97.31	2021.77	71.93	46.74
16	56.08	85.98	2023.03	71.86	56.54
17	64.85	97.40	2020.16	70.67	44.54
18	64.87	83.82	2022.10	67.83	56.44
19	75.05	79.06	2022.19	66.81	59.79
20	85.08	80.99	2021.97	67.63	55.97
21	95.09	65.78	2021.55	70.48	76.25
22	55.92	80.79	2016.71	67.90	51.94
23	65.03	83.18	2015.90	67.16	43.94
24	65.03	70.91	2016.16	65.42	62.09
25	75.21	75.98	2016.12	66.57	51.95
26	56.79	96.71	2520.04	75.89	33.77
27	57.00	75.83	2519.80	71.39	55.96
28	65.00	93.54	2519.67	77.99	34.84

29	65.02	73.83	2518.93	74.60	56.10
30	75.06	92.59	2519.62	75.51	30.88
31	75.03	70.98	2519.48	74.34	63.10
32	85.10	65.98	2519.17	72.65	70.52
33	89.97	70.77	2519.99	73.71	62.11
34	56.95	79.81	2522.41	69.84	45.46
35	57.02	61.06	2522.24	66.49	74.93
36	65.01	78.81	2521.57	68.59	47.04
37	65.03	61.04	2521.97	67.34	74.96
38	75.05	61.00	2522.29	68.18	73.18
39	80.14	76.09	2521.82	69.52	47.34

APPENDIX B
LIST OF PAPERS

1. Jia, N., Wang, J.W., Nuttall, K., Wei, J.L., Xu, H.M., Wyszynski, M.L., Qiao, J. and Richardson, M.J., 'HCCI Engine Modelling for Real-time Implementation and Control Development', IEEE/ASME Transactions on Mechatronics, Vol. 12, No. 6, 2007.

2. Jia, N., Wang, J.W., Nuttall, K., Wei, J.L., Xu, H.M., Wyszynski, M.L., Qiao, J. and Richardson, M.J., 'HCCI Engine Modelling for Control with Parameter Identification using GAs', The Proceedings of the 11th Mechatronics Forum Biennial International Conference (MX2008), Limerick, Ireland, 2008.

3. Xing, L., Jia, N., Shpanin, L. and Wang, J.H., 'An Energy Efficient Pneumatic-Electricity System Modelling Study of the Scroll Expender', The Proceedings of the 11th Mechatronics Forum Biennial International Conference (MX2008), Limerick, Ireland, 2008. (Best Paper Award)

4. Jia, N., Wang, J.W., Nuttall, K., Wei, J.L., Xu, H.M., Wyszynski, M.L., Qiao, J. and Richardson, M.J., 'HCCI Engine Modelling for the Purpose of Control Development', The Proceedings of the 18th International Conference on System Engineering, Coventry, UK, 2006

5. Wei, J.L., Jia, N., Wang, J.H., Nuttall, K., Xu, H.M., Qiao, J. and Richardson, M. 'Study of HCCI Engine Model and Control Strategy', The Proceedings of the 10th Mechatronics Forum Biennial International Conference (MX2006), PA, USA, 2006.